NOTE TO USERS

This reproduction is the best copy available.

uOttawa

L'Université canadienne
Canada's university

FACULTÉ DES ÉTUDES SUPÉRIEURES ET POSTOCTORALES

uOttawa

L'Université canadienne
Canada's university

FACULTY OF GRADUATE AND POSDOCTORAL STUDIES

Robin Everett C. Lee
AUTEUR DE LA THÈSE / AUTHOR OF THESIS

Ph.D. (Cellular and Molecular Medicine)
GRADE / DEGREE

Department of Cellular and Molecular Medicine
FACULTÉ, ÉCOLE, DÉPARTEMENT / FACULTY, SCHOOL, DEPARTMENT

The Non-Death Role for the Yeast Metacaspase: YCA1 Prevents the Accumulation of Insoluble Protein Aggregates

TITRE DE LA THÈSE / TITLE OF THESIS

Lynn Megeney
DIRECTEUR (DIRECTRICE) DE LA THÈSE / THESIS SUPERVISOR

CO-DIRECTEUR (CO-DIRECTRICE) DE LA THÈSE / THESIS CO-SUPERVISOR

Steffany Bennett

Jeffrey Dilworth

David Litchfield (U.W.O)

Michael Rudnicki

Gary W. Slater
Le Doyen de la Faculté des études supérieures et postdoctorales / Dean of the Faculty of Graduate and Postdoctoral Studies

The non-death role for the yeast metacaspase: YCA1 prevents the accumulation of insoluble protein aggregates

Robin E. C. Lee

Department of Cellular and Molecular Medicine

Faculty of Medicine

University of Ottawa

June 2010

This thesis is submitted as a partial fulfillment of the Ph.D. program in Cellular and Molecular Medicine.

Your file Votre référence
ISBN: 978-0-494-69104-5
Our file Notre référence
ISBN: 978-0-494-69104-5

Abstract:

The caspase family of proteases are regulators of cell fate contributing to apoptosis, proliferation and differentiation. The yeast metacaspase, YCA1, is an ancestral caspase protease that is an established mediator of death processes, however, contribution to non-apoptotic processes have not been explored. Using systems level proteomic analysis we have identified a novel role for the yeast metacaspase in the clearance of insoluble protein aggregates. This function contributes to the fitness and adaptability of wild-type yeast. Our observations suggest that death and non-death caspase function emerged in single celled eukaryotes.

Table of contents

Abstract: i

List of Tables v

List of Figures vi

List of Abbreviations viii

Acknowledgements xii

Foreword xv

CHAPTER 1 1

1.0 General Introduction 1

1.1 Caspases, metacaspases and YCA1 2

1.2 Capsase signalling pathways 7

1.3 Apoptotic cell death 9

1.4 Caspases and cell fate decisions 13

1.5 Yeast cell death and YCA1 16

1.6 Motivation 22

1.7 Hypothesis and objective 26

CHAPTER 2 27

A Non-death Role of the Yeast Metacaspase: YCA1 Alters Cell Cycle Dynamics 27

2.1 Manuscript 28

2.1.1 Author Contributions and Manuscript Information: 29

2.1.2 Abstract 30

2.1.3 Introduction 31

2.1.4 Results and Discussion 34
2.1.5 Materials and Methods:..... 49
2.1.6 Acknowledgements..... 54
2.2 Supplementary Information:..... 55
CHAPTER 3:..... 59
The Metacaspase YCA1 is required for Clearance of Insoluble Protein Aggregates... 59
3.1 Manuscript..... 60
3.1.1 Author Contributions and Manuscript Information..... 61
3.1.2 Abstract..... 62
3.1.3 Text body..... 63
3.1.4 Acknowledgements..... 74
3.2 Supplementary information:..... 75
3.2.1 Supplementary Materials and Methods..... 75
3.2.2 Supplementary Tables..... 82
3.2.3 Supplementary Figures..... 89
CHAPTER 4..... 96
4.0 General Discussion..... 96
4.1 A non-death role for the yeast metacaspase YCA1..... 97
4.1.1 YCA1 and the cell cycle..... 98
4.1.2 YCA1 and stress response chaperones..... 100
4.1.3 A model for YCA1 in aggregate removal..... 103
4.1.4 Caspases and amyloid aggregates..... 106
4.2 A paradigm shift for the interpretation of caspase activity..... 108

4.3 Conclusions and future directions 109

References: 114

Appendix 1. Extended Materials and methods 126

Appendix 2. Additional Publications 130

2.1 Article: The Yeast Kinome Displays Scale Free Topology with Functional Hub Clusters 131

2.2 Article: Reconstructing the regulatory kinase pathways of myogenesis from phosphopeptide data 141

2.3 Book Chapter: Reconstructing regulatory kinase pathways from phosphopeptide data: a bioinformatics approach 150

List of Tables

Manuscript 1:

Table 1. MS identification of protein species induced by yca1 ablation..... 45

Manuscript 2:

Table S1| iTRAQ analysis of *Δyca1* versus wild-type lysates..... 83

Table S2| List of yeast strains used in this study..... 87

Table S3| List of primers used in this study. The listed oligos were used to construct the indicated plasmids and yeast strains..... 88

List of Figures

Manuscript 1:

Figure 1: Cell cycle profiles during logarithmic growth..... 36

Figure 2: Derivation of the duration of cell cycle phases..... 38

Figure 3: Response of cells to nocodazole..... 40

Figure 4: G2/M response of caspase inhibited cells..... 42

Figure 5: Representative 2D gels of BY4741 and *Δyca1* proteomes..... 43

Figure 6: Downstream effects and oxidative stress..... 47

Figure S1: Expression of *yca1*..... 55

Figure S2: Flow cytometry gates for DNA analysis..... 56

Figure S3: Integration of the C297A construct into the *Δyca1* background strain..... 57

Figure S4: Expression of genes flanking *yca1*..... 58

Manuscript 2:

Figure 1| Proteomic analysis of *Δyca1* and TAP interactors reveal association with chaperone mediated protein quality control..... 65

Figure 2| YCA1 targets insoluble protein aggregates irrespective of its catalytic activity..... 67

Figure 3| Caspase mutants accumulate insoluble aggregate material during logarithmic growth..... 70

Figure 4| Model depicting the role of YCA1 in the balance of protein aggregate assembly and dissolution..... 73

Figure S1| iTRAQ analysis identifies protein species that undergo significant change *in* Δyca1 cells..... 90

Figure S2| *GO biological process* and *MIPS subcellular localization* Funspec clusters of proteins up-regulated in *Δyca1*..... 91

Figure S3| YCA1-TAP interacting proteins..... 92

Figure S4| YCA1 does not significantly co-localize with mRNA processing bodies (P-bodies)..... 93

Figure S5| YCA1-GFP foci form rapidly in response to heat stress..... 94

Figure S6| YCA1-GFP co-localizes with HSP104 foci formed in aged stationary cultures..... 95

List of Abbreviations

ADH – Alcohol Dehydrogenase

AIF – Apoptosis Inducing Factor

ANOVA – Analysis of Variance

APAF – Apoptotic Peptidase Activating Factor

BCL2 – B-cell CLL/lymphoma 2

BI-1 – Bax Inhibitor 1

BMP – Bone Morphogenetic Protein

CAD – Caspase Activated DNAse

CARD – Caspase Recruitment Domain

cAMP – cyclic AMP

CDC – Cell Division Cycle

CED – Cell Death abnormal

CytC – Cytochrome C

DED – Death Effector Domain

DHR123 – Dihydrorhodamine 123

DISC – Death Inducing Signaling Complex

DNA – Deoxyribonucleic Acid

DTT – Dithiolthreitol

EDTA – Ethylenediaminetetraacetic Acid

EGF – Epidermal Growth Factor

ER – Endoplasmic Reticulum

FITC – Fluorescin Isothiocyanate

FMK – Fluoromethylketone

GFP – Green Fluorescent Protein

GICD – Glucose Induced Cell Death

GO – Gene Ontology

H_2O_2 – Hydrogen Peroxide

HCl – Hydrochloric Acid

HeLa – Henrietta Lacks

HSP – Heat Shock Protein

HU – Hydroxyurea

ICAD – Inhibitor of Caspase Activated DNAse

ICE – Interleukin Converting Enzyme

IPG – Immobilized pH Gradient

iTRAQ – Isobaric Tagging for Relative and Absolute Quantitation

LC – Liquid Chromatography

LiAc – Lithium Acetate

MAC – Mitochondrial Apoptosis Induced Channel

MIPS – Munich Information Center for Protein Sequences

MOMP – Mitochondrial Outer Membrane Permeability

mRNA – Messenger Ribonucleic Acid

MS – Mass Spectrometry

MST1 – Mammalian Sterile Twenty-like Kinase

Na_3VO_4 – Sodium Orthovanadate

NCCD – Nomenclature Committee on Cell Death

NER – Nucleotide Excision Repair

ND – Nocodazole

NP-40 – Nonidet P-40

OD660 – Optical Density at 660 nm

PAGE – Polyacrylamide Gel Electrophoresis

P-Bodies – mRNA Processing Bodies

PCD – Programmed Cell Death

PCR – Polymerase Chain Reaction

PEG – Polyethylene Glycol

PI – Propidium Iodide

Poly-Q – Poly-Glutamine

PS – Phosphatidylserine

PTP – Permeability Transition Pore

PVDF – Polyvinylidene Fluoride

RAD23 –Radiation sensitivity abnormal

RFP – Red Fluorescent Protein

RIP – Ribosome Inactivating Protein

RNA – Ribonucleic Acid

ROS – Reactive Oxygen Species

SSA – Stress-Seventy Associated

TAP – Tandem Affinity Purification

TEM – Transmission Electron Microscopy

TNF – Tumor Necrosis Factor

TPE – Total Protein Extract

TRAIL – TNF-Related Apoptosis-Inducing Ligand

TSN –Tudor Staphylococcal Nuclease

TUNEL – Terminal Deoxynucleotidyl Transferase dUTP Nick End Labeling

UV – Ultraviolet

WT – Wild-Type

Y2H – Yeast Two Hybrid

YPD – Yeast extract Peptone Dextrose

Acknowledgements

Being a graduate student in molecular biology is a tumultuous roller coaster of ups and downs. With each and every one of our many experimental failures, our skin gets another layer thicker; eventually we will become frustrated with bruised egos as our hypotheses are disproven. The intensity increases with the length of the day as we try to determine 'what went wrong'. However, with a shift in our methodology and/or perspective we realize that each failure is, in fact, directing us away from a flaw in our approach or model. Eventually, experiments begin to work as our hypothesis is refined. We realize why previous experiments failed and we learn from the experience. In these times, each success can bring the joy, wonder and excitement like that of a child on Christmas morning. Well, kind of... It is, nonetheless, these successes that keep our skin from getting too thick. It is also these successes that lead to new questions which start the whole process over. It is easy enough to stay motivated when 'the science' works. However it is the people that participated in theoretical discussions, had confidence in me and cheered me on from the sidelines who kept me going through the majority of my days as a graduate student. Here I would like to express my gratitude to these people.

First and foremost, I thank Dr. Lynn Megeney. Lynn opened the doors of his lab to me as a new graduate of physics with no training in biology, molecular biology or wet lab experience. Lynn gave me an open environment to explore science. I had free run to make my own discoveries and to make my own mistakes. He never balked at the expense of these mistakes, nor did he ever suggest they weren't worth trying. When results were unclear he was a responsive and engaged supervisor. When things were on the upswing he was a muse. Whenever we approached a conclusion or a publication he was equally

excited and along for the ride. I have learned a great deal of things from Lynn personally and through his lab as a whole. Thank you for these Lynn.

I extend my gratefulness to all members of the Megeney lab past and present. I've learned from each and every student, technician and post doc from the Megeney lab. It was a privilege to work with all of you. In particular, I thank Dr. Lawrence Puente for being a knowledgeable collaborator from the very start. Thanks to Mohammad Abdul-Ghani for following me through a pipe dream and teaching me how to clone in the process. Finally, I thank Steve Brunette for being an outstanding technician, sharing knowledge and watching out for us lab-folk, you are a brother-at-arms. I also thank you for taking interest in the yeast project as a whole. This Bud's for you – metacaspase deficient budding yeast that is.

My graduate committee, Drs. Mads Kærn, Len Maler and Jeff Dilworth, offered challenges to me throughout my progression that helped me keep perspective of my work. Each of them also shared sound personal and professional advice that I will take with me wherever I end up in the future. In the end (and along the way) their support gave me confidence in myself and my work. Thanks to you all for this, and a special thanks to Mads for the numerous chats and for training me in the basics of yeast.

I thank my parents, my sister and her family for the conversations, their help, support and many hot meals. Thanks to my father, Dr. Wayne Lee, for sharing his stories and experiences in academia as a PhD student with me. I also thank my mother-in-law and father-in-law for all of their help. Their generosity and their general interest in science provided great relief in times of stress. Finally, I'd like to thank my wife Laila

Lee. Laila was neck deep with me in everything I went through. Her confidence in me never faltered. Words cannot express my gratitude. This thesis is dedicated to you.

Foreword

Early along the course of my graduate school training, my research project underwent a substantial shift in theme and methodology. The original research plan consisted of a systems level study of kinase activation dynamics comparing metacaspase deletion mutants to wild-type cells. The intent of the project was to screen the enzymatic activity of highly interactive kinases to determine if the yeast metacaspase, YCA1, contributed to non-death signalling pathways. Control data from our first cell-cycle experiments, however, immediately demonstrated a non-death function for YCA1 and offered a more direct route to study the role of YCA1 in ambient conditions. The preliminary research from the kinase network project contributed to the development of a novel network modeling tool and three publications (Lee and Megeney 2005; Puente, Voisin et al. 2006; Puente, Lee et al. 2009). The work in these publications does not directly contribute to the thesis topic herein; however, they do represent a portion of my efforts in my time in Dr. Megeney's lab. For the reader's interest, I have included these publications as an appendix to this thesis.

CHAPTER 1

1.0 General Introduction

"But in the world nothing can be said to be certain except death and taxes"

- Ben Franklin, 1789.

1.1 Caspases, metacaspases and YCA1

The caspase family of proteases are regulators of multiple cell behaviours including apoptotic programmed cell death (PCD), immune cell activation, enhanced motility and differentiation (Ellis and Horvitz 1986; Thornberry, Bull et al. 1992; Fernando, Kelly et al. 2002; Helfer, Boswell et al. 2006). Members of the caspase family are identified by domains, structures and features which together co-ordinate their unique function. Caspase proteases are notably absent in plants, fungi and protozoa; however, structural relatives to the caspase family have been identified. This emerging family, termed metacaspases, complements caspase function and serve as extensions to the caspase family in lower eukaryotes. Subsequently, metacaspase dependent apoptotic PCD has been observed in response to various challenges in these species thus implicating the caspase and metacaspase families as regulators of cell death across phyla. Particular attention has been given to the yeast metacaspase from which a yeast model of metacaspase-dependent apoptosis has been developed.

Caspases are clan CD cysteine-dependent aspartate specific proteases that cleave substrates after an aspartic acid. The caspase family contains conserved cysteine and histidine residues which together form a catalytic dyad essential for protease activity. Caspases are expressed as zymogens with an N-terminal pro-domain consisting of adaptor recruitment domains (DED and CARD). The fully mature enzyme is a heteromeric complex of catalytic fragments resulting from the removal of the pro-domain and cleavage events which separate the protein into P10 and P20 catalytic components. Mammalian caspases -2, -8 and -9 are able to undergo autocatalytic activation by induced proximity whereas others require proteolytic activation from other caspases or non-

caspase proteases (Muzio, Stockwell et al. 1998; Timmer and Salvesen 2007; Bouchier-Hayes, Oberst et al. 2009). Generally, apoptotic caspases have affinity for tetrapeptide motifs including a glutamate in the second position (termed P3), ending with an aspartate residue 'P1' and followed by a non-bulky uncharged residue 'P–1'. The cleavage event occurs between the charged aspartate '*P1*' and the uncharged residue '*P–1*', (i.e.: *P4-P3-P2-P1*↓*P–1*…) (Timmer and Salvesen 2007). For this reason the fluoromethyl-ketone conjugated peptide inhibitor zVAD (z.VAD-FMK) is a potent pan-caspase inhibitor (Van Noorden 2001) from which multiple designer peptide inhibitors have been optimized to target individual caspases.

The interleukin-1β-converting enzyme (ICE) was the first recognized caspase protease identified for mediating inflammatory responses via cleavage induced maturation of IL1β (Cerretti, Kozlosky et al. 1992). Ced-3, a homologue to the ICE protease in the nematode *C. elegans*, was identified in a mosaic screen for essential PCD genes in the developing hermaphrodite (Yuan and Horvitz 1990) where exactly 131 of the 1090 somatic cells are eliminated by PCD (Sulston, Schierenberg et al. 1983). Regulation of PCD by the caspase Ced-3 represents a generally conserved function of the caspase family; caspases are established apoptotic regulators. ICE and Ced-3 homologues were later re-named to Caspases-1 and -3 respectively. Numerous caspase proteases have been identified throughout metazoan phyla with different organisms expressing varying number of caspase family proteins. For example, over eleven caspases have been observed in humans whereas *D. melanogaster* express 7 and *C. elegans* only express four (Lamkanfi, Declercq et al. 2002).

There are no direct homologues to the caspase family in many lower metazoans and single celled organisms; however, bioinformatic investigation of distant ancestors to caspases uncovered a family of structural homologues in plants, fungi and protozoa termed metacaspases (Uren, O'Rourke et al. 2000). Metacaspases are divided into type-I and type-II variants based on the presence or absence of a pro-domain respectively. Metacaspases are distributed irregularly across various species. The mustard plant *Arabidopsis Thaliana* expresses nine metacaspases, three type-I (AtMCP1a-c) and six type-II (AtMCP2a-f) (Watanabe and Lam 2005). The parasitic protist *Trypanosoma brucei* has five type-I metacaspases (Szallies, Kubata et al. 2002). Fission yeast *Schizosaccharomyces pombe* and the baker's yeast *Saccharomyces cerevisiae* both express a single type-I metacaspase gene named PCA1 and YCA1 respectively (Madeo, Herker et al. 2002; Zhang, Chieu et al. 2003). Direct sequence homologues to metacaspases found in early eukaryotes are noticeably missing in animals, an observation which is complemented by the complete absence of caspase homologues in lower eukaryotes. Due to this phyletic distribution and conserved contributions to apoptotic cell fate, metacaspases in early eukaryotes are regarded as ancestral caspases (Uren, O'Rourke et al. 2000).

Consistent with mammalian caspases, yeast and plant metacaspases have a caspase fold and can undergo caspase-like processing in the formation of the mature protease. Similarly, maturation and enzymatic activity of metacaspases is dependent on the conserved catalytic cysteine (Madeo, Herker et al. 2002; Bozhkov, Suarez et al. 2005; Watanabe and Lam 2005). A model for an ancestral metacaspase (*Arabidopsis thaliana*) revealed differences in the active site from mammalian caspases suggesting that the P1

specificity pocket may not require a charged residue (Uren, O'Rourke et al. 2000). Indeed, upon examination for alternate specificity, cysteine dependent arginine/lysine-specific protease activity was observed from various recombinant type-I and -II metacaspases (Vercammen, van de Cotte et al. 2004; Watanabe and Lam 2005; Gonzalez, Desponds et al. 2007). Nevertheless, even with alternate specificity metacaspases have been observed to contribute to PCD pathways in these organisms. The Norway spruce (*Picea abies*) metacaspases mcII-Pa is required for PCD dependent patterning in plant embryogenesis (Bozhkov, Filonova et al. 2004; Suarez, Filonova et al. 2004; Bozhkov, Suarez et al. 2005). The type-II Arabidopsis metacaspases AtMCP-2e is activated and required for UV and H_2O_2 induced PCD in *A. thaliana* (He, Drury et al. 2008). Metacaspase activity similarly promotes H_2O_2 mediated PCD in the protozoan parasite *Leishmania donovani* (Lee, Gannavaram et al. 2007). Finally, the yeast metacaspase YCA1 is an integral component of *Saccharomyces cerevisiae* PCD in response to numerous stresses (Madeo, Herker et al. 2002). While the metacaspase specificity pocket may differ from mammalian caspases, the families share similar structure, cysteine dependence, auto-processing and apoptotic influence.

The yeast metacaspase MCA1/YCA1 (YOR197w) is the most comprehensively studied metacaspase. YCA1 contains the conserved catalytic cysteine-histidine dyad and undergoes caspase-like autocatalytic liberation of 10 kDa (P10) and 20 kDa (P20) fragments from a 50 kDa pro-enzyme (Madeo, Herker et al. 2002). In response to H_2O_2, *S. cerevisiae* are reported to undergo PCD with markers of apoptosis including TUNEL positive nuclei, chromatin condensation, phosphatidylserine exposure, caspase-like proteolytic activity and cytosolic accumulation of ROS (Madeo, Herker et al. 2002;

Khan, Chock et al. 2005). H_2O_2 induced PCD does not occur in the metacaspase knockout strain (*Δyca1*), the C297A catalytic inactivation mutant or in wild-type cells pre-treated with the pan-caspase inhibitor zVAD. These observations demonstrated a requirement for YCA1-dependent proteolytic activity and canonical caspase-like protease activity for progression of the apoptotic phenotype in yeast. Lysates from a strain over-expressing YCA1 co-treated with H_2O_2 displayed elevated caspase-8 and -6 like tetrapeptide affinity (Madeo, Herker et al. 2002) which suggested YCA1 was responsible for the observed caspase-like substrate specificity during H_2O_2 induced PCD; however, recombinant YCA1 expressed in *E. coli* did not have affinity for aspartate containing peptides *in vitro* but instead cleaved arginine and (to a lesser extent) lysine containing substrates similar to other members of the metacaspase family (Watanabe and Lam 2005).

YCA1 is a type-I metacaspase which is typified by an N-terminal pro-domain. Pro-domains of caspases generally contain DED and CARD domains which facilitate binding of the caspase with death adaptors and receptor complexes. The YCA1 pro-domain does not contain these structures but is instead rich in poly-Q/N repeats, a motif predicted to have prion-like function (Alberti, Halfmann et al. 2009). Indeed, when this region was fused to a truncation of the SUP35 prion lacking its own prion domain a new hybrid prion was formed (Nemecek, Nakayashiki et al. 2009). The prion domain of YCA1 is a feature which is likely to promote protein interactions, like the CARD and DED domains of animal caspases, targeting the metacaspase to regulatory structures or possibly even to substrates.

It has been repeatedly demonstrated that metacaspases are capable of influencing apoptotic phenotypes in plants, fungi and protozoa. The yeast metacaspase YCA1 has received particular attention for its contribution to yeast PCD. In a general context, YCA1 has a semblance of most caspase features. However, the actual substrate affinity of YCA1 is debatable. YCA1 is associated with VEIDase and IETDase proteolytic activity *in vivo* that contrast with its *in vitro* affinity (Madeo, Herker et al. 2002; Watanabe and Lam 2005; Guaragnella, Bobba et al. 2009). Intriguingly, a VEIDase activity that is required for cell death during plant embryogenesis in the Norway spruce is metacaspase dependent, yet mcII-Pa also has affinity for arginine/lysine containing peptides *in vitro* (Bozhkov, Filonova et al. 2004; Suarez, Filonova et al. 2004). In both of these cases canonical caspase peptide inhibitors (zVAD, IETD and VEID) mimic metacaspase knockout and catalytic inactivation mutants by inhibiting their capacity to undergo programmed cell death. While metacaspases share structural and regulatory similarities with mammalian caspases they may yet function upstream of another undetermined protease with caspase-like activity. It may alternatively suggest that the *in vivo* affinity of metacaspases is mediated by other cofactors that arbitrate substrate presentation or alter metacaspase conformation/specificity.

1.2 Capsase signalling pathways

Caspases are central components of the molecular signaling pathway of apoptosis. There are four known caspase dependent signaling pathways that result in apoptosis. The predominant pathways are the extrinsic receptor mediated pathway and the intrinsic mitochondria dependent pathway (Leist and Jaattela 2001). Additionally, caspases of the major pathways can be impinged on and activated via granule mediated delivery of

granzyme B (Talanian, Yang et al. 1997) and the ER stress pathways (Hitomi, Katayama et al. 2004).

The simplified extrinsic apoptotic pathway is triggered by the binding of a transmembrane death receptor such as TNF-1 receptor, TRAIL receptor or FAS (CD95) with its ligand (TNF, TRAIL and FasL respectively) (Pitti, Marsters et al. 1996). Receptor-ligand interactions promote the clustering and trimerization of the receptor with cytoplasmic adaptor proteins containing death domains, such as FADD, RIP and Daxx which then recruit initiator caspases (caspases-8 and caspase-10) forming the death inducing signaling complex (DISC). Initiator caspases are activated at the DISC through proximity-induced autocatalysis (Baker and Reddy 1998). Activated initiator caspases perpetuate the apoptotic program either through direct cleavage of downstream effector caspases (caspase-3, -6, -7) (Stennicke, Jurgensmeier et al. 1998; Boatright and Salvesen 2003) or through modulation of the intrinsic pathway via proteolytic activation of the pro-apoptotic BCL-2-family member BID (Bossy-Wetzel and Green 1999).

The second major pathway of apoptosis is the intrinsic mitochondrial pathway which is influenced by both positive and negative signals. The BCL-2-family of proteins contains both pro-apoptotic and anti-apoptotic counterparts that influence the integrity of the mitochondrial membrane (Korsmeyer, Shutter et al. 1993). Stress induced activation of the pro-apoptotic BCL-2 members, such as BAX, BAD and tBID, open the mitochondrial Permeability Transition Pore (PTP) and the mitochondrial apoptosis-induced channel (MAC) resulting in eventual mitochondrial depolarization (Hirsch, Marzo et al. 1997; Kinnally and Antonsson 2007). Alterations to the PTP and MAC promote the release of apoptotic signalling molecules such as apoptosis inducing factor

(AIF), cytochrome C (CytC), EndoG and ROS/Ca^{2+} from mitochondria. CytC promotes downstream caspase activation by binding APAF-1 and pro-caspase-9 to form the apoptosome, an efficient processing plant for activating caspase-9 (Li, Nijhawan et al. 1997). Processed caspase-9 then regulates the activity of downstream effector caspases (Kuida, Haydar et al. 1998) culminating in an apoptotic fate.

The pathways that contribute to completion of PCD are relative to the speed of the individual pathways that are provoked. Stimulation of the same receptor may lead to different morphological outcomes depending on the environmental and intracellular circumstances (Vandenabeele, Vanden Berghe et al. 2006). For example in the absence of sufficient caspase activity TNF can induce an apoptotic fate mediated by cathepsin-b in human primary tumors (Foghsgaard, Wissing et al. 2001). Extrinsic death receptor mediated apoptosis commonly results in activation of the mitochondrial pathway by cross-communication through the BCL-2-family of proteins (Basu, Castle et al. 2006). Similarly, the apoptosome can activate initiator caspases in the absence of a death-receptor bound ligand (Bao and Shi 2007). As such, observation of caspase activity during PCD does not necessarily identify the general intrinsic or extrinsic pathways as the initiating cue for death.

1.3 Apoptotic cell death

All things living are destined to an eventual death; however, the timing and specific type of cell death are variable, dependent on the age, function and environment of the cell. Cell death falls within the two general categories of necrosis and apoptotic PCD. Necrotic cell death is a passive or accidental phenotype that is characterized by loss of cell membrane integrity in response to inappropriate signalling or acute

injury/challenges. Necrosis is typified by cellular lysis which exposes surrounding cells and tissue to signalling molecules, lytic enzymes and/or reactive oxygen species (ROS). Exposure to these factors can propagate a necrotic fate to neighbouring cells advancing an inflammatory response in affected tissue. Apoptosis is an orchestrated form of PCD whereby a damaged or dying cell actively deconstructs/packages itself in both an energy dependent and non-inflammatory manner. The physical characteristics of apoptotic cells were first described in mammalian systems by Kerr, Wyllie and Currie in 1972 (Kerr, Wyllie et al. 1972). The morphology of apoptosis is the primary factor distinguishing it from necrotic cell death and autophagy, an arguable form of programmed cell death (Levine and Yuan 2005; Madeo, Eisenberg et al. 2009). The molecular pathways and signals that regulate apoptosis are broadly studied; however, various other forms of programmed and accidental cell death share morphological hallmarks and have stimulated much debate on the specific requirements for an accurate diagnosis of apoptotic death (Kroemer, El-Deiry et al. 2005).

In the presence of an apoptogenic cue or insult a complex signaling network is initiated that induces a predictable morphology in affected cells. Under transmission electron microscopy (TEM) apoptotic cells shrink, become rounded with eosinophilic cytoplasm, their cell membrane blebs (zeiosis), chromatin condenses into compact geometric crescent shapes (at the nuclear periphery) and cells decompose into apoptotic bodies with intact membranes (Leist and Jaattela 2001). Phosphatidylserine (PS) is a membrane phospholipid that is asymmetrically distributed on the inner leaflet of the membrane bilayer. During apoptosis affected cells rapidly translocate PS to the outer leaflet where it can be detected by Annexin V (Fadok, Voelker et al. 1992; Vermes,

Haanen et al. 1995). Exposed PS on cells and apoptotic bodies then serve as an attractant for scavenging and destruction by phagocytosis, thereby limiting any excess inflammatory response (Fadok, Voelker et al. 1992).

Substantial caspase activity is commonly regarded as the point of no return in the decision to engage apoptosis (Boatright and Salvesen 2003). Active caspases can be detected via antibodies or with fluorogenic caspase substrates. Caspase mediated degradation of ICAD, the inhibitor of the cytoplasmic endonuclease CAD (caspase activated DNAse) promotes the degradation of chromosomal DNA in linker regions between nucleosomes (Liu, Zou et al. 1997). A DNA ladder is formed (DNA fragments of 200 base pair multiples) when the nucleic content of apoptotic cells is resolved by agarose gel electrophoresis (Duke, Chervenak et al. 1983). Caspases also target numerous cytosolic and nuclear protein substrates in apoptotic cells resulting in the eventual destabilization of DNA repair machinery and the nuclear-cytoplasmic barrier (Faleiro and Lazebnik 2000). The strictest definition of apoptosis requires activation of members of the caspase family of proteases.

Mitochondrial outer membrane permeability (MOMP) contributes to the intrinsic mitochondrial death pathway and promotes apoptosis in response to DNA damaging radiation, ROS, or toxins. MOMP permits the release of several mitochondrial factors in apoptotic cells. Mitochondrial CytC is released to the cytosol during MOMP contributing to downstream apoptosome formation and caspase activation. Accordingly, cytoplasmic localization of CytC and ROS are used as markers of apoptosis. In addition to CytC and ROS, other competing factors are released from mitochondria during MOMP that can contribute to apoptosis-like death without the requirement for caspase activity. One form

of caspase-independent apoptosis is mediated by release of AIF from mitochondria. Unconfined AIF rapidly translocates from the mitochondria to the nucleus inducing the compaction of chromatin upon release and apoptosis-like death during murine embryogenesis (Susin, Lorenzo et al. 1999; Joza, Susin et al. 2001). Similarly, the mitochondrial endonuclease EndoG is released, stimulating nucleosomal DNA fragmentation and again encouraging death in a caspase-independent manner (Li, Luo et al. 2001). As such, caspase inhibition under some circumstances may not preclude death but rather just delay an apoptosis-like fate (Chipuk and Green 2005) or promote completely different death pathways (Vandenabeele, Vanden Berghe et al. 2006).

The multitude of apoptotic markers underpins the requirement for distinct criteria to diagnose apoptosis. Aside from recognizing the morphological properties, multiple biochemical observations are used to distinguish actual apoptosis from other forms of cell death such as apoptosis-like PCD which commonly results in a necrotic fate (Leist and Jaattela 2001). Furthermore the finding that apoptosis can occur in the absence of one or more of the morphological and biochemical hallmarks has complicated the interpretation of experimental observations. The Nomenclature Committee on Cell Death [NCCD] has made recommendations to clarify the requirements for apoptosis. Specifically they recognize that apoptosis can occur in the absence of a DNA ladder. As such, DNA laddering is not an absolute requirement to distinguish apoptosis (Kroemer, El-Deiry et al. 2005). Moreover, the NCCD recognizes the existence of caspase-independent apoptosis. Thus 'caspase activity' has been partially separated from the canon of 'apoptosis' even though caspase activity is still considered to be a hallmark apoptotic feature.

1.4 Caspases and cell fate decisions

Caspase activity is requisite for the completion of apoptotic PCD which, in turn, promotes organism fitness. Caspase dependent PCD contributes to the patterning of developing organisms and homeostatic maintenance in adult organisms. In this capacity, deregulation of apoptosis contributes to multiple pathological states. However, the benefits of caspase activity to the organism do not lie exclusively in their ability to cull unnecessary or damaged cells. Caspase activity also promotes proliferation and differentiation of individual progenitor cells in the absence of cell death triggers (Kennedy, Kataoka et al. 1999; Gilot, Serandour et al. 2005; Fernando and Megeney 2007). Together, these observations argue that the caspase family is a mediator of larger cell fate decisions.

Caspase dependent apoptosis has positive roles during development and growth as demonstrated in developing nematode *C. Elegans* where caspase dependent PCD limits the number of somatic cells (Sulston, Schierenberg et al. 1983; Yuan, Shaham et al. 1993). Similarly, apoptosis is a fundamental process in the formation of hollow organ lumen in other metazoans (Jacobson, Weil et al. 1997). For example, caspase-8 null mice are embryonic lethal with impaired heart development (Varfolomeev, Schuchmann et al. 1998). Indeed, caspase dependent apoptosis contributes to the patterning of the outflow tract, valve and atrial septum of the developing heart (Fisher, Langille et al. 2000). PCD also patterns at the organism level by the removal of vestigial structures during development. For example, fetal digitation requires the removal of the inter-digit webbing by an apoptotic process (Zuzarte-Luis and Hurle 2005). In the maintenance of tissue homeostasis apoptosis is the counterpart to mitosis, ensuring that an organ does not

become overpopulated with cells (Wilson, Close et al. 2000). Apoptotic processes play a pivotal role in cell restriction and sculpting of developing tissue.

Based on these observations it is not surprising that deregulation of caspase dependent apoptosis is also a central mechanism that advances pathological states in adult organisms. For example, premature apoptosis is a key factor in neurodegenerative diseases such as Alzheimer's disease, Parkinson's disease and Huntington's disease (Desjardins and Ledoux 1998). Impaired apoptosis exacerbates the pathology of cancerous tumours. Here the capability of a cancer cell to continue proliferating is not countered by the capacity to die in a controlled fashion (Itoh, Semba et al. 2002). To this effect, failure to undergo anoikis (an apoptotic fate upon detachment from the cell matrix) is fundamental in metastasis, a mechanism that facilitates the transport of cancer cells through the circulatory system to distal locations (Grossmann 2002). Furthermore, chronological ageing of cells is concomitant with build up of potentially damaging ROS, a by-product of mitochondrial respiration which predisposes older cells to apoptosis. Thus, apoptosis can protect surrounding cells from secondary injury and inflammation resulting from exposure to ROS or lysosomal enzymes from the lysate of an aged cell. Together, these examples demonstrate that caspase dependent apoptosis influences the fate of organs/tissues in the developing and adult organism.

Beyond the benefits of a caspase dependent programmed cell death pathway to the larger organism, caspase activity also promotes non-apoptotic processes influencing the fate of individual cells. Enucleation is a final step in the terminal differentiation of lens fibre epithelial cells, keratinocytes and erythrocytes which requires the enzymatic activity of caspase-3 (Ishizaki, Jacobson et al. 1998; Weil, Raff et al. 1999; Zermati,

Garrido et al. 2001). Transient caspase-3 activation and cleavage of the Mammalian Sterile Twenty-like Kinase (MST1) is requisite for the timely differentiation of skeletal myoblasts (Fernando, Kelly et al. 2002). A similar temporary pulse of caspase-3 activity promotes the completion of neuronal differentiation after neuronal specification in a murine neurosphere model (Fernando, Brunette et al. 2005). These observations suggest that caspase targeted therapies intended to reduce apoptotic death resulting from acute neuromuscular damage may also markedly impair the eventual re-growth and repair of damaged tissue.

Delayed ossification and reduced bone mineral density were also observed in caspase-3 deficient heterozygous mice. Caspase-3 inhibited explants of bone marrow stromal stem cells have a decreased osteogenic potential (Miura, Chen et al. 2004). Similarly, caspases -2, -3 and -8 inhibited osteoblasts were incapable of entering the G0 quiescent state in response to BMP-4 induced osteoblastic differentiation (Mogi and Togari 2003). These results strongly implicate caspase function with bone formation and remodelling, a function which comes with a strong caveat against the clinical administration of caspase inhibitors due to a likely contribution to the development of osteoporosis in post-menopausal women (Miura, Chen et al. 2004).

Finally, caspase activity functions in proliferation and the mitotic cell cycle. To this effect, caspase-8 activity is required for activation and rapid proliferation of T lymphocytes (Alam, Cohen et al. 1999; Kennedy, Kataoka et al. 1999; Bell, Leverrier et al. 2008). Similarly, Caspase-3 alters the timing of mitotic checkpoint of HeLa and human hepatoma cell lines (Kim, Murphy et al. 2005; Hsu, Yu et al. 2006). Collectively,

these results demonstrate that caspase activity promotes proliferation in addition to differentiation independent of apoptotic outcomes.

Apoptosis, differentiation and division represent the major bifurcation points requiring complete commitment to an irreversible fate. These distinct endpoints require massive morphological changes resulting from large-scale cytoskeletal, phospholipid and chromatin remodelling events. Dividing cells must carefully duplicate and distribute templates and cellular material to their soon-to-be independent progeny. Differentiating cells undergo massive alterations adopting the conformation of their committed lineage; sometimes requiring multiple fusion events as is the case in the formation of mature multinucleate myofibers. Finally, dying cells effectively package themselves into consumable packets in an organized and timely manner. Together, caspase activity is apparent and required during times of extreme morphological change, suggesting that caspases may contribute to these fates as a necessary remodelling factor (Fernando and Megeney 2007). Similarly, these observations demonstrate that caspase enzymatic activity is required for altering cell fate in general.

1.5 Yeast cell death and YCA1

S. cerevisiae is a tractable model system with a fully sequenced genome that has contributed to our understanding of many fundamental cell mechanisms. Expression of various apoptotic mediators in yeast has elucidated their regulation and their ability to promote apoptosis-like cell death in yeast. Heterologous expression of caspase-like proteases promotes apoptosis and can complement the apoptotic capacity of caspase deficient yeast. Yeast apoptosis can be initiated by numerous environmental stresses which generally promote cell death in a metacaspase dependent manner. Additionally,

aged cells and compromised cells that are incapable of mating may be specifically targeted to undergo apoptosis to promote population fitness.

Expression of exogenous apoptotic regulators in yeast has revealed novel interactions and protein function. For example, cytosolic interaction between the DED domain of RIP and the FAS receptor were discovered in yeast by Y2H (Stanger, Leder et al. 1995). Functional studies of the dimerization and physical interactions between BCL-2-family members have exposed the mechanisms of their influence on mitochondrial permeability in the yeast model (Sato, Hanada et al. 1994; Sedlak, Oltvai et al. 1995; Gross, Jockel et al. 1998). Specifically, expression of the pro-apoptotic BCL-2-family member, BAX, has a lethal effect in budding yeast which is dependent on respirative metabolism and is corrected by co-expression of anti-apoptotic BCL-2, BCL-xl and BI-1 (Hanada, Aime-Sempe et al. 1995; Greenhalf, Stephan et al. 1996; Matsuyama, Schendel et al. 1998; Xu and Reed 1998). BAX expression in yeast encourages the release of CytC and ROS from a mitochondrial pore (Manon, Chaudhuri et al. 1997; Shimizu, Narita et al. 1999) and the concomitant death is accompanied by markers of apoptosis (Ligr, Madeo et al. 1998). Expression of pro-apoptotic tBID in yeast is similarly toxic, however, tBID and BAX induced lethality are independent of YCA1 (Guscetti, Nath et al. 2005). Consistent with mammalian PCD, other mitochondrial factors are released in yeast with compromised mitochondrial membranes which can influence PCD. In response to apoptogenic insults, or during ageing, the yeast AIF homologue (AIF1) is released from mitochondria and translocates to the nucleus where it promotes DNA degradation and death (Wissing, Ludovico et al. 2004). The death resulting from AIF1 is potentiated by YCA1 but death will still occur in its absence. In similar conditions the EndoG

homologue, NUC1, translocates from mitochondria promoting apoptosis-like death independent of YCA1 and AIF1 (Buttner, Eisenberg et al. 2007). These findings argue that the molecular machinery capable of promoting lethality downstream of mitochondrial depolarization is conserved in yeast. The resulting death can be either YCA1 dependent or independent.

Yeast strains expressing various genes encoding for caspases and metacaspases were developed to study their autocatalytic regulation and contribution to yeast cell death. Heterologous expression of initiator caspases -8 and -10 in yeast results in autocatalytic processing of the zymogens into their mature form. Moreover, caspase-8 expression in yeast is cytotoxic and can be abrogated by mutating the active cysteine or by co-expressing the pan-caspase inhibitor p35 (Kang, Schaber et al. 1999). Co-expression of the 17 and 10 kDa catalytic fragments of caspase-3 in yeast resulted in dose dependent inhibition of cell growth but does not result in cytotoxicity (Wright, Han et al. 1999). The roles of more evolutionarily distant caspases and apoptotic proteins have also been examined in yeast. Expression of the *C. elegans* orthologue of caspase-3 (CED-3) promotes death in budding yeast (Jabbour, Ho et al. 2004). Similar toxicity after expression of CED-4 (APAF-1 in mammals) in *S. cerevisiae* (Tao, Walke et al. 1999) mimics observations in *S. pombe* where further apoptotic markers such as chromatin condensation have been noted (James, Gschmeissner et al. 1997). Death associated with expression of CED-4, an adaptor protein seems curious but might suggest that APAF-1 may also support a caspase independent form of cell death.

Finally, metacaspases from plants and protozoa have been observed to functionally complement oxidative stress induced apoptosis in the metacaspase deletion

yeast strain *Δyca1*. Type-I and type-II metacaspases of *A. thaliana* (AtMCP-1b and AtMCP-2b) promote death in *Δyca1* with cytosolic accumulation of ROS and TUNEL positive nuclei (Watanabe and Lam 2005). This apoptosis-like death is prevented by co-treatment with the pan-caspase inhibitor zVAD. The *L. major* metacaspase LmjMCA is autoprocessed and promotes death with externalization of PS in metacaspase deficient yeast (Gonzalez, Desponds et al. 2007). The *T. brucei* metacaspase promotes clonal death in *Δyca1* cells by impairing respirative competency (Szallies, Kubata et al. 2002). Heterologous expression of metacaspases complements the apoptosis-like process promoted by oxidative stress in YCA1-deficient yeast. However, the cytotoxic effects of mammalian and nematode caspases in yeast appear without additional stresses and may be due to rupture of the nuclear/plasma membranes independent of YCA1 and AIF1 (Puryer and Hawkins 2006).

Yeast is an adaptive organism that is capable of survival in many environments. Fermentive growth would naturally occur in the acidic environment of a fruit yet in the exclusive presence of a non-fermentable carbon source yeast can grow by respirative metabolism. It is therefore unexpected that an adaptive organism would readily engage PCD in response to environmental challenges. Hydrogen peroxide is a thoroughly established promoter of YCA1 dependent PCD with most apoptotic markers in yeast (Madeo, Frohlich et al. 1999; Madeo, Herker et al. 2002; Khan, Chock et al. 2005). The presence of some organic acids such as acetic acid can similarly provoke an apoptotic fate with the requirement for YCA1, CytC and ROS (Mazzoni, Herker et al. 2005; Guaragnella, Bobba et al. 2009). Exposure to hypochlorous acid promotes apoptosis-like death in yeast but the involvement of YCA1 in this process is currently unknown (King,

Hannum et al. 2004). Apoptosis in these cells is not simply the result of an acidic environment as yeast readily grow in media acidified with inorganic acids such as hydrochloric acid (Giannattasio, Guaragnella et al. 2005). Ion disequilibrium induced by high concentration of salt also produces an apoptotic phenotype that can be rescued by ectopic expression of anti-apoptotic BCL-2 (Huh, Damsz et al. 2002). Yeast are a robust organism that can promptly enter a G0-like quiescence in the absence of nutrients (Granot and Snyder 1993). Counter intuitively, in the absence of other nutrients and the presence of glucose yeast rapidly produce ROS and die with apoptotic morphology known as glucose induced cell death (GICD). GICD is dependent on both YCA1 and CytC (Granot, Levine et al. 2003; Silva, Sotoca et al. 2005). Yeast cells that are unable to phosphorylate hexose are resistant to GICD suggesting that the actual cause of death is a metabolic byproduct rather than the glucose itself (Granot and Dai 1997).

Yeast apoptosis can also be initiated by the presence of competing organisms or by host defense mechanisms. For example, killer yeast strains bear cytoplasm inherited double stranded RNA viruses that can be used to competitively kill foreign yeasts by means of toxin secretion (Schmitt and Breinig 2006). These killer yeasts are immune to the toxins they secrete. When exposed to low concentrations of the toxin, sensitive strains accumulate ROS which act as a trigger for YCA1 mediated apoptosis (Reiter, Herker et al. 2005). Similarly, osmotin is an anti-fungal protein/peptide produced in plants that acts as a host defense against microbial growth. It has been demonstrated that osmotin is able to promote apoptosis in *S. cerevisiae* by suppressing the RAS/cAMP metabolic/stress response pathway and stimulating ROS production (Narasimhan, Damsz et al. 2001).

Together these data demonstrate that some organisms have evolved mechanisms that impinge on the apoptotic pathway of yeast.

There is also limited evidence that apoptosis can be induced via physiological situations relevant to the natural course of yeast life. Interestingly, in the presence of large amounts of mating pheromone and the absence of a mating partner, yeast cells die with accumulated ROS, PS exposure and chromatin compaction (Severin and Hyman 2002). This reaction has been regarded as an apoptotic failsafe whereby cells that are unable to mate are removed from the gene pool to prevent asexual propagation of a sterile genome. Apoptotic markers accompany pheromone induced death, however, the actual mode of death arguably results from multiple YCA1-independent waves of necrosis (Zhang, Dudgeon et al. 2006). Aged yeast cells accumulate cytosolic ROS and are predisposed to an apoptotic fate. In addition to chronological age (lifespan during the post-diauxic shift/stationary phase) relating to the deterioration of a cell over time, yeast also age in a replicative context. The replicative age of a yeast cell is the number of asymmetric divisions that the particular cell has undergone. Both replicative and chronological aged yeast display typical markers of apoptosis marked by the time dependent accumulation of ROS possibly due to retention of inferior mitochondria during division (Laun, Pichova et al. 2001; Fabrizio, Battistella et al. 2004; Herker, Jungwirth et al. 2004). Aging *Δyca1* cells have a short overall gain in life expectancy; however, wild-type cells tend to overgrow disruptants in competitive growth assays. Furthermore, caspase deficient yeast are completely incapable of re-growth after long pre-culturing periods (Herker, Jungwirth et al. 2004). This is a perplexing finding suggesting that the influence of YCA1 may not be exclusive to death.

Yeast does not express direct homologues to known death receptors or BCL-2 family regulators of MOMP during cell death; however, many stresses that induce cytosolic accumulation of ROS also promote YCA1 dependent apoptotic death (Mazzoni and Falcone 2008). The methods by which YCA1 promotes PCD remain obscure as YCA1 has no known substrates. Being the only yeast metacaspase, it is possible that YCA1 may act both upstream and downstream of mitochondrial death pathways. However, the regulation of YCA1 dependent PCD generally appears to be ROS dependent suggesting that the role for YCA1 mediated death is downstream of mitochondrial and oxidative stress. Much like its mammalian counterpart, the apoptosis-like phenotype in yeast can be either YCA1-dependent or –independent. Similarly numerous apoptogens are able to generate a *mostly* apoptotic morphology whereby death occurs in the presence of most, but not all, morphological hallmarks.

1.6 Motivation

S. cerevisiae appear to have the molecular machinery required to commit to a metacaspase dependent apoptotic fate; however, the concept of metacaspase-dependent PCD has been met with considerable controversy (Vercammen, Declercq et al. 2007). The discovery of the metacaspase family in plants, protozoa and fungi supports the argument that the apoptotic program originated as early as single-celled organisms. While metacaspase-dependent apoptosis benefits metazoans and plants by coordinating embryonic patterning (Bozhkov, Filonova et al. 2004), a metacaspase dependent death program does not provide a similar advantage to single-celled fungi and protozoa. In this regard it is not clear what selective pressure would promote the retention of a death-specific pathway, and indeed the caspase family, from single celled eukaryotes to

vertebrate and invertebrate animals. In yeast, metacaspase-dependent death is argued to result from altruistic roots whereby an aged or defective cell will preferentially die in stress conditions to feed and thus preserve its nearby progeny in a colony. However, one must then ask how the apoptotic morphology would benefit the colony more than an autophagic or necrotic fate.

Development and adult life of metazoan organisms requires the multi-faceted influence of apoptosis (Jacobson, Weil et al. 1997), but what is the advantage of an autonomous cell death program to a single celled eukaryote? Most arguments to this point discuss the growth of yeast as an organism-like colony even though yeast growth is optimal in liquid-phase. Yeast apoptosis has been described as an altruistic system whereby a ROS damaged cell can rapidly cease its metabolic function and die thus preserving scarce nutrients (Frohlich and Madeo 2000). Aged yeast cells accumulate ROS. In the absence of nutrients and in the presence of glucose these older cells may rapidly apoptose distributing scarce amino acids to the younger population. One experiment demonstrated the advantage of death in a colony whereby removal of the older cells in the central region of a yeast colony reduced the longevity of the younger cells in the margin of the colony (Vachova and Palkova 2005). This suggested that the dying/aged cells promote colony life in the younger periphery. The second major argument considers apoptosis induced by mating pheromone. Here the death of cells that are unable to mate is encouraged in order to prevent wasting nutrients on a sterile genome. It is similarly argued as a mechanism to favour the diploid state and promote evacuation by sporulation in the absence of nutrients (Severin and Hyman 2002; Knorre, Smirnova et al. 2005; Buttner, Eisenberg et al. 2006). While this is an intriguing

hypothesis the resulting death has since been demonstrated to be YCA1-independent and is debatably necrotic (Zhang, Dudgeon et al. 2006). It is thus an unconvincing argument to explain the retention of metacaspase-dependent PCD pathways.

The 'colony as an organism' suggests that altruistic preservation of younger isogenic descendents benefits the greater population of the colony; yet, it is still unclear why the apoptotic morphology is the favoured form of death in these conditions. For example, exposure of PS ensures the rapid removal of apoptotic cells and apoptotic bodies by macrophages. Given that this is requirement for non-inflammatory cell death, what purpose does PS exposure fulfill in a yeast colony or suspension? Does it recruit wandering phagocytic cells to a damaged colony to clean up the potentially damaging detritus? How is membrane exposure of PS detected by nearby cells when the yeast membrane is enclosed by a cell wall? Similarly, would lysis not serve an efficient distribution mechanism to feed nearby cells in the absence of nutrients? Many of the proposed hypotheses loosely argue the minutiae of yeast population dynamics; however, no single model has been generally accepted. This is likely to be due to the exceptional importance of cell removal in metazoan organisms during development and disease that is not reflected in yeast.

Non-death functions of the caspase family at the cell level have been demonstrated in vertebrate and invertebrate animals; however, the discovery of metacaspases in plants, fungi and protozoa has promoted investigations biased to apoptotic regulation in these systems. The function of YCA1 has been exclusively examined in response to death inducing chemical and genetic insults. These are commonly non-physiological insults yeast would not encounter in natural conditions such

as H_2O_2, valproic acid and ectopic protein expression (Mitsui, Nakagawa et al. 2005). However, limited evidence exists demonstrating that metacaspases may also influence cell fate independent of death. Particularly, expression of the *L. major* metacaspase LmjMCA is tightly regulated and required for proliferation where its deletion is lethal and its over-expression results in aneuploidy (Ambit, Fasel et al. 2008). Similarly, deletion of the two *Aspergillus fumigatis* metacaspases results in a growth detriment in conditions of ER stress (Richie, Miley et al. 2007). These observations suggest that non-death functions of caspases may be similarly conserved from metacaspases.

Overall, yeast apoptosis is clearly not identical to that of mammalian models. The complete absence of death receptors and ligands punctuates this fact. However, the individual pathways involved with yeast apoptosis do bear striking similarity to their mammalian counterparts. Central to these is the yeast caspase YCA1. A substantial hurdle to the use of yeast as an evolutionary model of caspase-dependent apoptosis is defining why it exists and how it can benefit a unicellular organism; an obstacle which may be addressed by examining non-apoptotic metacaspase function. Furthermore, the non-apoptotic molecular pathways that mammalian caspases contribute are relatively uncharacterized. In this context examination of the yeast metacaspase in non-apoptotic conditions might contribute to our understanding of non-death molecular pathways that caspases regulate in higher eukaryotes.

1.7 Hypothesis and objective

The yeast metacaspase YCA1 has been characterized as an ancestral caspase functioning as a conserved apoptotic regulator in yeast. However, it is unclear why an apoptotic protease would be conserved from a single celled organism where a death-centric pathway offers no clear benefit to the organism. Alternatively, we hypothesize that the yeast metacaspase YCA1 contributes to non-apoptotic functions that promote yeast fitness and proliferation.

Objective: Use a systems-level approach to investigate the yeast metacaspase YCA1 during log-phase growth conditions and characterize its functions in a non-apoptotic context.

CHAPTER 2

A Non-death Role of the Yeast Metacaspase: YCA1 Alters Cell Cycle Dynamics

2.1 Manuscript

A Non-death Role of the Yeast Metacaspase: YCA1 Alters Cell Cycle Dynamics

Robin E. C. Lee[2, 1], Lawrence G. Puente[1], Mads Kærn[3, 2, 4] and Lynn A. Megeney[1, 2, 3,*]

1. Regenerative Medicine Program,
   Ottawa Health Research Institute,
   Sprott Centre for Stem Cell Research,
   Ottawa, Canada

2. Department of Cellular and Molecular Medicine,
   University of Ottawa,
   Ottawa, Canada

3. Ottawa Institute of Systems Biology,
   University of Ottawa,
   Ottawa, Canada

4. Department of Physics,
   University of Ottawa,
   Ottawa, Canada

* To whom correspondence should be addressed.
  Email: lmegeney@ohri.ca
  Mail box 511
  501 Smyth Rd
  Ottawa, Ontario, Canada
  K1H8L6
  Phone: 613 737 8618

2.1.1 Author Contributions and Manuscript Information:

RECL: Designed the study, performed experiments, analyzed the data and wrote the manuscript.

LGP: Designed experiments, performed experiments, analyzed data and wrote the manuscript.

MK: Designed experiments and contributed materials.

LAM: Designed the study, contributed materials and wrote the manuscript.

This research was originally published in PLoS ONE. Lee REC, Puente LG, Kærn M, Megeney LA (2008) A Non-Death Role of the Yeast Metacaspase: Yca1p Alters Cell Cycle Dynamics. PLoS ONE 3(8): e2956. doi:10.1371/journal.pone.0002956

2.1.2 Abstract

Caspase proteases are a conserved protein family predominantly known for engaging and executing apoptotic cell death. Nevertheless, in higher eukaryotes, caspases also influence a variety of cell behaviors including differentiation, proliferation and growth control. *S. cerevisiae* expresses a primordial caspase, *yca1*, and exhibits apoptosis-like death under certain stresses; however, the benefit of a dedicated death program to single cell organisms is controversial. In the absence of a clear rationale to justify the evolutionary retention of a death only pathway, we hypothesize that *yca1* also influences non-apoptotic events. We report that genetic ablation and/or catalytic inactivation of YCA1 leads to a longer G1/S transition accompanied by slower growth in fermentation conditions. Downregulation of YCA1 proteolytic activity also results in failure to arrest during nocodazole treatment, indicating that YCA1 participates in the G2/M mitotic checkpoint. 20s proteasome activity and ROS staining of the *Δyca1* strain is indistinguishable from its isogenic control suggesting that putative regulation of the oxidative stress response by YCA1 does not instigate the cell cycle phenotype. Our results demonstrate multiple non-death roles for *yca1* in the cell cycle.

2.1.3 Introduction

The timely and organized form of programmed cell death known as apoptosis has vital functions in the development and pathologies of complex metazoan life forms. Apoptosis is regulated by conserved signaling pathways that activate caspase proteases leading to target protein cleavage and cell death. Morphological features typical of apoptosis have been recognized in single cell organisms and structural homologues of the caspase family (metacaspases) have been identified (Madeo, Frohlich et al. 1999; Uren, O'Rourke et al. 2000; Kroemer, El-Deiry et al. 2005). Metacaspase proteases have since been characterized as apoptotic regulators in plants, fungi and protozoa supporting the concept of a widely conserved cell death pathway (Madeo, Herker et al. 2002; Watanabe and Lam 2005).

A single metacaspase, YOR197w, was identified in the genome of *S. cerevisiae* and named Yeast Caspase 1, (YCA1 also known as MCA1). YCA1 demonstrates enzymatic peptidase activity analogous to mammalian caspase activity, and is inhibited in the presence of the fluoromethyl ketone (FMK) conjugated caspase-inhibitory substrate z-VAD-FMK (Madeo, Herker et al. 2002). In addition to canonical caspase substrate specificity YCA1 has secondary substrate specificity directed at arginine-lysine motifs (Watanabe and Lam 2005). Furthermore, YCA1-mediated apoptosis has been observed in a variety of apoptogenic situations including senescence and following insults such as hydrogen peroxide (H_2O_2) and acetic acid (Madeo, Herker et al. 2002; Khan, Chock et al. 2005; Buttner, Eisenberg et al. 2006; Guaragnella, Pereira et al. 2006; Frohlich, Fussi et al. 2007). These findings have promoted the view of yeast as an evolutionarily distant

model of metazoan apoptosis and numerous orthologous pathways have since been reported.

Despite the discovery of homologues to apoptotic proteins in yeast, there was limited consensus that yeast engaged a death program similar to that of multi-cellular metazoans. Arguments to rationalize apoptosis in yeast have included altruism in the presence of reactive oxygen species or killer toxins, a program to execute cells that fail to mate in response to pheromone and a mechanism for lateral gene transfer (Frohlich and Madeo 2000; Severin and Hyman 2002; Buttner, Eisenberg et al. 2006; Koren 2006). In addition, the apoptotic pathway in yeast has been suggested to act as a mechanism to protect surrounding cells from the potentially damaging cellular constituents of dead or dying cells (Vachova and Palkova 2007). However, the validity of these hypotheses has yet to be fully explored and may not justify the development and retention of a biochemical pathway devoted solely to cell death. Without an incontrovertible justification for an apoptotic response in yeast, it is also reasonable to conjecture that proteins such as YCA1 may have initially developed or co-evolved other vital non-death functions (Fernando, Kelly et al. 2002; Fernando and Megeney 2007).

Caspase activity is an inductive signal for non-death functions such as cell cycle progression, proliferation, cell migration and differentiation in mammalian cell lines (Fernando and Megeney 2007; Li, Brieher et al. 2007). Enzymatic processing of target proteins by caspase-3 at key time points promotes differentiation in mammalian precursor and progenitor cells (Fernando, Kelly et al. 2002; Fernando, Brunette et al. 2005). The enzymatic activity of caspases has also been associated with the proper activation and release from the mitotic checkpoint. In HeLa cells, disruption of microtubule dynamics

results in caspase mediated cleavage of the mitotic checkpoint protein BUBR1, augmenting the duration of mitosis (Kim, Murphy et al. 2005). Similarly, inhibition of caspase activity in human hepatoma cells causes the failure of metaphase arrest in the presence of microtubule depolymerizing nocodazole (Hsu, Yu et al. 2006). Various apoptogenic insults can promote death at specific phases in the cell cycle indicating that the cell-cycle and apoptosis are intimately linked (Coquelle, Mouhamad et al. 2006). Apoptosis of G2/M arrested cells is a widespread observation in the literature (DiPaola 2002). Finally, caspase-8 is activated in EGF-stimulated primary hepatocytes and participates in mitogenic signaling as a positive regulator of G1/S transition (Gilot, Serandour et al. 2005). Collectively these findings suggest that a non-death role for caspases in the mammalian cell cycle exists and, depending on the system/conditions, can modulate the fidelity of major cell cycle checkpoints.

In this study we describe a non-death role for the yeast metacaspase YCA1. DNA content analysis of *Δyca1 vs.* wild-type shows that YCA1 accelerates G1/S and antagonizes G2/M transitions granting YCA1-expressing cells an increased fitness in fermentive conditions. Analysis of a YCA1 catalytic inactivation mutant revealed that enzymatic activity of YCA1 is upstream of the G1/S transition phenotype. The slow growth phenotype of the *Δyca1* strain was exacerbated in the presence of the catalytic inactivation mutant resulting in an even longer procession through the S and G2/M cell cycle phases. Furthermore, genetic or chemical inhibition of YCA1 results in desensitization to nocodazole. These findings support the hypothesis that the canonical apoptotic proteins also regulate critical non-death functions in single cell organisms.

2.1.4 Results and Discussion

Ablation of *yca1* alters DNA content profiles

Mammalian caspase activity can alter cell cycle timing when observed under specific conditions. As a preliminary query to investigate a cell cycle role for YCA1, we examined the Saccharomyces Genome Database (www.yeastgenome.org) for cell cycle specific changes in *yca1* expression (Spellman, Sherlock et al. 1998). The CDC15 synchronization time-course presented a marked peak of *yca1* expression at a time following the second G1/S transition post release from growth-repressive conditions (fig. S1, t =150min). The single surge of *yca1* expression at the second G1/S transition may have been related to a phenomenon whereby a fraction of daughter cells in synchronized cultures do not separate from the mother cells until the second division after release from arrest (Allen, Buttner et al. 2006). This observation suggested a link between YCA1 and G1/S associated cell cycle dynamics. DNA content of wild-type BY4741 and YCA1 disrupted (*Δyca1*) yeast strains were quantified to examine this hypothesis. Strains were grown to mid-exponential phase and DNA content was analyzed by flow cytometry (see Fig. S2 for example distributions, gating and controls). Our first experiments performed in standard YPD media exhibited no observable changes between the wild-type and mutant strains (data not shown).

Yeast is an adaptive organism that survives in a variety of environments by modulating protein expression and activity, such as during the fermentation phase (Causton, Ren et al. 2001) where the natural habitat of the yeast is commonly the acidic surrounding of a fruit or within its confines. Given that fermentive growth may be more typical of yeast's natural environment, the experiment was repeated in acidified media.

Wild-type BY4741 cells displayed no discernable change in DNA distribution between acidic and neutral media. However, *Δyca1* grown in acidic media consistently exhibited a substantial increase in the proportion of G1 cells (1-copy of DNA) and a proportionate decrease in G2/M phase cells (2-copies of DNA) when compared with wild-type controls in the same media (Fig. 1 a, b). From this we conclude that genetic ablation of *yca1* promotes a shift in the equilibrium between the 1-copy (G1) and 2-copy (G2/M) DNA populations of yeast during fermentative growth.

Enzymatic activity of YCA1 promotes the G1/S transition and increases the robustness of log-phase yeast

Enzymatic inactivation of YCA1 via mutation of the catalytic cysteine at position 297 to alanine has been described (Madeo, Herker et al. 2002). To examine whether the enzymatic activity of YCA1 influenced cell cycle progression/equilibrium, the YCA1-C297A mutant was constructed and expressed under its endogenous promoter with the selectable trophic marker leu2 in the *Δyca1* background strain (Fig. S3). The resulting mutant strain (referred to henceforth as C297A) and a control strain consisting of only the selectable marker *leu2* in the *yca1* locus of the same background strain (referred to as the LEU2 strain) were used. In all cell cycle experiments, the LEU2 strain behaved identically to the *Δyca1* strain indicating that the selectable marker did not influence cell cycle behaviour (unpublished observation). Furthermore, reverse transcriptase PCR was used to test if modifications to *yca1* affect the expression of the genes that flank the *yca1* locus. It was observed that expression of the flanking *bfr1* and *lip5* genes were unaltered in the *Δyca1* and the C297A strains in comparison to BY4741 (Fig. S4) indicating that the disruptions were specific to *yca1*.

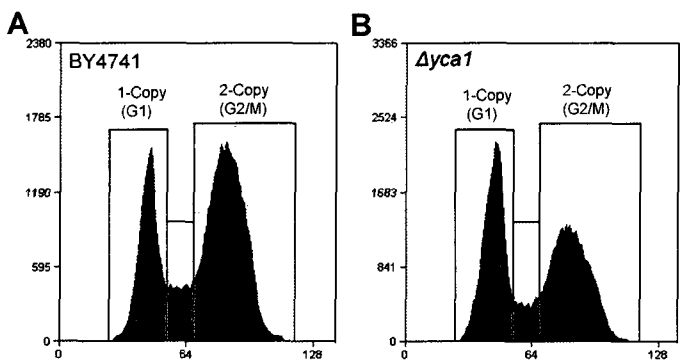

Figure 1: Cell cycle profiles during logarithmic growth.

Representative DNA content profiles for exponentially growing (a) BY4741 and (b) *Δyca1* cells. The percentage of cells in the 1-copy and 2-copy gated regions is indicative of the percentage of cells in the respective G1 and G2/M phases of the cell cycle.

Samples were collected at multiple time points during mid-log growth and DNA content was analyzed (see fig S2 for example time course). The percentage of cells in each gate were quantified and averaged for all samples over the indicated time points. The averages of biological replicates were compared for the different strains and summarized as pie charts (Fig. 2 a). The doubling time of the exponentially growing cultures was then calculated based on optical density measurements. We observed that both the *Δyca1* and C297A strains had a protracted progression through the cell cycle suggesting that endogenous expression of YCA1 improves robustness of yeast cells in fermentive conditions (Fig. 2 b). The actual time spent in each phase of the cell cycle was derived by multiplying the percentage of cells in a particular phase by the observed doubling time (Fig. 2 c). One-way ANOVA confirmed significant variation of the mean within the group of different strains for each observed phase of the cell cycle (G1, S and G2/M; $P < 0.01$). During exponential growth the time required for *Δyca1* cells to pass from G1 to S is significantly extended, passage through G2/M is accelerated and the S-phase was relatively unaffected when compared to BY4741 (Fig. 2 c). The C297A strain displayed a comparable delay through the G1/S transition just as the *Δyca1* strain suggesting that timely G1/S transition is dependent on the enzymatic activity of YCA1. The time required for the C297A strain to pass through G2/M was comparable to that of BY4741 implying that the accelerated transition through G2/M observed for the *Δyca1* could be corrected by replacement of YCA1 without regard to its proteolytic activity. Interestingly, the C297A strain also demonstrated a protracted progression through S phase when compared to both the BY4741 and *Δyca1* strains. It is not immediately apparent how the C297A strain could alter S phase when the comparable knockout strain

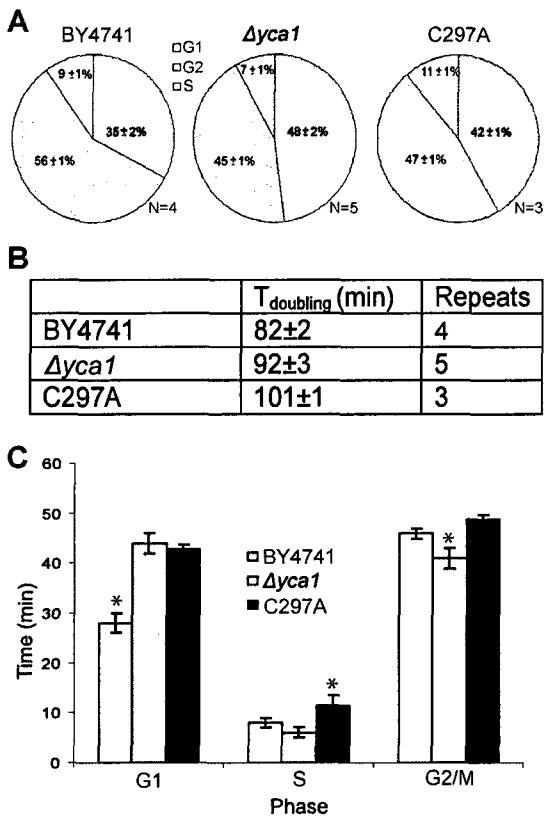

	$T_{doubling}$ (min)	Repeats
BY4741	82±2	4
Δyca1	92±3	5
C297A	101±1	3

Figure 2: Derivation of the duration of cell cycle phases.

(a) BY4741 (wild-type), *Δyca1* and C297A catalytic inactivation mutant were grown to mid-logarithmic phase in acidic YPD media. Cells were collected at regular intervals over multiple time courses and analyzed by flow cytometry. Results shown indicate the percentage of cells found in the different phases of the cell cycle. (b) Doubling time of exponentially growing cells in YPD pH 3.5 media. (c) Time spent in specific phases of cell cycle derived by multiplying the doubling time and the phase population. (* $P \leq 0.05$ heteroscedastic unpaired 2-tailed t-test, ± SEM for all).

did not yield a similar effect. However, the substantial delay of the doubling time observed in the C297A strain suggests that YCA1-C297A may be acting in a dominant inhibitory fashion, interacting with the YCA1 targets and limiting their respective activity. Such an interaction could convey an illusory correction of the G2/M timing phenotype that is observed. Together, these results clearly implicate a role for the yeast meta-caspase protein in a cell cycle timing function, modulating both G1/S and G2/M progression.

YCA1 activity is required for appropriate activation of the nocodazole induced G2/M checkpoint

Enzymatic activity of Caspase-3 in human hepatoma cells has been identified as a requirement for appropriate cell cycle arrest in response to nocodazole (Hsu, Yu et al. 2006). The observation that the G2/M timing was accelerated in the absence of the yeast caspase (Fig. 2 c) led us to hypothesize that YCA1 may perform a similar function. The following experiments were performed to test if YCA1 similarly affected the G2/M checkpoint. When cells were treated with 15 ug/mL nocodazole in YPD media, exponentially growing BY4741 and *Δyca1* strains were predominantly arrested in G2 within 100 minutes (data not shown). BY4741 cells similarly treated in acidified media were observed to respond more slowly but did reach a primarily G2 arrested state within 180 min (Fig. 3 a). Intriguingly, the *Δyca1* cells were desensitized to the arresting agent in acidified media. Only a marginal increase in the size of the G2 population was observed (Fig. 3 b), suggesting that loss of YCA1 causes the cells to bypass the G2/M check point and continue the cell cycle proper (Fig. 3 c, d).

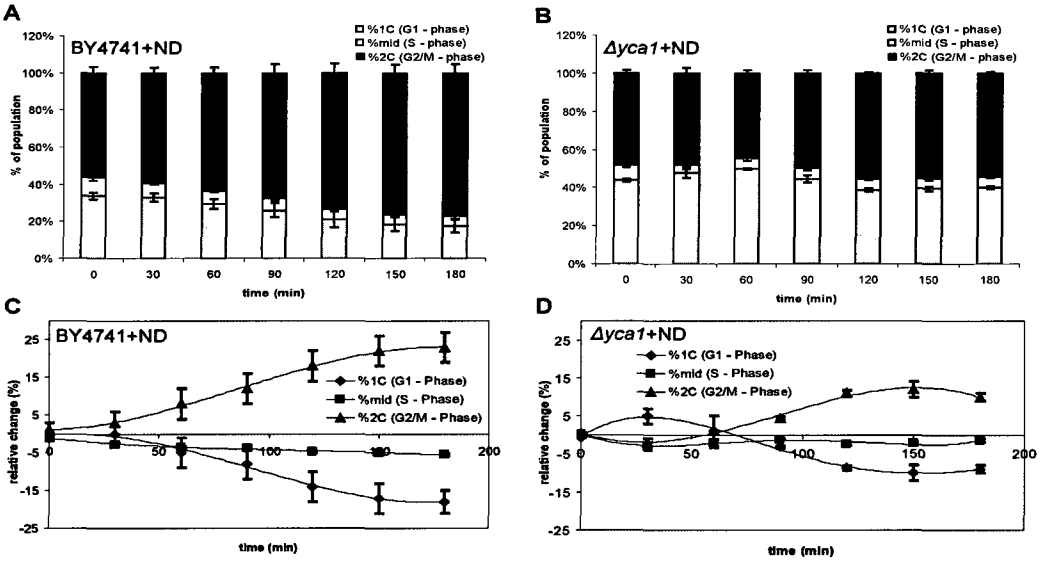

Figure 3: Response of cells to nocodazole.

DNA content profile of wild-type (a) BY4741 and (b) *Δyca1* cells over time after treatment with 15ug/mL nocodazole. Relative change in population between nocodazole treated and untreated (c) BY4741 and (d) *Δyca1* cells. For each phase the value represents the difference between population of nocodazole treated and untreated cells (value = treated – untreated). (N = 3, ± S.E.M. for all).

To test whether or not the G2/M defect derived from the enzymatic activity associated with YCA1, BY4741 cells were pre-treated with the pan-caspase inhibitor z-VAD-FMK before the addition of nocodazole. The characteristic increase in the G2/M population and decrease in the G1/S population were eliminated in the presence of the caspase inhibitor. This result paralleled the response of the C297A strain to nocodazole in identical conditions, indicating that the enzymatic activity of YCA1 is required for the nocodazole response (Fig 4 a). Protease activity analogous to mammalian caspases 6 and 8 has been observed in yeast responding to H_2O_2 (Madeo, Herker et al. 2002). Caspase 6 and 8 specific peptide inhibitors were tested for their capacity to inhibit cell cycle arrest in response to nocodazole (Fig. 4 b). The response to both inhibitors was similar to that observed with the C297A strain and zVAD treatment, however, BY4741 cells responded with greater sensitivity to the caspase 8 inhibitor in comparison to the -6 inhibitor. To verify that the results of these experiments were not skewed by the presence of cell death in response to nocodazole (Verdoodt, Decordier et al. 1999; Kim, Murphy et al. 2005) the sub-G1 populations of both BY4741 and *Δyca1* cells were quantified (Fig. 4 c). Only a very small proportion of cells died in response to nocodazole (< 2%). As such, the additional cell death in BY4741 (< 1% of cells) may be explained as an apoptotic response to nocodazole activated YCA1. We conclude that the nocodazole induced G2/M checkpoint is dependent on the enzymatic activity of YCA1.

The cell cycle phenotype is not caused by excessive oxidative stress

We sought to identify proteins that could modify the G1/S checkpoint in response to *yca1* by using comparative proteomics. Whole cell lysates derived from BY4741 and

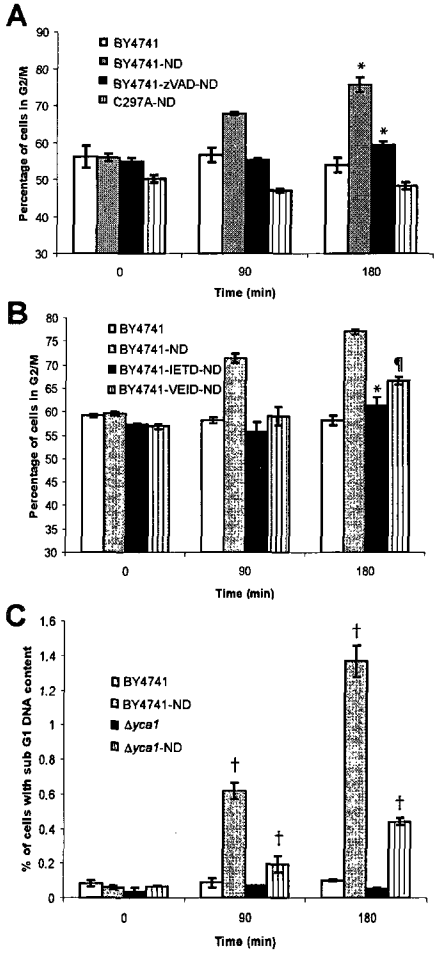

Figure 4: G2/M response of caspase inhibited cells.

(a) G2/M content of C297A caspase catalytic inactivation mutant or wild-type BY4741 cells pre-treated for 30 minutes with 20μM pan-caspase inhibitor z-VAD-FMK in response to 15 μg/mL nocodazole. (b) BY4741 cells pre-treated for 30 minutes with 20μM Caspase 6 (z-VEID-FMK) and caspase 8 (z-IETD-FMK) specific peptide inhibitors before exposure to 15μg/mL nocodazole. (c) Sub G1 population of BY4741 and Δyca1 cells either untreated or exposed to 15μg/mL nocodazole over time (N = 3, ± S.E.M., P ≤ 0.05 heteroscedastic unpaired 2-tailed t-test between paired *, ¶ and † symbols; note figure 4a is a composite of multiple experiments).

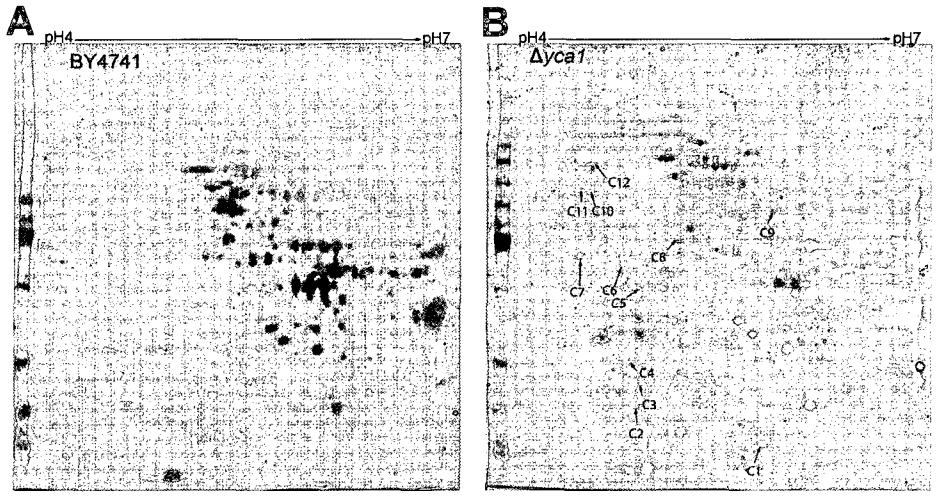

Figure 5: Representative 2D gels of BY4741 and *Δyca1* proteomes.

(a) BY4741 and (b) *Δyca1* cells separated along pH 4-7 IPG strips. The BY4741 gels were relatively over-stained to expose yca1 inducible protein species in the *Δyca1* gel. Arrowheads depict spots that appear unique to *Δyca1* lysates. Alphanumeric designation corresponds with identities summarized in table 1.

Δyca1 were resolved by 2D SDS-PAGE (Fig. 5) and examined for altered mobility in response to *yca1*ablation. We observed numerous changes to the yeast proteome between gels; particularly a number of protein species unique to *Δyca1* strain that were not apparent in protein lysates from the BY4741 strain. These spots were excised and analyzed by MS (Table 1). The list of *yca1* enriched/responsive proteins included mitochondria-associated factors and proteins functioning in the oxidative stress response, the 20s proteasome and nucleotide excision repair (NER) process.

Increased oxidative damage and compensatory activity of the 20s proteasome occurs in the absence of YCA1 (Khan, Chock et al. 2005). As such, we reasoned that altered expression of mitochondrial, stress response and DNA repair proteins might reflect the presence of oxidative DNA damage which might be responsible for the extended G1/S transition in the *Δyca1* strain. We assessed intracellular reactive oxygen species (ROS) via bivariate flow cytometry using dihydrorhodamine 123 (DHR123) as an indicator of ROS and propidium iodide (PI) as a marker of membrane integrity/viability (Wysocki and Kron 2004). When treated with 3mM H_2O_2 for 2 hours before analysis, BY4741 cells were observed to be predominantly ROS positive with a smaller percentage of non-viable PI positive cells co-staining with DHR123. Untreated exponentially growing BY4741 and *Δyca1* cells, however, were largely negative for both PI and DHR123 (Fig. 6 a). We also assessed the chymotrypsin-like activity of the 20s proteasome in BY4741 and *Δyca1* cell lysates (Fig. 6 b). We did not observe any change between the BY4741 and *Δyca1*strains which indicated that the 20s proteasome was not abnormally activated. These results suggest that the cell cycle effects and proteomic

Spot	Name	Score/peptides	Notes [a]
C1	PST2	72/2	Mitochondrial; Oxidative stress response protein induced by YAP1
C3	MRP8	52/2	Putative mitochondrial ribosomal protein
C4	PUP2	73/3	Alpha subunit of 20S proteasome
C5	LIA1	171/5	deoxyhypusine hydroxylase; Possible role in mitochondrial positioning
C6	SGT2	151/5	Similarity to human SGT which negatively regulates HSP70
C7	PEP4	155/4	Aspartate protease involved in metabolic degradation (pepsin like); important for protein turnover after oxidative damage
C8	TIF2	347/9	eIF4a homolog
C10	PYK1	90/5	Pyruvate kinase
C11	RAD23	181/4	Nucleotide excision repair; DNA damage checkpoint role normally degraded during G1/S transition
C12	PDI1	227/7	Protein disulfide isomerase involved in formation and management of scrambled protein disulfide bonds

[a]Notes derived from ORF descriptions available at www.yeastgenome.org.
doi:10.1371/journal.pone.0002956.t001

Table 1. MS identification of protein species induced by *yca1* ablation

changes seen in *Δyca1* cells are not due to oxidative stress or abnormal proteasome activity.

We identified RAD23 as a potential *yca1* modulated protein. RAD23 stabilizes DNA damage repair machinery (G1 checkpoint) and is a cofactor to the ubiquitin/proteasome pathway (Schauber, Chen et al. 1998). Increased expression of RAD23 in the *Δyca1* strain was confirmed by western blot (Fig. 6 c). RAD23 is usually degraded at the G1/S transition. Given the preponderance of G1 cells in the *Δyca1* strain, the increased presence of RAD23 in these cells suggests the potential activation and stabilization of the NER associated checkpoint (Ortolan, Chen et al. 2004). We examined the possibility of direct interaction between YCA1 and RAD23; however, we were unable to demonstrate any association through co-immunoprecipitation of RAD23 with the YCA1-TAP strain or YCA1 with the RAD23-TAP strain (unpublished observations). The lack of Rad23p cleavage products in the western blots in addition to the failure to co-immunoprecipitate suggests that the RAD23 response is secondary to YCA1 activity. However, the increase in RAD23 in the *Δyca1* strain might suggest the occurrence of alternate DNA processing events which may contribute to the G1/S phenotype. Low-level ROS has been reported to act as a proliferative signal, stimulating G1/S progression (Sattler, Winkler et al. 1999; Deng, Gao et al. 2003). We cannot discount the possibility that retention of RAD23 and the G1/S transition phenotype result from subtle differences in ROS levels that are not detectable by our methods. However, the absence of 20s proteasome activity and ROS staining suggest that oxidative stress-associated DNA damage is not directly invoking an NER response in *Δyca1* cells. In fermentive

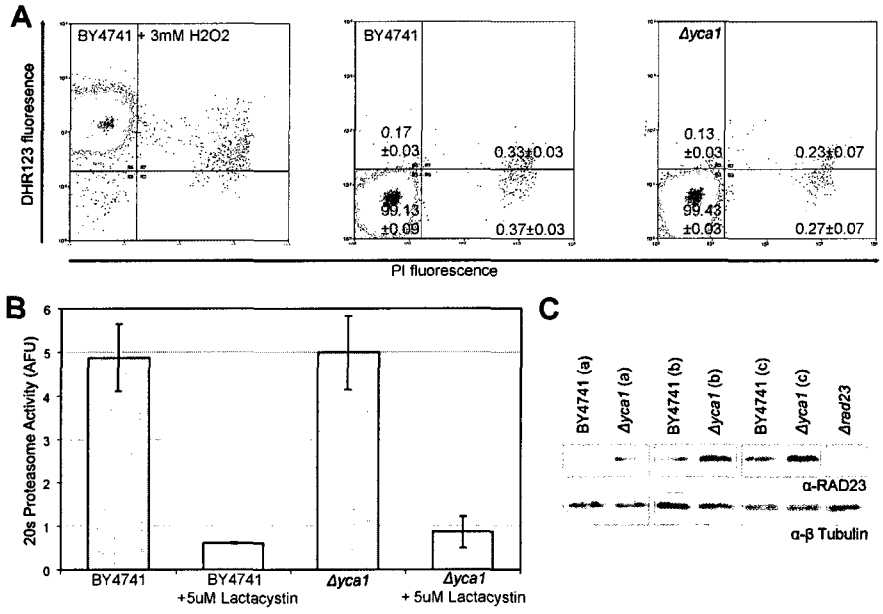

Figure 6: Downstream effects and oxidative stress.

(a) Bivariate flow cytometry analysis of H2O2 treated BY4741, BY4741 and *Δyca1* cells dual stained with propidium iodide (PI) and ROS stain dihydrorhodamine 123 (DHR123). (N=3, ± SEM). (b) 20s proteasome activity from BY4741 and *Δyca1* lysates (N=3, ± SEM). (c) Western blot for 3 biological replicates of BY4741, *Δyca* and Δrad23 (100 μg protein for each). Δrad23 appears as a negative control. The RAD23 antibody was obtained from Santa Cruz Biotechnology (SCBT, Santa Cruz, CA), β-tubulin (Iowa State University Hybridoma Bank) was used as a loading control.

conditions, both strains grow in a healthy manner free of excessive oxidative stress or cell death suggesting that these are not the direct causes of the cell cycle phenotype.

In conclusion, our results demonstrate a previously unrecognized role for the yeast metacaspase YCA1 in cell cycle progression. YCA1 accelerates the G1/S transition and slows the G2/M transition. In the first instance YCA1 confers a growth advantage by promoting the transition between G1 and S phase. Secondly, our results show that YCA1 antagonizes cell growth by limiting the G2/M transition. Furthermore, we observed that *Δyca1* and YCA1 inhibited cells are similarly desensitized to the nocodazole induced G2/M checkpoint. Reduced response to nocodazole has been detected in mammalian systems in which the YCA1 related enzyme caspase-3 is inhibited (Hsu, Yu et al. 2006). Based on these observations, we speculate that the disparate ability of metacaspases to both promote and antagonize different cell cycle checkpoints may represent an early form of the proliferation/differentiation regulating activity exhibited by metazoan caspases.

2.1.5 Materials and Methods:

Yeast strains and growth conditions. S. cerevisiae strains used in this study include wild-type haploid BY4741 (MATa his3Δ1 leu2Δ0 met15Δ0 ura3Δ0) and the knockout *Δyca1* strain from the BY4741 background (Open Biosystems, Huntsville, AL). Yeast cultures were grown in yeast extract peptone dextrose (YPD) medium (2% glucose, 2% Bacto peptone, and 1% yeast extract; pH adjusted to 3.5 with HCL; agar was added for solid plates to a final concentration of 2%). Overnight starter cultures grown from a single S. *cerevisiae* colony were used to inoculate large YPD cultures to a final optical density (OD660) of 0.05. These cultures were grown at 30° C with 250 RPM orbital rotation into mid-logarithmic phase at which point samples were collected as described in the *Exponential growth, caspase inhibition and cell cycle arrest* section below.

Construction of the C297A strain. The YCA1 open reading frame in the BG1805 plasmid (Open Biosystems, Huntsville, AL.) was used as a template for site directed mutagenesis. A mutagenic fragment was generated using a mutagenic primer 5'-TGTTTGACTCTGCTCATTCGGGTAC-3' and a reverse primer with a flanking HindIII site 5'-GGGAAGCTTCTACATAATAAATTGCAGAT-3. The 487 bp mutagenic fragment was then used in a second PCR reaction with a primer directed at the 5' end of *yca1* 5'-GGGGGATCCATGAAGATGAGCCTCGAAGT-3' with a flanking BamH1 site. We cloned the C297A construct into the BamH1/HindIII site of the pSSB08 plasmid; obtained by introducing two silent mutations (F: TTC to TTT ; E: GAA to GAG) to remove the EcoRI site in the Leu2 selection marker of the pRS405 backbone (Brachmann, Davies et al. 1998) created by Simon St-Pierre. The construct was amplified

using primers containing 41-mer regions of homology to the endogenous *yca1* locus and 20-mers directed at the construct 5'-CTATTGAAAAAGCATGGCTTCGCATTAATAGGAGCCAAAAATATGAAGATGAGCCTCGAAG-3' and 5'-CTATTGAAAAAGCATGGCTTCGCATTAATAGGAGCCAAAAATCCCCGGGCTGCAGGAATTCGA-3'. The *Δyca1* strain was transformed with the double stranded DNA product using a standard LiAC/SS carrier DNA/PEG method.

Protein extraction. *S. cerevisiae* cells were pelleted, washed twice and resuspended in 500μL of ice cold modified RIPA buffer (50mM Tris-HCL, 1% NP-40, 150mM NaCl 1mM EDTA 1% Glycerol) containing protease inhibitors. 0.7g of acid washed glass beads (Sigma Aldrich, Ontario, Canada) were added and cells were lysed with a Disruptor Genie (Scientific Industries, New York, USA) at 4°C. Lysates were clarified by centrifugation at 5000 × g for 20 minutes and the soluble fraction was retained for analysis.

Exponential growth, caspase inhibition and cell cycle arrest. For exponential growth experiments BY4741, Δ*yca1* or C297A strains were grown to OD660 of 0.4 - 0.5 at which point optical density was recorded and aliquots were collected at regular intervals. To inhibit endogenous caspase-like enzymatic activity cells were pretreated with 20μM of either z-VAD-FMK, z-VEID-FMK or z-IETD-FMK (BioVision, Mountain View, CA) at an OD660 of 0.3. Cultures were allowed to grow in the presence of inhibitor for an additional 45 minutes before further treatment with 15 μg/mL nocodazole (Sigma, Saint

Louis, MO) and subsequent time course sample collection. For cell cycle arrest, BY4741, Δ*yca1* or C297A cells were grown to OD660 of 0.4 - 0.5 before addition of 15 μg/mL nocodazole. In all cases, OD660 measurements and 1 mL aliquots were collected regularly over 3 hours. Collected samples were immediately fixed in cold 70% ethanol and stored at 4°C overnight before further analysis. Optical density at 660nm (OD660) of liquid yeast culture was determined using an Ultrospec 2100 PRO spectrophotometer.

DNA staining. 3.5×10^6 cells were collected from ethanol fixed samples, washed with 50mM sodium citrate and resuspended in sodium citrate containing 0.2 mg/mL RNase A (GE Healthcare, Pittsburgh, PA). Samples were incubated at 37°C for 22 hours to promote hydrolysis of endogenous RNA. Sytox green (Molecular Probes, Burlington, Ontario) was added to a final concentration of 3.75μM and samples were incubated in the dark at room temperature for 1 hour. Finally, samples were pelleted and resuspended in PBS before analysis by flow cytometry. DakoCytomation Summit version 4.0 software was used to gate and quantify cells after flow acquisition (see fig. S2 for example gating).

Flow cytometry. Flow cytometry data acquisition was performed with a Coulter MoFlo (Fullerton, California, USA), all samples were excited by a 488 nm Spectra- Physics Argon laser, Sytox green dye and DHR123 fluorescence was detected with a 530/40 bandpass filter. PI was detected with a 630/30 bandpass filter. 50000 cells per sample were counted. Dual compensation was performed to remove signal bleed between the PI and DHR123 channels. Flow data was analyzed with DakoCytomation Summit version 4.0 software.

2D gel electrophoresis. Samples were diluted in isoelectric focusing buffer (7M urea, 2M thiourea, 4% CHAPS, 1% DTT) and absorbed into 17 cm ReadyStrip™ IPG strips (Biorad) following the manufacturer's directions. Isoelectric focusing was performed on a Protean IEF Cell (Biorad) with the following program: 200 V for 1 hour, 500 V for 1 hour, 5000 V ramp for 5 hours, 5000 V for 80000 VH. For the second dimension, IPG strips were overlaid onto 10% SDS-PAGE gels and electrophoresed in a Protean II apparatus (Biorad).

Mass spectrometry. Silver stain and in-gel digest were performed using a standard method (Shevchenko, Wilm et al. 1996). Sample cleanup was performed using ZipTip (Millipore). Tandem mass spectra were collected on an Applied Biosystems/SciEX QSTAR XL with oMALDI2 ion source. Spectra were analyzed using Mascot 2.0 (Matrix Science, UK) and the NCBI non-redundant protein sequence database (version 20070306). MS/MS tolerance was ±0.4 Da.

20s Proteasome activity assay. 50 μg of clarified whole cell extract was analyzed using the Proteasome Activity Kit (Chemicon, California, USA). Fluorescent AMC liberated from the 20s proteasome substrate suc-LLVY-AMC was detected for 90 minutes at 37°C as per instructions on a Fluoroskan Ascent FL microplate fluorometer (Thermo Scientific, USA) with excitation at 380nm and emission at 460 nm.

Supplementary Information. Fig. S1 shows expression pattern of YCA1 following release from CDC15 synchronization. Fig. S2 displays G1 and G2/M gating controls in addition to example gating as used for time course DNA profiles. Fig. S3 depicts the verification of the C297A strain. Fig. S4 demonstrates the invariability of the genes immediately flanking the YOR197w open reading frame.

2.1.6 Acknowledgements

The authors would like to thank Simon St-Pierre, Caroline Vergette, Paul Oleynik, Laila Lee and Dr. Pasan Fernando for helpful discussions and technical advice. L.A.M. holds the Mach-Gaennslen Chair in Cardiac Research.

2.2 Supplementary Information:

A Non-death Role of the Yeast Metacaspase: YCA1 Alters Cell Cycle Dynamics

Robin E. C. Lee[2,1], Lawrence G. Puente[1], Mads Kærn[3,2,4] and Lynn A. Megeney[1,2,3,*]

[1]Ottawa Health Research Institute, Sprott Centre for Stem Cell Research, The Molecular Medicine Program Ottawa, Canada

[2]University of Ottawa, Department of Cellular and Molecular Medicine Ottawa, Canada

[3]Ottawa Institute of Systems Biology, University of Ottawa Ottawa, Canada

[4]University of Ottawa, Department Physics Ottawa, Canada

*To whom correspondence should be addressed. Email: lmegeney@ohri.ca Phone: 613 737 8618

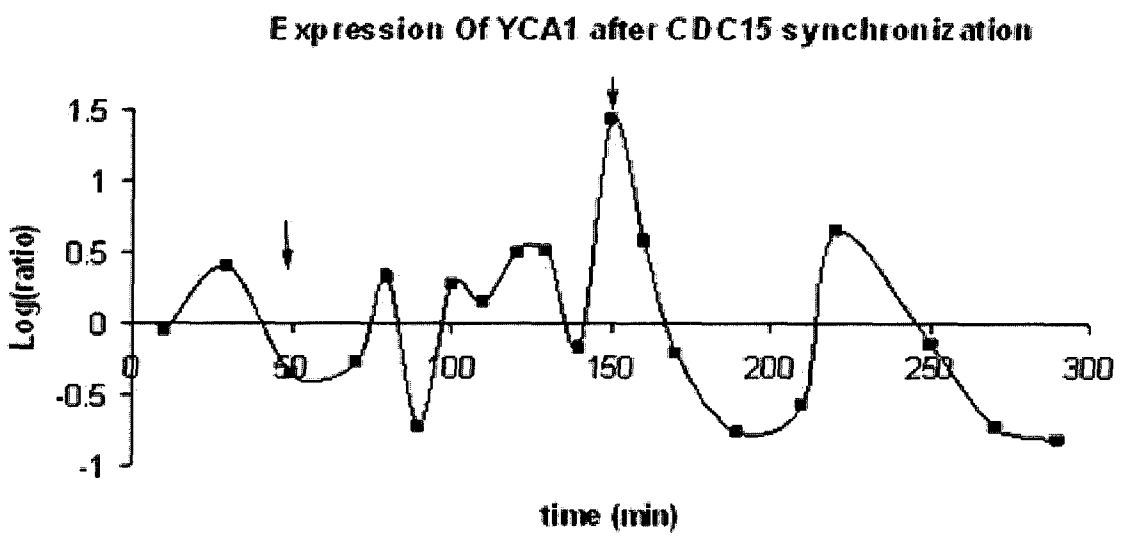

Figure S1: Expression of *yca1*

Adaptation of data from Spellman et al. (Mol Biol Cell 9, 3273-97 1998) depicting expression of *yca1* after CDC15 synchronization. Arrows denote the first observation of new buds. Peak expression after 150 minutes release coincides with second appearance of small buds indicative of the G1/S transition in budding yeast.

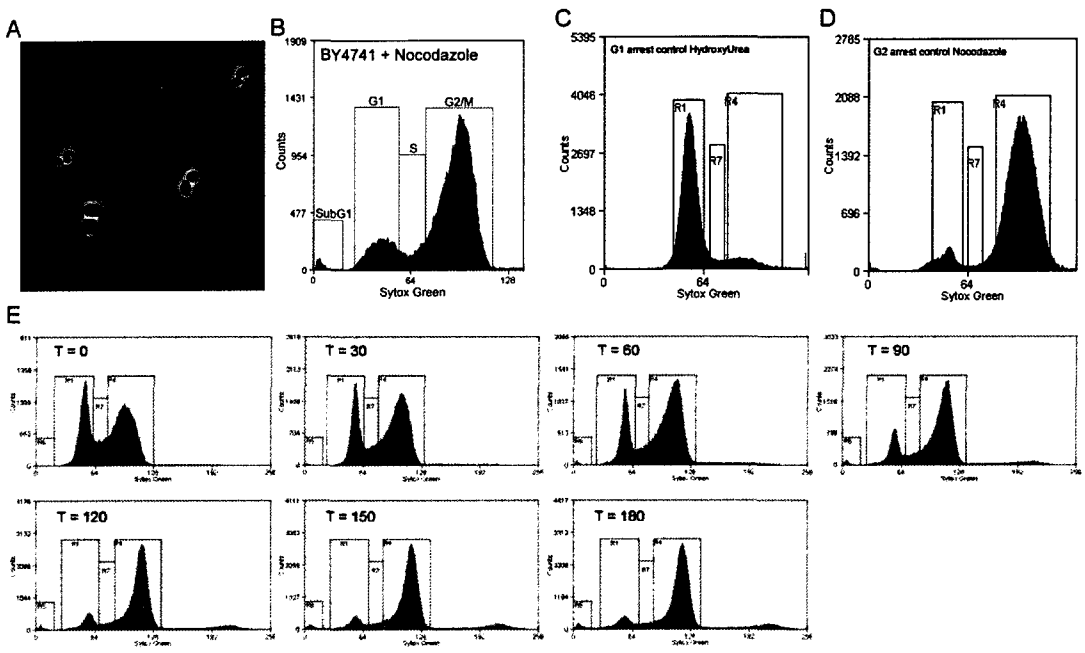

Figure S2: Flow cytometry gates for DNA analysis

(a) 63x phase contrast/FITC microscope merge of sytox green stained yeast cells arrested with nocodazole. Microscopy was performed on an Axioplan 2 compound microscope fitted with a Zeiss Axiocam. Fixed cells were suspended in 50mM sodium citrate, slide mounted and viewed at 63x magnification with a PlanApochromat 1.4 NA objective lens at 22°C. Phase contrast and FITC channel images were merged using Axiovision 3.1 software (Carl Zeiss, Toronto Canada). (b) Control DNA content profile demonstrating gating used to quantify cell cycle populations for nocodazole treated BY4741 cells. The histogram abscissa represents relative fluorescent intensity of fixed cells incubated with the nucleic acid stain Sytox green. (c,d) Example of gating used to identify G1 and G2 peaks. Cells were arrested at the G1/S transition with (c) the ribonucleotide reductase inhibitor Hydroxyurea or in the G2/M phase with (d) Nocodazole. (e) Example time response (in minutes) and gating of wild-type BY4741 cells to 15 µg/mL nocodazole. The montage demonstrates a progressive decay of the G1 population concurrent with an enlargement of the G2 population consistent with G2 arrest.

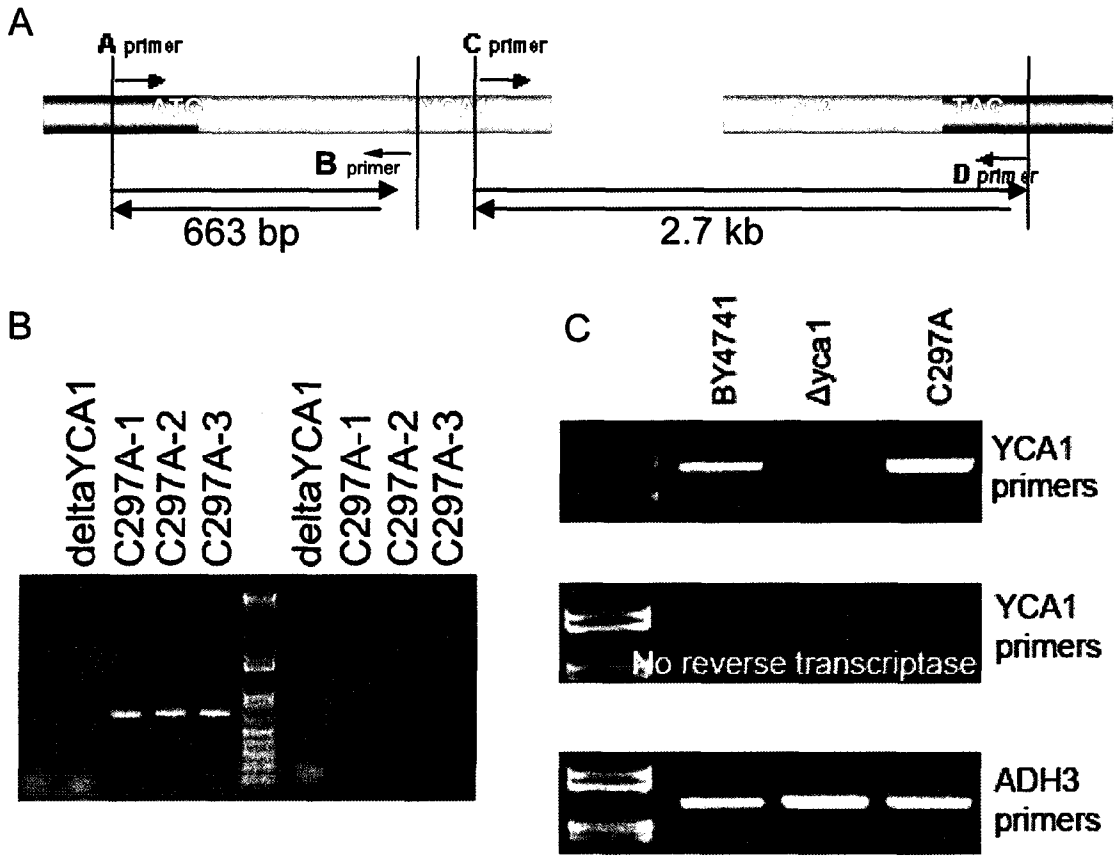

Figure S3: Integration of the C297A construct into the *Δyca1* background strain.

(a,b) The location of integration and expression of integrants were verified using A-B and C-D primers designed for the systematic deletion project (http://www-sequence.stanford.edu/group/yeast_deletion_project/confirmation.html) predicted 663 bp and 2.7 kb fragments were observed. (c) Reverse transcriptase PCR confirming the presence of the C297A transcript. ADH3 was used as a loading control.

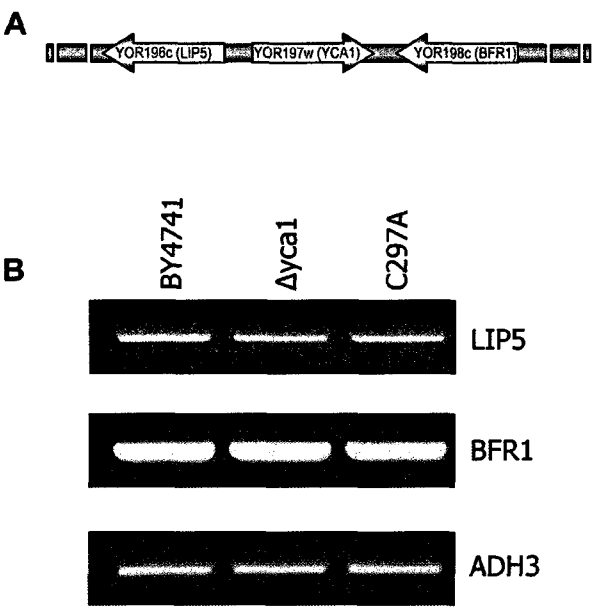

Figure S4: Expression of genes flanking *yca1*

a) Region of chromosome XV depicting genes flanking *yca1*. b) Reverse transcriptase PCR of flanking genes demonstrates invariable expression in the *Δyca1* and C297A strains when compared to the congenic BY4741 background strain. ADH3 was used as a loading control.

CHAPTER 3:

The Metacaspase YCA1 is required for Clearance of Insoluble Protein Aggregates

3.1 Manuscript

The Metacaspase YCA1 is required for Clearance of Insoluble Protein Aggregates

Robin E. C. Lee[1,2], Steve Brunette[2], Lawrence G. Puente[2], Lynn A. Megeney[1,2,3]

[1] Department of Cellular and Molecular Medicine, University of Ottawa, Ottawa, Canada
[2] Ottawa Hospital Research Institute, Sprott Centre for Stem Cell Research, Ottawa, Canada
[3] To whom correspondence should be addressed

One sentence summary: The ancestral caspase YCA1 acts in a non-death role to limit the formation of insoluble protein aggregates.

3.1.1 Author Contributions and Manuscript Information:

RECL: Designed the study, performed experiments, analyzed the data and wrote the manuscript.

SB: Performed experiments and analyzed data.

LGP: Analyzed data and wrote the manuscript.

LAM: Designed the study, contributed materials and wrote the manuscript.

This article has been submitted to *Science*.

3.1.2 Abstract:

Caspase proteases influence numerous cell functions independent of inducing programmed cell death/apoptosis. In single cell eukaryotes, metacaspases have been demonstrated to engage apoptosis, yet non-death roles are currently undefined. We report an essential non-death role for the *S. cerevisiae* metacaspase YCA1 in protein quality control. Quantitative proteomic analysis of *Δyca1* cells identified significant alterations to protein catabolism and stress response pathways. YCA1 protein complexes are enriched for aggregate remodeling chaperones that together co-localize with YCA1-GFP fusions on insoluble protein plaques. Finally, deletion and inactivation mutants of YCA1 accrue protein aggregates and autophagic bodies during log-phase growth. Together, our experiments demonstrate that YCA1 acts to clear insoluble protein aggregates, a remodeling activity that may represent the evolutionary precursor to the breadth of caspase function in metazoans.

3.1.3 Text body:

In complex organisms, caspase proteases mediate a variety of cell behaviors including programmed cell death (PCD/apoptosis), immune cell activation, enhanced motility and differentiation (Ellis and Horvitz 1986; Thornberry, Bull et al. 1992; Fernando, Kelly et al. 2002; Helfer, Boswell et al. 2006). The yeast metacaspase (YCA1/MCA1) is an established mediator of yeast PCD in response to oxidative stress and environmental insults (Madeo, Herker et al. 2002; Herker, Jungwirth et al. 2004; Khan, Chock et al. 2005); However, YCA1 also promotes competitive fitness and the fidelity of cell cycle checkpoints through undefined mechanisms (Herker, Jungwirth et al. 2004; Lee, Puente et al. 2008). The involvement of YCA1 in apoptotic and non-apoptotic functions mimics that of caspase proteases in vertebrate and invertebrate animals (reviewed in (Fernando and Megeney 2007)). Nevertheless, the actual molecular role of YCA1 remains uncharacterized during ambient growth conditions in the absence of severe environmental challenges.

To investigate the non-death function of YCA1 we measured relative proteomic changes induced by YCA1 ablation in physiologic growth conditions. Trypsin digested peptides from wild-type and *Δyca1* cell lysates were labeled with iTRAQ mass tag labels, combined and analyzed by LC/MS-MS. Proteins with significant iTRAQ ratios ($1.20 <$ *Δyca1*/wild-type < 0.80) were selected along with those previously identified in 2D gel experiments (Lee, Puente et al. 2008). The 67 up-regulated proteins and 13 down-regulated proteins (Fig. S1 and table S1) were separately clustered using the Funspec cluster interpreter (Robinson, Grigull et al. 2002) to identify any significant alterations in

GO biological process and *MIPS subcellular localization* (Fig. S2). We did not see significant clusters form from the down-regulated proteins; however, a substantial over-representation of proteins involved with vacuolar catabolism, stress response and growth/metabolism based on *GO biological process* categories were observed (Fig. 1a). Of these proteins, five of the six known peptidases responsible for catabolic processes within the vacuolar lumen were increased by over 40% (on average). *Δyca1* lysates were also enriched for proteins associated with stress response including HSP70 family chaperones (SSA1, SSA2 and SSA4) and HSP104, a chaperone involved with active re-solubilization of protein aggregates (Parsell, Kowal et al. 1994) (Fig. 1b, c).

To discern if alterations to the size, number or morphology of the vacuoles in the caspase mutant contributed to the presence of vacuolar peptidases in our iTRAQ screen, live cells were labeled with the vital dye FM4-64. Most wild-type cells had 1-3 well defined vacuoles whereas a subpopulation of cells was multi-vacuolated with greater than 3 vacuolar structures per cell. We quantified the proportion of cells with normal or multi-vacuolated appearance and observed a 2.5-fold increase in the number of multi-vacuolated cells in the *Δyca1* strain and a 2-fold accumulation of these structures in the C297A strain (a catalytic inactivation mutant of YCA1) (Madeo, Herker et al. 2002; Lee, Puente et al. 2008) when compared to wild-type (Fig. 1d, e). The de-localized stain and the multiple intra-vacuolar structures within the larger vacuolar space of *Δyca1* cells was consistent with the morphology of autophagic bodies (Journo, Winter et al. 2008). The proteomic alterations and the accumulation of autophagic bodies in the *Δyca1* strain suggested activation of a chaperone mediated autophagy or microautophagic process. Furthermore, the various stress response chaperones induced by YCA1 deletion

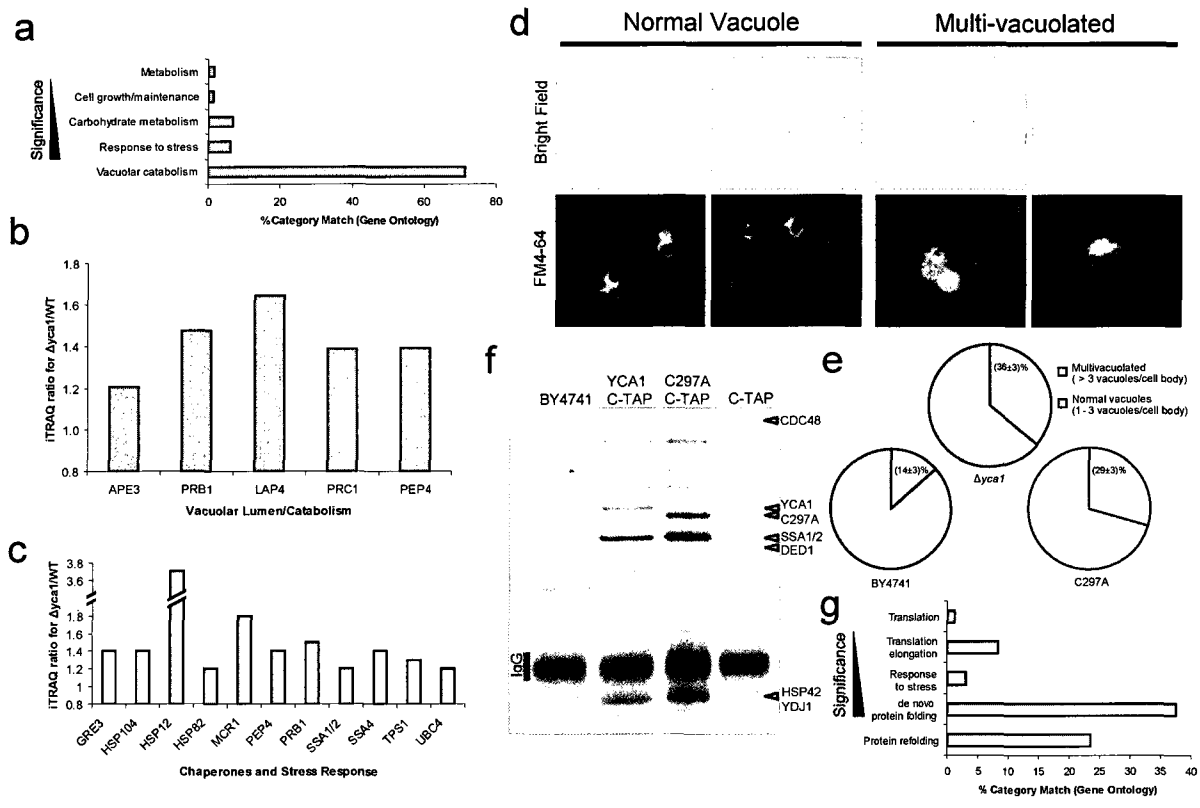

Figure 1| Proteomic analysis of *Δyca1* and TAP interactors reveal association with chaperone mediated protein quality control.

a, GO biological process clusters (Funspec, phypergeometric < 5x10-5, Bonferroni correction enabled) of proteins up-regulated in *Δyca1* lysates as determined by iTRAQ. **b, c,** iTRAQ ratios for proteins involved with (**b**) vacuolar catabolism (**c**) stress response. **d,** FM4-64 vacuole stain depicting normal and multi-vacuolated morphology **e,** Quantification of multi-vacuolated wild-type, YCA1 catalytic inactivation mutant C297A and *Δyca1* cells during log growth (N = 3, ± s.e.m.). **f,** YCA1/C297A-TAP associating proteins are enriched for aggregate remodeling proteins and chaperones. **g,** GO biological process clusters of YCA1-TAP associated proteins as determined by Funspec (Robinson, Grigull et al. 2002) (phypergeometric < 3x10-4, no Bonferroni correction).

demonstrated that log-phase yeast are challenged without the action of YCA1, an observation consistent with our previous cell cycle analysis (Lee, Puente et al. 2008).

To further explore the relationship between YCA1 and the altered stress response, we used a single step magnetic bead TAP purification system to identify YCA1 associated complexes. Proteins that consistently co-purified with YCA1-TAP and C297A-TAP and did not associate with wild-type and TAP expressing control strains (Fig. 1f) were identified by LC-MS and clustered using the Funspec cluster interpreter (Robinson, Grigull et al. 2002) (Fig. 1g, and fig. S3). Based on the association of YCA1-TAP with protein translation machinery and the DEAD box helicase DED1 we hypothesized that YCA1 may directly interact with or impinge upon the formation of mRNA processing bodies (P-Bodies) (Beckham, Hilliker et al. 2008). To address this possibility we expressed a centromeric plasmid containing EDC3-mCh as an *in-situ* marker of cytosolic P-Bodies (Buchan, Muhlrad et al. 2008) in wild-type, YCA1-GFP and *Δyca* backgrounds (Fig. S4). We did not observe any difference in the size or number of P-Bodies nor did we note significant co-localization of YCA1-GFP with EDC3-mCH positive foci suggesting that the *Δyca1* phenotype cannot be explained by a P-body dependent effect. YCA1 co-purified with SSA1/SSA2 (HSP70), HSP42, YDJ1 (HSP40) chaperones and the AAA ATPase CDC48 (Fig. 1f), a cell cycle control protein associated with the formation of aggresomes and polyglutamine aggregates (Fu, Ng et al. 2003; Wang, Meriin et al. 2009). This observation complemented our iTRAQ data whereby the HSP70 and HSP104 aggregate remodeling chaperones are expressed in compensation of YCA1 deletion. Together these data suggest that YCA1 may directly interact with protein

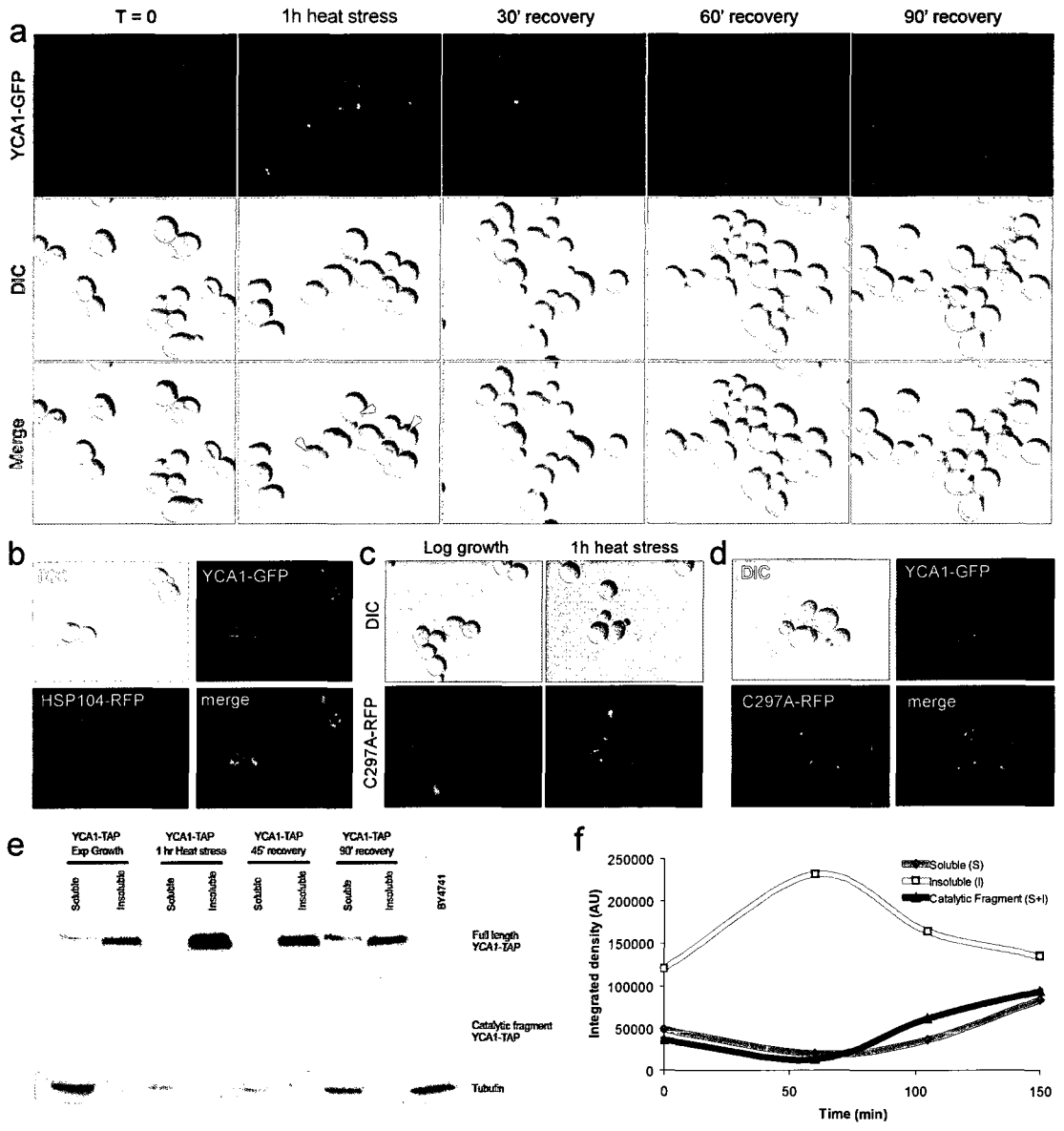

Figure 2| YCA1 targets insoluble protein aggregates irrespective of its catalytic activity.

a, YCA1-GFP reversibly condenses into discrete foci during heat stress. Arrows depict co-localization between YCA1-GFP and visible features of the DIC channel. **b,** YCA1-GFP co-localizes with HSP104-RFP during heat stress. **c, d,** Catalytic inactivation of YCA1 (C297A-RFP expressed in *Δyca1*) does not affect its aggregate targeting function. **e, f,** Western blot of soluble and insoluble fractions confirm association of full-length YCA1 with the insoluble phase during heat stress. Quantified by densitometry in (**f**).

aggregates or the HSP40/HSP70/HSP104 protein aggregate remodeling complex (Glover and Lindquist 1998; Cashikar, Duennwald et al. 2005; Haslbeck, Miess et al. 2005).

To test if YCA1 targets cytosolic protein aggregates we used a genomic YCA1-GFP fusion protein expressed under its native promoter and monitored the localization of the GFP signal. We observed that YCA1-GFP is diffuse throughout the cell and generally excluded from vacuoles in baseline logarithmic growth conditions (Fig. 2a, T=0). However, when subjected to 42°C heat stress to promote the formation of cytosolic protein aggregates, YCA1-GFP converged into discrete foci which co-localize with visible features of the cells as viewed by nomarski optics (Fig 2a). The formation of the YCA1-GFP foci were apparent as early as 7 minutes after exposure to heat and dispersed into the cytosol within 60-90 minutes after return to 30°C (Fig. 2a, and fig. S5). We expressed HSP104-RFP under its own promoter in a centromeric plasmid as an *in-situ* marker of protein aggregates (Erjavec, Larsson et al. 2007) and observed robust co-localization of YCA1-GFP with RFP positive aggregates during heat stress (Fig. 2b). Furthermore, we observed formation and co-localization of YCA1-GFP and HSP104-RFP foci in aged stationary phase cultures (Fig. S6), a second physiologic stress capable of promoting protein aggregation (Maisonneuve, Ezraty et al. 2008). The C297A catalytic inactivation mutant was fused to RFP and expressed in wild-type, YCA1-GFP and *Δyca1* backgrounds (Fig 2.c, d). C297A also converged into discrete foci during heat stress in all backgrounds and C297A-RFP co-localized strongly with YCA1-GFP indicating that the catalytic core of YCA1 is not required for its aggregate targeting function. Finally, lysates from YCA1-TAP expressing cells were separated into soluble and insoluble fractions by differential centrifugation (Fig. 2e, f). During log growth YCA1-TAP is

distributed between the soluble and insoluble fractions. After 1 hour of heat stress full length YCA1-TAP expression increased in the insoluble fraction and both full length and catalytic fragments were depleted from the soluble fraction. Within 90 minutes of recovery the pattern of YCA1-TAP returned to baseline albeit with slightly higher expression levels. The distribution of full length C297A-TAP behaved similarly over the time course with the exception of the catalytic fragment which does not form in the mutant. Together these data demonstrate that YCA1 is actively expressed in response to heat stress and shuttles to insoluble protein aggregates in a manner that does not require the catalytic cysteine of the protease.

We reasoned that YCA1 in the insoluble fraction may actively remodel or disassemble protein aggregates during exponential growth. To examine this possibility we measured the nonidet P40-insoluble protein aggregate fraction from log-phase wild-type, *Δyca1* and C297A protein lysates by filter trap analysis (Fig. 3a, b). We observed a 2-fold increase of insoluble aggregates in *Δyca1* when compared with equal amounts of wild-type protein lysate. Unexpectedly, we observed a 1.4-fold increase in the insoluble aggregate fraction in the C297A catalytic inactivation mutant suggesting that the expression of YCA1 can significantly reduce the retention of protein aggregates even in the absence of its catalytic activity. The contents of the insoluble fraction were further analyzed. HIS tagged SSA1 was expressed from its genomic locus and found to accumulate in the insoluble fraction of *Δyca1* cells when compared to wild-type (Fig. 3c). Similarly, insoluble aggregates from equal amounts of total protein extract were separated by 1D PAGE and silver stained (Fig. 3d). Consistent with the filter trap assay, the intensity of the bands in the aggregate fraction from *Δyca1* lysates were directly

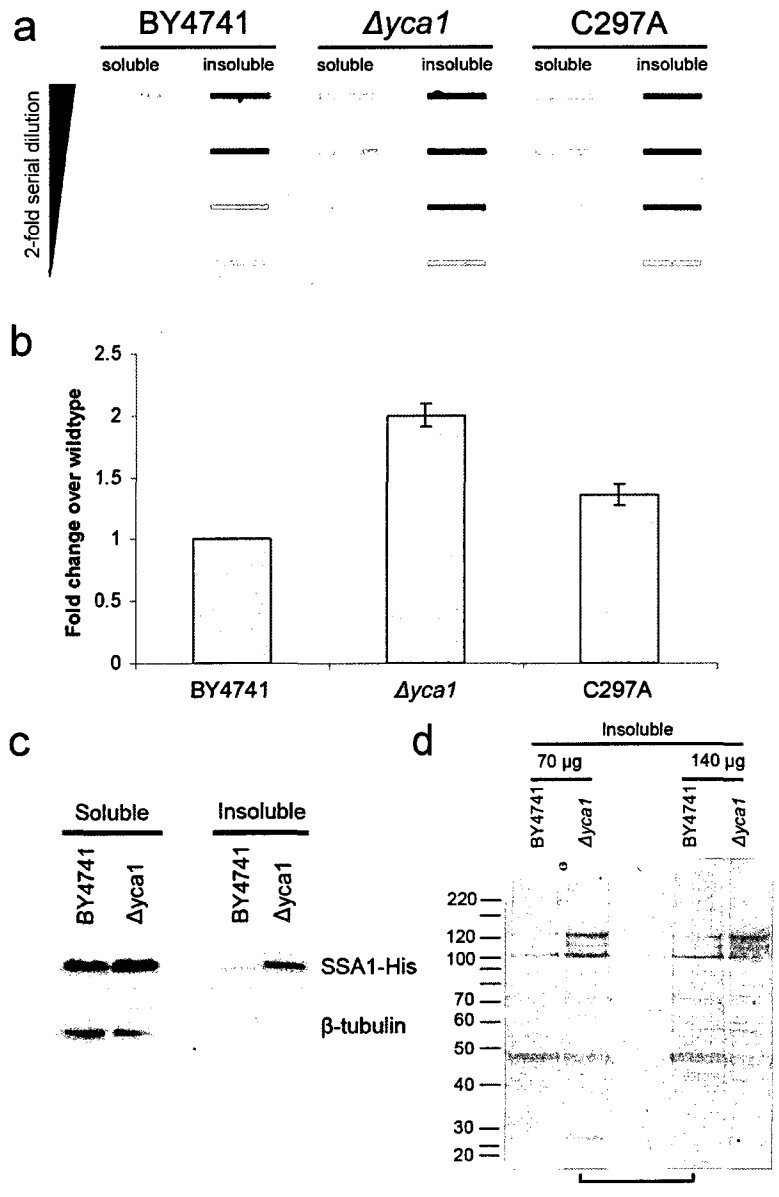

Figure 3| Caspase mutants accumulate insoluble aggregate material during logarithmic growth.

a, Filter trap analysis of soluble and insoluble fractions from equal amounts of total wild-type (BY4741), *Δyca1* and C297A lysates. **b,** Densitometry analysis of insoluble fractions from filter trap assays (N=3, ± s.e.m.). **c,** Anti-HIS western blot of genomic HIS tagged SSA1 in the BY4741 and *Δyca1* backgrounds. **d,** Silver stained 1D PAGE gel of insoluble fractions from mid-logarithmic phase BY4741 and *Δyca1* lysates.

comparable with the intensity of the aggregate fraction from twice as much wild-type protein. Furthermore, the pattern of protein bands between the *Δyca1* and wild-type samples was not altered suggesting that the *Δyca1* strain accumulate protein aggregates of a non-specific composition rather than targeting individual protein species.

The molecular mechanism that directs YCA1 to insoluble protein aggregates is not clear. Interestingly, both full length YCA1 and the C-terminal catalytic fragment of YCA1 were observed to associate with the insoluble fraction (Fig. 2e). YCA1 contains a prion-like Q/N-rich amino-terminal domain (Alberti, Halfmann et al. 2009; Nemecek, Nakayashiki et al. 2009), a structural feature that may provide the aggregate targeting capacity for the yeast caspase. Here the C-terminal domain could remain associated with the insoluble fraction through dimerization with full length YCA1 or its N-terminal fragments. Localization of YCA1 with insoluble material might also be mediated by other protein interaction domains or regulatory co-factors independent of the prion domain. In these scenarios, the innate caspase-like proteolytic (Madeo, Herker et al. 2002) and trypsin-like (Uren, O'Rourke et al. 2000; Watanabe and Lam 2005) peptidase activity of YCA1 could act on aggregates to directly promote their clearance. To this effect, a general or co-factor dependent substrate affinity for YCA1 would explain why physiological substrates of YCA1 remain elusive. Finally, we observed that genomic expression of C297A can partially alleviate, but not correct, the autophagic and aggregate accumulation phenotypes. These observations are indicative of a non-proteolytic function whereby YCA1 might additionally stabilize aggregate remodeling complexes at the aggregate surface.

The current study suggests that the evolutionary origin of caspase function is rooted in both death and vital non-death roles. We propose a model whereby YCA1 acts to target and limit the formation of insoluble protein aggregates during the mitotic cell cycle and chronological aging (Fig. 4). In our model, the accumulation of protein aggregates in the absence of YCA1 leads to compensatory expression of stress response genes and autophagy mediated aggregate clearance (reviewed in (Komatsu, Ueno et al. 2007)). Intriguingly, mammalian caspases directly converge upon inclusions formed by ectopic expression of extended polyglutamines resulting in proximity induced casapse activation (U, Miyashita et al. 2001). Caspase mediated cleavage of amyloidogenic proteins has furthermore been hypothesized to be a primary contributing factor to the pathogenesis of multiple neurodegenerative disorders before commitment to apoptosis (Canu, Dus et al. 1998; Weidemann, Paliga et al. 1999; Wellington, Singaraja et al. 2000). In light of our current findings, caspase targeting and cleavage of aggregate prone proteins during neurodegeneration may also represent a general aggregate remodeling activity conserved from early eukaryotic metacaspases.

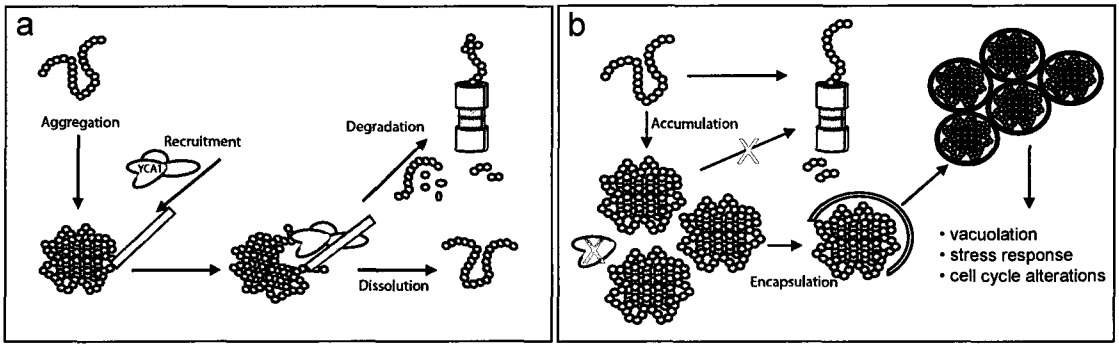

Figure 4| Model depicting the role of YCA1 in the balance of protein aggregate assembly and dissolution.

A schematic diagram illustrating a role for YCA1 in the regulation of protein aggregate accumulation in **a,** wild-type and **b,** *Δyca1* yeast strains. In wild-type cells (a), YCA1 targets insoluble protein aggregates and co-operates with heat shock proteins to promote aggregate clearance. The improved aggregate clearance in the C297A inactivation mutant suggests that YCA1 may participate in a recruitment process to regulate aggregate remodeling complexes at the aggregate surface. In caspase deletion mutants (**b**), the balance of aggregate formation and disassembly is disrupted favoring their accumulation. The amassing aggregates are too large to be processed by the 20s proteasome pathway and instead require autophagic encapsulation and a concomitant stress response for efficient removal.

3.1.4 Acknowledgements:

The authors would like to thank Drs. Jeff Dilworth, Michael Rudnicki and Valerie Wallace for insightful discussion. In addition the authors would like to thank Leslie Mitchell, Derek Smith and Laila Lee for assistance and support. R.E.C.L. was supported by an Ontario Graduate Student Scholarship. This study was supported by grants to L.A.M. from the Canadian Institutes of Health Research. L.A.M. is the Mach-Gaennslen Chair in Cardiac Research.

3.2 Supplementary information:

The Metacaspase YCA1 is required for Clearance of Insoluble Protein Aggregates

Robin E. C. Lee[1,2], Steve Brunette[2], Lawrence G. Puente[2], Lynn A. Megeney[1,2,3]

[1] Department of Cellular and Molecular Medicine, University of Ottawa, Ottawa, Canada

[2] Ottawa Hospital Research Institute, Sprott Centre for Stem Cell Research, Ottawa, Canada

[3] To whom correspondence should be addressed

3.2.1 Supplementary Materials and Methods:

Strains and growth conditions:

All *S. cerevisiae* strains used in this study were derived from the wild-type haploid BY4741 (MATa his3Δ1 leu2Δ0 met15Δ0 ura3Δ0) strain. The *Δyca1* and the YCA1-TAP strains were obtained from Open Biosystems (Huntsville, AL.). The YCA1-GFP strain was obtained from Invitrogen (Burlington, Canada). The C297A-TAP, TAP control strain and SSA1-HTF strains were generated via genomic integration as described in the molecular biology section. RFP fusion proteins were expressed from centromeric plasmids. Samples were grown in YPDm (1% yeast extract, 2% peptone, 2% glucose pH buffered to 3.5 with HCl) for protein expression, fractionation and vacuole morphology experiments. To examine the localization of fluorescent fusion proteins, samples were grown in synthetic media (complete or with trophic marker dropout as required). All samples were inoculated from starter cultures then grown at 30° C with 250 RPM orbital rotation into mid-logarithmic phase unless otherwise stated. All of the strains used in this study are summarized in supplementary table 2.

Microscopy:

To examine the effect of caspase deletion and inactivation on vacuolar morphology BY4741, ΔYCA1 and C297A strains were grown to log phase in YPDm (1% yeast extract, 2% peptone, 2% glucose pH buffered to 3.5 with HCl) and diluted to an OD660 of 0.2 in the same pre-warmed media at 30°C. The cultures continued to grow for 2 hours (OD660 = 0.4-0.5) at which point FM4-64 (Molecular Probes, Burlington, Ontario) was added to a final concentration of 20μM. The cultures were incubated in FM4-64 over the 40 minute pulse period. The cells were then pelleted, washed and resuspended in an equal volume of fresh pre-warmed media. Cultures continued to grow over the 2 hour chase period allowing more than sufficient time for the dye to label vacuoles exclusively. Post-chase cells were immediately viewed with an Axioplan 2 compound microscope fitted with a Zeiss Axiocam (63× magnification, PlanApochromat 1.4 NA objective lens, 22°C). Live cells expressing GFP and RFP fusions were grown in synthetic media (dropout or complete as required) and viewed similarly with appropriate filters.

Immunoblots:

Samples for immunoblots were grown to mid-logarithmic phase in YPDm. Protein was extracted in buffer C (50 mM Tris-HCL, 1% NP-40, 150mM NaCl 1mM EDTA 1% Glycerol, supplemented with 5 mM Na_3VO_4 and 10 μg/mL each aprotinin, pepstatin, leupeptin and PMSF) via glass bead disruption, separated by PAGE and blotted onto a PVDF membrane. Immunodetection was performed using anti-TAP (Open Biosystems, Huntsville, AL.), anti-HIS 27E8 monoclonal antibody (Cell Signaling, Beverly,

Massachusetts) and anti-ß-tubulin (Iowa State University Hybridoma Bank) primary antibodies. Soluble and insoluble fractions were separated in buffer C as described for the filter trap experiment (Supplementary methods). Insoluble fractions were resuspended in equivalent volumes of lysis buffer and vortexed at 4°C for 5 minutes. Insoluble protein samples were then boiled for 10 min in Laemmli buffer before separation by PAGE.

Molecular biology:

The C-TAP tag construct (Rigaut, Shevchenko et al. 1999) was amplified from the pBS1479 plasmid (Euroscarf, Frankfurt, Germany) and inserted into the pSSB08 vector (a generous gift of Mads Kaern) on its own or as a C-terminal fusion of the C297A catalytic inactivation mutant (Lee, Puente et al. 2008). The C297A-TAP construct was amplified and inserted into the endogenous *yca1* gene locus with Leu2 as a prototrophic marker as described previously (Lee, Puente et al. 2008). The TAP construct with an in-frame start codon was similarly expressed from the *ade2* genomic locus and the resulting strain was grown in media supplemented with adenine hemisulfate (Sigma-Aldrich, Ontario). The C-terminal HisTevFlag tag construct was amplified from the pBRIT-Pax7-CTAP (McKinnell, Ishibashi et al. 2008) vector (kind gift of Michael Rudnicki). This construct was inserted into the EcoR1/Asc1 sites of pRS406 and used as a template to create genomic C-terminal HTF fusion strains with *ura3* prototrophy.

The pRP1574 (generous gift of Roy Parker) plasmid harboring the EDC3-mCherry was expressed in various background to mark P-Bodies (Buchan, Muhlrad et al. 2008; Nissan and Parker 2008). HSP104 was amplified from the *hsp104* gene locus along with its 334 base pair promoter region (Grably, Stanhill et al. 2002). The construct was

fused to RFP using the Sal1/BamH1 restriction sites of the pRP1186 vector (kind gift of Roy Parker) to generate HSP104-RFP fusion strains. The C297A-RFP fusion strain was constructed by amplifying the C297A with the 249 bp of the *yca1* promoter region from the C297A strain described previously (Lee, Puente et al. 2008). This construct was similarly ligated between the Sal1/BamH1 restriction sites of pRP1186.

Genomic and plasmid integrants were constructed using standard LiAc transformation methods (Gietz and Schiestl 2007). All primer sequences that were used for plasmid based integration or integration of constructs into genomic loci are summarized in supplementary table S3.

iTRAQ:

Wild-type and *Δyca1* strains were grown to log phase in YPDm. Samples were lysed by glass bead agitation in buffer A (50 mM Hepes, 4 M Urea and 0.1% SDS) and clarified by centrifugation at 15000×g for 20 minutes at 4°C. 100 µg of protein was processed, trypsin digested, iTRAQ labeled and analyzed at the University of Victoria-Genome BC Proteomics Centre as described previously (Lippert, Ralph et al. 2009). Data files were processed using the Protein Pilot software (Applied Biosystems, Foster City) with a detected protein confidence threshold above 95% (unused Protscore of 1.3).

Filter TRAP and 1D gel analysis of protein aggregates:

Soluble and aggregate fractions of protein lysates were collected and processed as described (Cashikar, Duennwald et al. 2005; Haslbeck, Miess et al. 2005; Rand and Grant 2006) with the following adjustments. Cells were grown to mid-logarithmic phase in

YPDm. An equal number of cells (30 A_{660} units) were pelleted and stored at -80°C for later processing. The pellets were thawed in equal volumes (500 µL) of buffer B (0.1% NP-40, 50 mM Tris pH7.4, 1 mM EDTA, 1% glycerol supplemented with 5 mM Na_3VO_4 and 10 µg/mL each aprotinin, pepstatin, leupeptin and PMSF) and acid washed glass beads (Sigma-Aldrich, Ontario). A crude yeast lysate was formed using a Disruptor Genie (Scientific Industries, New York) with six alternating cycles of 1 minute on followed by 1 minute off at 4°C. Cell debris was removed by sequential spins of 2000 and 3000 RPM at 4°C in a 5417r microcentrifuge (Eppendorf, Ontario). 300 µL of supernatant was carefully collected yielding a total protein extract (TPE). The protein concentrations of all samples were determined via the Bradford assay and normalized. Equal volumes of TPE were centrifuged at 15000×g for 15 minutes at 4°C to separate the soluble and insoluble fractions. The insoluble fractions were washed in 320 µL buffer B supplemented with 80 µL of 10% NP-40 followed by centrifugation at 15000×g for 15 minutes. The wash step was repeated two times to remove membrane proteins. The protein aggregate fractions were then re-suspended in an equal volume of buffer B. Serial dilutions of soluble and insoluble fractions resulting from 300 µg of TPE material were subjected to either vacuum filtration through a 0.45 µM Immobilon PVDF membrane (Sigma Aldrich, Ontario, Canada) using a BioDot SF microfiltration apparatus (Bio-Rad Laboratories, Hercules, CA) or 1D PAGE separation for silver stain. Filter trap membranes were stained with coomassie blue and slot intensity was determined by densitometry with ImageJ software. A standard curve was generated using the serial dilutions of the wild-type sample to correct for non-linearity and comparison with bands from caspase mutant lysates.

TAP pulldown:

YCA1-TAP associated protein complexes were purified by one-step affinity purification essentially as described (Mitchell, Lambert et al. 2008) with the following modifications. Yeast cultures were grown into log phase in YPDm, collected, washed and lysed in buffer D (20 mM HEPES, pH 7.4, 0.1% Tween 20, 2 mM $MgCl_2$, 300 mM NaCl supplemented with protease inhibitors) by glass bead disruption at 4°C. Lysates were clarified by centrifugation at 20000 ×g for 15 minutes and protein concentration was determined by Bradford assay. 100 µL of magnetic Dynabeads (Invitrogen) conjugated to rabbit IgG (Chemicon) were added to 17 mg of lysate in a normalized volume of buffer D. YCA1-TAP associated proteins were precipitated over 3 hours at 4°C. Beads were washed, YCA1-TAP and associated proteins were eluted as described (Mitchell, Lambert et al. 2008). Samples were resolved on a 10% polyacrylamide gel and silver stained. YCA1-TAP interacting bands were identified by mass spectrometry.

MS analysis of TAP bands:

In-gel digest was performed by the method of Shevchenko (Shevchenko, Tomas et al. 2006). Liquid chromatography - tandem mass spectrometry (LC-MS/MS) was performed at the OHRI Proteomics Facility (Ottawa, Canada) using a Thermo LTQ linear ion trap mass spectrometer. Spectra were matched to protein identities using Mascot 2.0 (Matrix Science, UK) and the NCBI non-redundant protein sequence database. Parameters used for data analysis were MS tolerance +/- 1.6 Da, MS/MS tolerance +/- 0.8

Da, <=1 miscut, variable modifications: oxidation of methionine, carbamidomethylation of cysteine. The complete list of identified proteins appears in Supplementary Fig. 3.

The Metacaspase YCA1 is required for Clearance of Insoluble Protein Aggregates

Robin E. C. Lee[1,2], Steve Brunette[2], Lawrence G. Puente[2], Lynn A. Megeney[1,2,3]

[1] Department of Cellular and Molecular Medicine, University of Ottawa, Ottawa, Canada

[2] Ottawa Hospital Research Institute, Sprott Centre for Stem Cell Research, Ottawa, Canada

[3] To whom correspondence should be addressed

3.2.2 Supplementary Tables

Supplementary tables S1 – S3

Table S1| iTRAQ analysis of *Δyca1* versus wild-type lysates.

Summary of protein species observed to undergo greater than 20% regulation in the *Δyca1* strain compared to wild-type.

Name	Ordered locus name	yca1-:wt	Name
AAC2	YBL030C	1.3794	ADP,ATP carrier protein AAC2 precursor - yeast (Saccharomyces cerevisiae)
ACO1	YLR304C	1.4282	aconitate hydratase (EC 4.2.1.3) precursor - yeast (Saccharomyces cerevisiae)
APE3	YBR286W	1.208	aminopeptidase Y (EC 3.4.11.-) precursor, vacuolar - yeast (Saccharomyces cerevisiae)
ARP3	YJR065C	1.2108	actin-related protein ARP3 - yeast (Saccharomyces cerevisiae)
BAT2	YJR148W	0.8026	branched-chain-amino-acid transaminase (EC 2.6.1.42) BAT2, cytosolic - yeast (Saccharomyces cerevisiae)
CHC1	YGL206C	1.2143	clathrin heavy chain 1 - yeast (Saccharomyces cerevisiae)
COR1	YBL045C	1.6738	ubiquinol-cytochrome-c reductase (EC 1.10.2.2) 44K core protein precursor - yeast (Saccharomyces cerevisiae)
CYT1	YOR065w	1.7671	Cytochrome c1 (Fragment).- Saccharomyces cerevisiae (Baker's yeast).
DAK1	YML070W	1.5204	hypothetical protein YML070w - yeast (Saccharomyces cerevisiae)
DBP5	YOR046C	1.342	probable RNA helicase CA5/6 - yeast (Saccharomyces cerevisiae)
DDR48	YMR173W	1.382	heat shock protein DDR48 - yeast (Saccharomyces cerevisiae)
DED82	YHR020W	0.793	multifunctional amino acid-tRNA ligase homolog - yeast (Saccharomyces cerevisiae)
END3	YNL084C	1.2158	END3 protein - yeast (Saccharomyces cerevisiae)
ENO1	YGR254W	1.21	phosphopyruvate hydratase (EC 4.2.1.11) 1 - yeast (Saccharomyces cerevisiae)
GLK1	YCL040W	1.5253	glucokinase (EC 2.7.1.2) - yeast (Saccharomyces cerevisiae)
GLN1	YPR035W	0.7969	glutamate-ammonia ligase (EC 6.3.1.2) - yeast (Saccharomyces cerevisiae)

GPD1	YDL022W	1.293	Glycerol-3-phosphate dehydrogenase [NAD+] 1 (EC 1.1.1.8).- Saccharomyces cerevisiae (Baker's yeast).
GRE3	YHR104W	1.4273	hypothetical protein YHR104w - yeast (Saccharomyces cerevisiae)
GSY2	YLR258W	1.849	glycogen(starch) synthase (EC 2.4.1.11) 2 - yeast (Saccharomyces cerevisiae)
GTT1	YIR038C	1.5134	hypothetical protein YIR038c - yeast (Saccharomyces cerevisiae)
HEM15	YOR176W	1.2253	ferrochelatase (EC 4.99.1.1) precursor - yeast (Saccharomyces cerevisiae)
HSP104	YLL026W	1.3584	endopeptidase Clp (EC 3.4.21.-) ATP-binding chain HSP104 [similarity] - yeast (Saccharomyces cerevisiae)
HSP12	YFL014W	3.7433	heat shock protein 12 - yeast (Saccharomyces cerevisiae)
HSP82	YPL240C	1.2313	heat shock protein 90 - yeast (Saccharomyces cerevisiae)
LAP4	YKL103C	1.6466	SCAPE1 NID: - Saccharomyces cerevisiae
LAT1	YNL071W	1.2517	dihydrolipoamide S-acetyltransferase (EC 2.3.1.12) precursor - yeast (Saccharomyces cerevisiae)
LSP1	YPL004C	1.3869	hypothetical protein YPL004c - yeast (Saccharomyces cerevisiae)
MCR1	YKL150W	1.8044	cytochrome-b5 reductase (EC 1.6.2.2), mitochondrial outer membrane form - yeast (Saccharomyces cerevisiae)
MIR1	YJR077C	1.2866	phosphate transport protein MIR1, mitochondrial - yeast (Saccharomyces cerevisiae)
MSC1	YML128C	2.2414	probable membrane protein YML128c - yeast (Saccharomyces cerevisiae)
PEP4	YPL154C	1.3918	saccharopepsin (EC 3.4.23.25) precursor - yeast (Saccharomyces cerevisiae)
PGM2	YMR105C	2.1375	phosphoglucomutase (EC 5.4.2.2) PGM2 - yeast (Saccharomyces cerevisiae)
POR1	YNL055C	1.2399	SCPORIN NID: - Saccharomyces cerevisiae
PRB1	YEL060c	1.4756	cerevisin (EC 3.4.21.48) precursor - yeast (Saccharomyces cerevisiae)
PRC1	YMR297W	1.3872	carboxypeptidase C (EC 3.4.16.5) precursor [validated] - yeast (Saccharomyces cerevisiae)
PRD1	YCL057W	1.2472	saccharolysin (EC 3.4.24.37) - yeast (Saccharomyces cerevisiae)
PST2	YDR032C	1.394	hypothetical protein YDR032c - yeast (Saccharomyces cerevisiae)

REP2	R0040C	0.5189	REP2 protein - yeast (Saccharomyces cerevisiae) plasmid
RIB4	YOL143C	1.2522	SEQUENCE 7 FROM PATENT WO9411515.- Saccharomyces cerevisiae (Baker's yeast).
RNH70	YGR276C	1.3055	hypothetical protein YGR276c - yeast (Saccharomyces cerevisiae)
RNR1	YER070W	0.7807	ribonucleotide reductase (EC 1.17.4.-) large chain 1 - yeast (Saccharomyces cerevisiae)
RPA49	YNL248C	0.671	DNA-directed RNA polymerase (EC 2.7.7.6) A chain RPA49 - yeast (Saccharomyces cerevisiae)
RPC37	YKR025W	0.8038	hypothetical protein YKR025w - yeast (Saccharomyces cerevisiae)
RPL14B	YHL001W	1.2238	ribosomal protein L14.e.B, cytosolic - yeast (Saccharomyces cerevisiae)
RPL33B	YOR234C	1.6706	ribosomal protein L35a.e.c15, cytosolic - yeast (Saccharomyces cerevisiae)
RPL4B	YDR012W	0.7734	60S ribosomal protein L4-B (L2B) (RP2).- Saccharomyces cerevisiae (Baker's yeast).
RPN12	YFR052W	0.7595	26S proteasome regulatory complex chain RPN12 - yeast (Saccharomyces cerevisiae)
RPN8	YOR261C	1.2928	26S proteasome regulatory particle chain RPN8 - yeast (Saccharomyces cerevisiae)
SEC27	YGL137W	1.3294	coatomer complex beta' chain - yeast (Saccharomyces cerevisiae)
SOD2	YHR008C	1.2455	superoxide dismutase (EC 1.15.1.1) (Mn) precursor - yeast (Saccharomyces cerevisiae)
SSA1	YAL005C	1.2139	Heat shock protein SSA1 (Heat shock protein YG100).- Saccharomyces cerevisiae (Baker's yeast).
SSA4	YER103W	1.3618	Heat shock protein SSA4.- Saccharomyces cerevisiae (Baker's yeast).
SSO1	YPL232W	1.2189	syntaxin-related protein SSO1 - yeast (Saccharomyces cerevisiae)
TCB3	YML072C	1.2409	probable membrane protein YML072c - yeast (Saccharomyces cerevisiae)
TDH1	YJL052W	1.8609	Glyceraldehyde-3-phosphate dehydrogenase 1 (EC 1.2.1.12) (GAPDH 1).- Saccharomyces cerevisiae (Baker's yeast).
TMA108	YIL137C	1.3241	hypothetical protein YIL137c - yeast (Saccharomyces cerevisiae)
TPS1	YBR126C	1.278	alpha,alpha-trehalose-phosphate synthase (UDP-forming) (EC 2.4.1.15) 56K chain - yeast (Saccharomyces cerevisiae)
TPS2	YDR074W	1.8997	trehalose-phosphatase (EC 3.1.3.12) - yeast (Saccharomyces cerevisiae)

UBC4	YBR082C	1.2021	ubiquitin-protein ligase (EC 6.3.2.19) UBC4 - yeast (Saccharomyces cerevisiae)
UGP1	YKL035W	1.484	probable UTP-glucose-1-phosphate uridylyltransferase (EC 2.7.7.9) - yeast (Saccharomyces cerevisiae)
UTR2	YEL040W	0.7816	UTR2 protein - yeast (Saccharomyces cerevisiae)
WTM1	YOR230W	1.2279	transcription modulator WTM1 - yeast (Saccharomyces cerevisiae)
YBR056W	YBR056W	1.4557	probable glucan 1,3-beta-glucosidase (EC 3.2.1.58) YBR056w - yeast (Saccharomyces cerevisiae)
YBT1	YLL048C	1.3999	probable membrane protein YLL048c - yeast (Saccharomyces cerevisiae)
YCP4	YCR004C	1.37	hypothetical protein YCR004c - yeast (Saccharomyces cerevisiae)
YET3	YDL072C	1.3235	probable membrane protein YDL072c - yeast (Saccharomyces cerevisiae)
YKR043C	YKR043C	0.7768	hypothetical protein YKR043c - yeast (Saccharomyces cerevisiae)
YME2	YMR302C	1.3095	RNA12 protein - yeast (Saccharomyces cerevisiae)
YOL057W	YOL057W	1.4033	hypothetical protein YOL057w - yeast (Saccharomyces cerevisiae)
YOR051C	YOR051C	0.6977	hypothetical protein YOR051c - yeast (Saccharomyces cerevisiae)
YRA1	YDR381W	0.6807	SCU72633 NID: - Saccharomyces cerevisiae
ZWF1	YNL241C	1.2006	YSCG6PD NID: - Saccharomyces cerevisiae

Table S2| List of yeast strains used in this study.

StrainID	Construct	Background strain	Source	Notes	Auxotrophic marker
BY4741	-	-	a		-
ΔYCA1	-	BY4741	a		-
YCA1-C-TAP	-	BY4741	a	Genomic C-TAP - YCA1 locus	-
YCA1-GFP	-	BY4741	b	Genomic C-TAP - YCA1 locus	-
yLM0001	C297A	ΔYCA1	c	Genomic Integration - YCA1 locus	Leu2
yLM4001	C297A-C-TAP	ΔYCA1	This Study	Genomic Integration - ADE2 locus	Leu2
yLM4002	C-TAP	BY4741	This Study	Genomic Integration - ADE2 locus	Leu2
yLM1002	HSP104-RFP	YCA1-GFP	This Study	Plasmid Expression (pLMxxxx)	Ura3
yLM1004	C297A-RFP	ΔYCA1	This Study	Plasmid Expression (pLMxxxx)	Ura3
yLM1005	C297A-RFP	YCA1-GFP	This Study	Plasmid Expression (pLMxxxx)	Ura3
yLM3000	SSA1-HTF	BY4741	This Study	Genomic C-HTF - SSA1 locus	Ura3
yLM3004	SSA1-HTF	ΔYCA1	This Study	Genomic C-HTF - SSA1 locus	Ura3

a - Open Biosystems
b - Invitrogen
c - doi:10.1371/journal.pone.0002956

Table S3| List of primers used in this study. The listed oligos were used to construct the indicated plasmids and yeast strains.

For strain/plasmid	Notes	Template	Sequence
pC297A-C-TAP	C-TAP_HINDIII_F	pBS1479	GGGAAGCTTGGAGGATCCATGGAAAAGAG
pC297A-C-TAP	C-TAP XHO1 R	pBS1479	GGGCTCGAGTCAGGTTGACTTCCCCGCGG
pC297A-C-TAP	C297A_BAMH1_F	*C297A gDNA	GGGGGATCCATGAAGATGAGCCTCGAAGT
pC297A-C-TAP	C297A HINDIII R	*C297A gDNA	GGGAAGCTTCTACATAATAAATTGCAGAT
pLM1002	HSP104_RFP_SAL1_F	BY4741 gDNA	GGGGTCGACAACCCTCCATCGTGGTAGTGTTTGCTGTTC CTAAC
pLM1002	HSP104_RFP_BAMH1_R	BY4741 gDNA	GGGGGATCCATCTAGGTCATCATCAATTTCCATACTGTCC TCAT
pLM1004	C297A_RFP_SAL1_F	*C297A gDNA	GGGGTCGACATTATTGTGGCTTAACAGTTCTCCTTAAAAT CCAC
pLM1004	C297A_RFP_BAMH1_R	*C297A gDNA	GGGGGATCCCATAATAAATTGCAGATTTACGTCAATAGG GTGTG
pLMHTF	HTF_ECOR1_F	pBRIT-Pax7-CTAP	GGGGAATTCCATCACCATCACCATCACG
pLMHTF	HTF_ASC1_R	pBRIT-Pax7-CTAP	GGGGGCGCGCCATCTCTAGACTACTTGTCATCG
yLM3000 & yLM3004	SSA1_HTF_F	pLMHTF	AGCTCCAGAGGCTGAAGGTCCAACCGTTGAAGAAGTTG ATCATCACCATCACCATCACG
yLM3000 & yLM3004	SSA1_HTF_R	pLMHTF	GACATTTTCGTTATTATCAATTGCCGCACCAATTGGCTTAT GTGAGTTTAGTATACATGC
yLM4001	yca1 locus integration F	pC297A-C-TAP	CTATTGAAAAAGCATGGCTTCGCATTAATAGGAGCCAAA AATATGAAGATGAGCCTCGAAG
yLM4001	yca1 locus integration R	pC297A-C-TAP	ACCAGTCTGAATACATCTACCAACGTACACATTCATATAT TTTTTTTAAGCAAGGATTTTCT

* C297A (yLM0001) strain described in doi:10.1371/journal.pone.0002956

The Metacaspase YCA1 is required for Clearance of Insoluble Protein Aggregates

Robin E. C. Lee[1,2], Steve Brunette[2], Lawrence G. Puente[2], Lynn A. Megeney[1,2,3]

[1] Department of Cellular and Molecular Medicine, University of Ottawa, Ottawa, Canada

[2] Ottawa Hospital Research Institute, Sprott Centre for Stem Cell Research, Ottawa, Canada

[3] To whom correspondence should be addressed

3.2.3 Supplementary Figures:

Supplementary figures S1 – S6

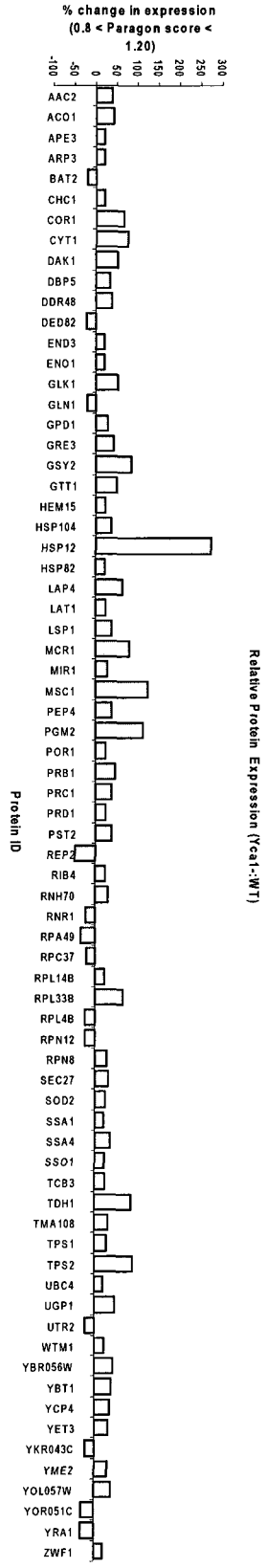

Figure S1| iTRAQ analysis identifies protein species that undergo significant change in Δyca1 cells. Ratios of protein species from Δyca1 and wild-type cells (Δyca1/WT) based on iTRAQ results. Proteins with greater than 20% change in expression were retained resulting in 59 up-regulated and 13 down-regulated proteins. The remaining 493 proteins identified in the iTRAQ experiment were considered unchanged.

a

Category	Hypergeometric p-value	In Category from Cluster	found	known
vacuolar protein catabolism [GO:0007039]	**1.288e-09**	**APE3 PRB1 LAP4 PRC1 PEP4**	**5**	**7**
response to stress [GO:0006950]	2.277e-07	UBC4 TPS1 GPD1 TPS2 PRB1 SSA4 HSP12 GRE3 MCR1 HSP104 PEP4 HSP82	12	199
carbohydrate metabolism [GO:0005975]	2.831e-07	TPS1 GLK1 TPS2 ENO1 GRE3 TDH1 UGP1 GSY2 ACO1 PGM2 ZWF1	11	165
cell growth and/or maintenance [GO:0008151]	2.716e-06	SSA1 PET9 COR1 UBC4 TPS1 APE3 GLK1 PRD1 GPD1 TPS2 PRB1 SSA4 HSP12 SEC27 CHC1 ENO1 RNH70 RPL14B SOD2 GRE3 GTT1 TDH1 ARP3 MIR1 UGP1 LAP4 MCR1 HSP104 YBT1 GSY2 ACO1 DAK1 MSC1 PGM2 DDR48 PRC1 PRP12 POR1 LAT1 END3 ZWF1 RIB4 DBP5 CYT1 HEM15 WTM1 RPL33B RPN8 PEP4 SSO1 HSP82	51	3657
metabolism [GO:0008152]	2.85e-06	SSA1 COR1 UBC4 TPS1 APE3 GLK1 PRD1 TPS2 PRB1 SSA4 HSP12 SEC27 ENO1 RNH70 RPL14B SOD2 GRE3 GTT1 TDH1 UGP1 LAP4 MCR1 HSP104 GSY2 ACO1 DAK1 MSC1 PGM2 DDR48 PRC1 PRP12 POR1 LAT1 ZWF1 RIB4 DBP5 CYT1 HEM15 RPL33B RPN8 PEP4 SSO1 HSP82	43	2693

b

Category	Hypergeometric p-value	In Category from Cluster	found	known
vacuolar lumen	7.145e-10	APE3 PRB1 LAP4 PRC1 PEP4	5	6
cytoplasm	4.401e-07	SSA1 CDC19 UBC4 TPS1 GLK1 PRD1 GPD1 TPS2 SSA4 CHC1 ENO1 RPL14B TDH1 TIF2 HSP104 GSY2 ACO1 PGM2 ZWF1 RPL33B HSP82	21	593
vacuole	2.054e-05	APE3 PRB1 LAP4 YBT1 PRC1 PEP4	6	54
mitochondria	4.59e-05	PET9(AAC2) COR1 PRD1 TPS2 SOD2 MIR1 MRP8 MCR1 ACO1 PRP12(YME2) POR1 LAT1 CYT1 HEM15	14	388

c

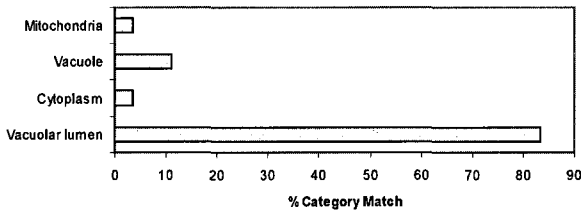

Figure S2| GO biological process and MIPS subcellular localization Funspec clusters of proteins up-regulated in *Δyca1*.

a, b, Protein species up-regulated in the *Δyca1* strain were used to identify clusters based on (**a**) GO biological process and (**b**) MIPS subcellular localization with a p-value cutoff 5x10-5. **c,** % Category match based on MIPS subcellular localization.

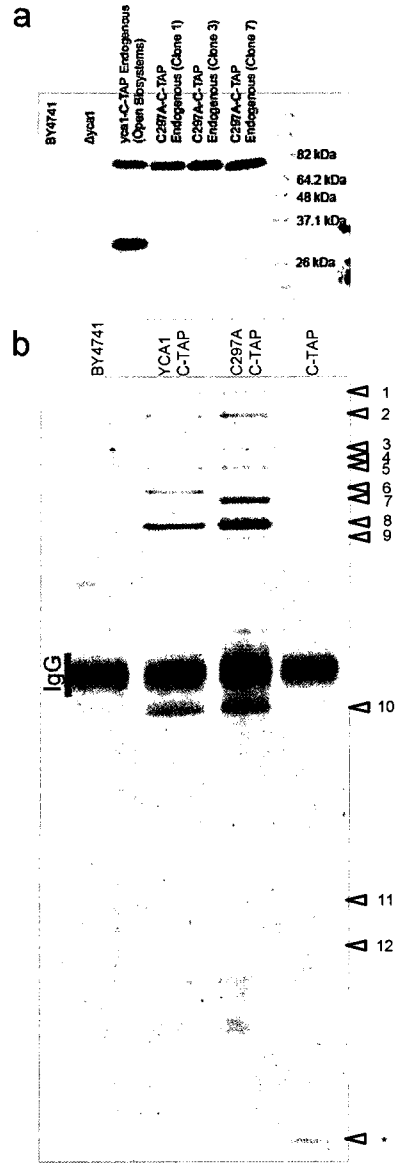

c

Band Number	Name	Predicted MW	Band Size	Mascot Score	
1	RNR1	99.6	100	249	
1	CDC48	92	100	662	
2	EFT2	93.2	95	1347	
2	SEC26	108	95	175	
2	SEC27	99.4	95	494	
3	MKT1	94.5	92	529	
4	PRT1(CDC63)	88.1	88	73	
5	HSC82	80.9	85	506	
5	HSP90	81.5	85	426	
6/7	YCA1/C297A	78	78	300	
8	SSA1/2(HSP70)	69.5	70	347	
9	DED1	65.5	67	246	
9	SSB1/2	66.5	67	572	
10	HSP42	42.8	44	113	
10	YDJ1(HSP40)	44.6	44	63	
10	TEF1	50	44	555	
11	SEC28	41.5	35	94	
11	RPP0	33.7	35	178	
11	RPL5	33.7	35	122	
12	RPS0A	28	30	121	
12	RPS3	26.5	30	128	
12	ASC1	34.8	30	227	
*	C-TAP	20	20	X	

d

Category	*Hypergeometric* p-value	In Category from Cluster	known	found
protein refolding [GO:0042026]	1.752e-07	SSA1 HSC82 YDJ1 HSP82	4	17
'de novo' protein folding [GO:0006458]	1.537e-06	HSC82 YDJ1 HSP82	3	8
response to stress [GO:0006950]	2.37e-05	SSA1 SSB1 HSP42 HSC82 YDJ1 HSP82	6	196
translational elongation [GO:0006414]	0.0001851	EFT2 RPP0 TEF1	3	36
translation [GO:0006412]	0.0002615	SSA1 SSB1 EFT2 RPS0A RPP0 RPS3 DED1 RPL5 TEF1	9	755

Figure S3| YCA1-TAP interacting proteins.

a, The C297A-TAP catalytic inactivation mutant fusion was expressed under the YCA1 promoter from the *yca1* gene locus and compared to a commercial C-terminal YCA1-TAP fusion strain. As described previously (Madeo, Herker et al. 2002), the catalytic fragment of the C297A-TAP does not form. **b,** Complete silver stained gel of TAP fusion interactors with the wild-type BY4741 and C-TAP controls. For the C-TAP strain the TAP construct was expressed in the *ade2* locus. **c,** List of protein IDs based on mass spectrometry of the silver stained protein bands. **d,** Funspec clusters of YCA1-TAP interacting proteins.

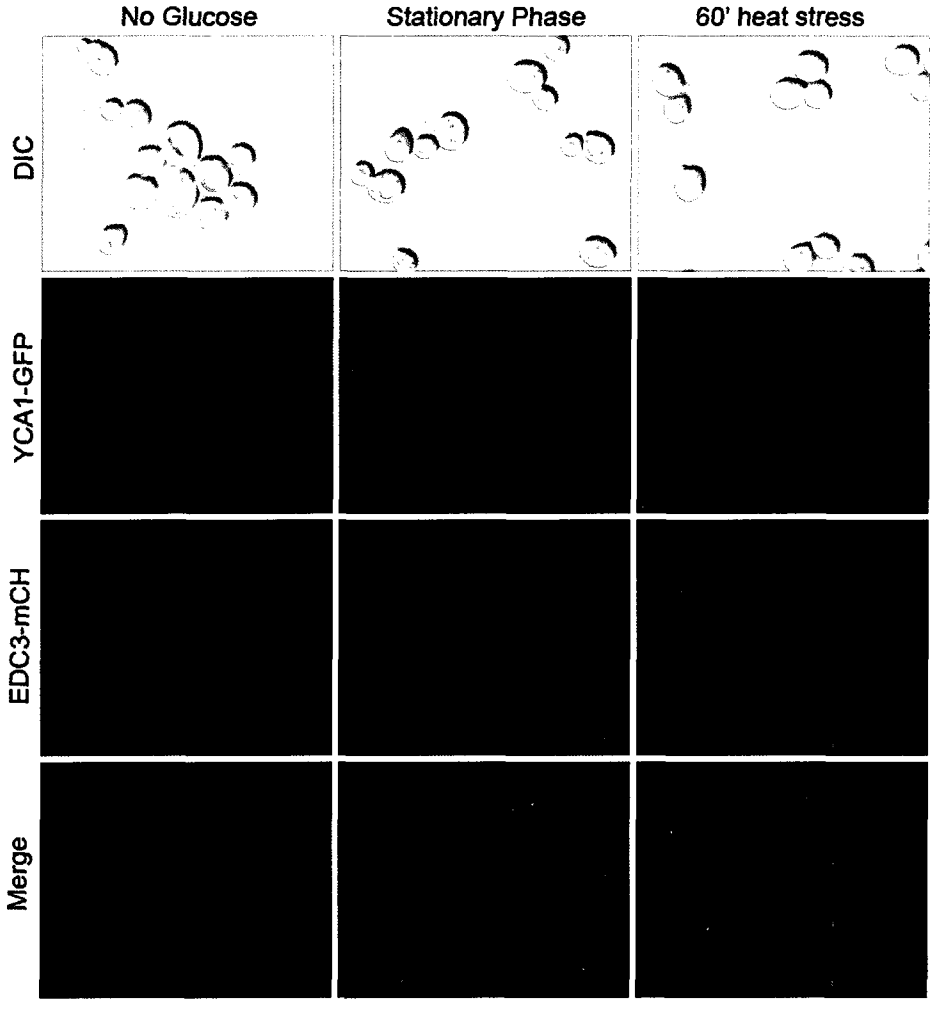

Figure S4| YCA1 does not significantly co-localize with mRNA processing bodies (P-bodies).

EDC3-mCherry was expressed under the control of its own promoter from the centromeric pRP1574 plasmid (Buchan, Muhlrad et al. 2008) (generous gift of Roy Parker). P-bodies were induced by glucose depletion for 10 minutes, by growing cultures into stationary phase (24 hour culture) or by 60 minutes of 42°C heat stress. When expressed in the YCA1-GFP background during glucose limitation or stationary phase there was no alterations to the YCA1-GFP localization within the cytoplasm. When cells were subjected to heat stress we observed the occasional co-localization of GFP and RFP foci, however, for the most part the GFP and RFP foci were distinct. Finally, when the pRP1574 plasmid was expressed in wild-type and Δyca1 backgrounds we did not observe any changes in the size or number of P-bodies in the various backgrounds (data not shown). Together these data suggest that YCA1 does not significantly influence p-body formation.

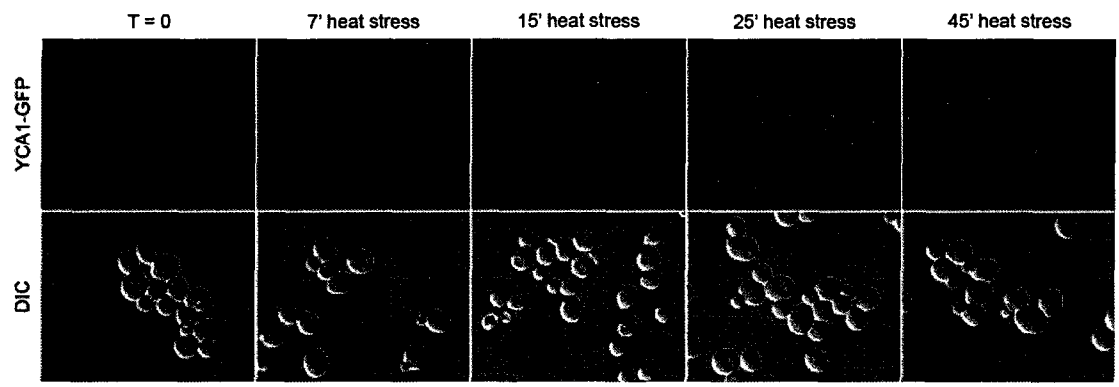

Figure S5| YCA1-GFP foci form rapidly in response to heat stress.

YCA1-GFP expressing cells were exposed to 42°C heat stress for the indicated amount of time. Seeds of GFP foci were apparent as early as 7 minutes after addition of heat. Within 15-25 minutes most cells had well developed GFP foci. After 45 minutes all cells have distinct foci.

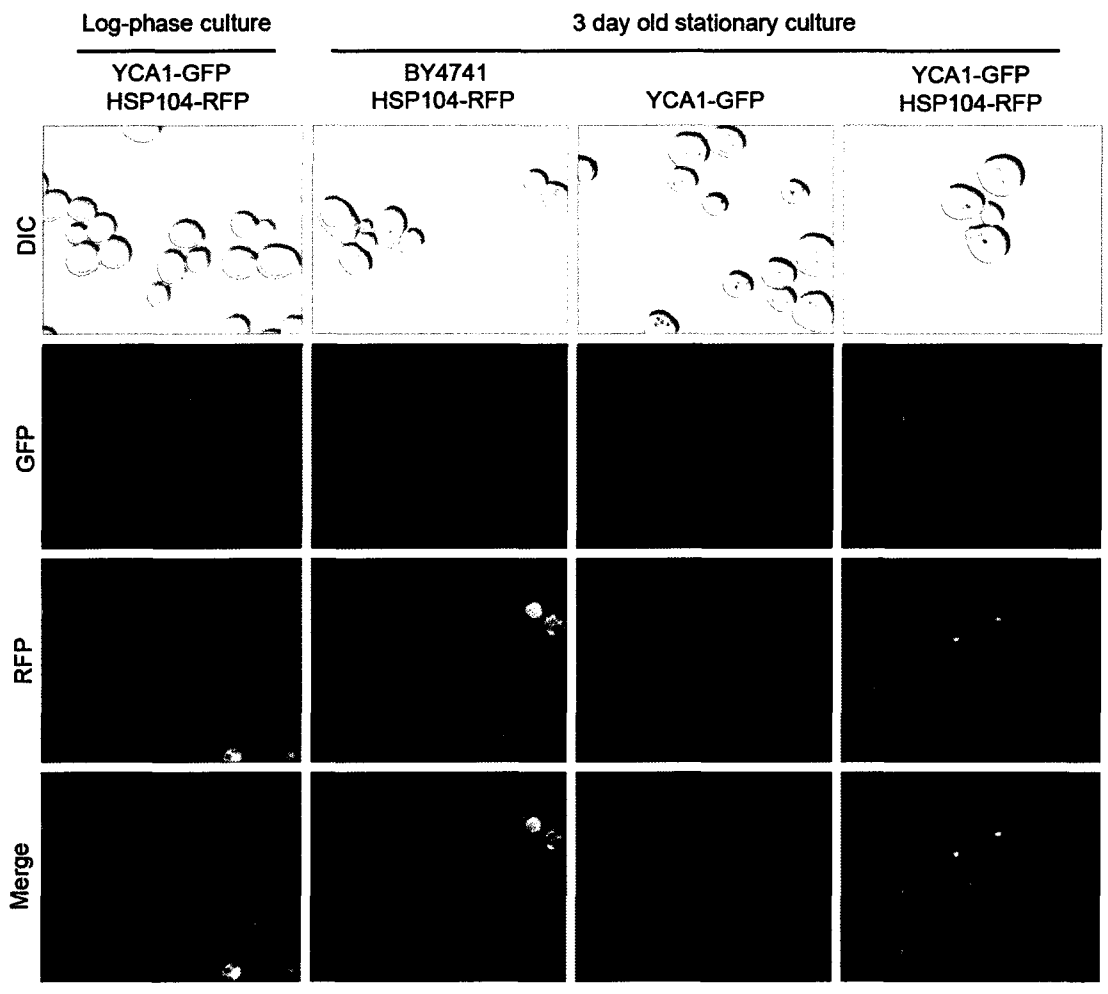

Figure S6| YCA1-GFP co-localizes with HSP104 foci formed in aged stationary cultures.

HSP104-RFP was expressed under its own promoter from a centromeric plasmid. During log-phase growth YCA1-GFP and HSP104-RFP were both diffuse within the cytosol. When cultures were grown well into stationary phase we observed the formation and co-localization of YCA1-GFP and HSP104-RFP foci suggesting that YCA1 targets to HSP104 positive protein aggregates in aged cultures.

CHAPTER 4

4.0 General Discussion

4.1 A non-death role for the yeast metacaspase YCA1

Here, we provide evidence that the yeast metacaspase YCA1 has an integral non-apoptotic function. We observed numerous alterations between *Δyca1* and wild-type in growth and proteomic studies that suggest caspase ablation affects multiple cell behaviours in logarithmic phase yeast. Specifically, we observed that caspase ablation and inhibition delay the progression through the cell cycle with phase-specific effects. Our proteomic study identified significant expression of vacuolar proteases and stress response proteins in *Δyca1*. Substantial vacuolation of the *Δyca1* strain validated this observation which together suggested an enhanced autophagic response in caspase ablated cells. We examined interactors of TAP tagged YCA1 and saw enrichment for chaperones associated with protein re-folding and stress response. The YCA1 localization experiments demonstrated that YCA1 forms discreet foci during heat stress and aging, foci that co-localize with the aggregate re-modeling chaperone HSP104. Finally, caspase deletion and inactivation strains accumulate insoluble aggregates during log-phase growth. Together these data support the premise that the yeast metacaspase co-operates with protein quality control machinery in baseline growth conditions to promote yeast fitness and adaptability in the absence of death-inducing environmental challenges. Specifically, we propose a role whereby YCA1 acts to directly target and degrade insoluble aggregates or to serve as a platform to promote aggregate clearance in co-operation with aggregate remodelling chaperones.

4.1.1 YCA1 and the cell cycle

YCA1 ablation and inactivation mutants demonstrate a slow growth phenotype during log phase conditions, with accelerated G2/M phases of the cell cycle and a prolonged G1/S transition. YCA1 inactivation mutants and wild type cells pre-treated with caspase inhibitors were all desensitized to the nocodazole (ND) induced mitotic checkpoint. Thus, YCA1 inactivation has pleiotropic effects on the cell cycle of log phase yeast in the absence of apoptotic stimulation.

Caspase and metacaspase activity have been previously observed to influence the G2/M spindle checkpoint machinery in animals and protozoa. For example, activated mammalian caspase-2 maintains the DNA damage-induced G2/M checkpoint in mouse embryonic fibroblasts allowing for additional time to repair damaged DNA (Shi, Vivian et al. 2009). Caspase-3 is expressed and activated specifically at the G2/M transition in human hepatoma and HeLa cells. Consistent with our findings in yeast, caspase-3 activity in HeLa cells is required for ND induced mitotic arrest (Hsu, Yu et al. 2006). The protozoan *L. major* metacaspase LmjMCA associates with mitotic spindle microtubules during mitosis. Expression of LmjMCA is tightly regulated whereby its knockout is lethal and over-expression causes both aneuploidy and slow growth (Ambit, Fasel et al. 2008). The slow growth and polyploidy phenotypes suggests that LmjMCA over-expression interferes with components of the mitotic checkpoint; however, the lethality induced by metacaspase deletion demonstrates that LmjMCA is also performing an essential but undefined function. Together these data suggest that the (meta)caspase-dependent influence on mitotic timing and the ND induced mitotic checkpoint is a conserved function.

Conceivably, a caspase/metacaspase dependent cleavage event may promote either a gain or loss of function for a protein regulator associated with the mitotic checkpoint. However, there is a paucity of known caspase-2 and LmjMCA substrates that could contribute to control of mitotic timing. Alternatively, caspase-3 has been observed to promote cleavage of at least 2 mitotic checkpoint regulators. Cleavage of the mitotic spindle checkpoint protein BUBR1 in HeLa cells is caspase-3 dependent and promotes cell death after prolonged exposure to ND possibly due to accumulation of toxic BUBR1 fragments (Kim, Murphy et al. 2005). Similarly, cleavage of the mitotic spindle checkpoint kinase BUB1 by caspase-3 potentiates etoposide induced apoptosis (Perera and Freire 2005). These data suggest that limited caspase/metacaspase action may be a conserved regulator of spindle checkpoint fidelity with the proviso that augmented caspase activity may promote apoptosis by targeting elements of the same checkpoint. Yeast homologues to these mitotic checkpoint genes are established regulators of the ND-induced mitotic checkpoint (Wang and Burke 1995) suggesting that YCA1 may target these proteins in a heterologous manner; however, true understanding of how YCA1 contributes to this process will require knowledge of the *in-vivo* substrate pool of YCA1.

Metacaspase deletion and inactivation mutants have prolonged doubling times due to substantial elongation of the G1 phase of the cell cycle. The influence of a caspase(s) on G1/S transition in higher eukaryotes is not well documented. Nevertheless, there is evidence to suggest that caspases may function in a similar capacity. For example, the initiator caspase, caspase-8 has a positive role in the G1/S transition of hepatocytes, by promoting the EGF-stimulated re-entry of quiescent cells into the cell cycle (Gilot, Serandour et al. 2005). This observation may directly complement an

observation in yeast whereby quiescent *Δyca1* cells fail to re-enter the cell cycle and establish new colonies when plated from aged cultures (Herker, Jungwirth et al. 2004). Additionally, heterologous expression of human initiator caspase-8 or -10 in yeast caused cells to bypass the HU induced G1/S checkpoint through an unknown mechanism (Lisa-Santamaria, Neiman et al. 2009). The analogous effect of YCA1 on the HU-induced checkpoint in yeast has not been determined. These findings suggest that mammalian caspases may also function in an essential process during the G1/S checkpoint. It is possible that the G1/S transition is supported by YCA1-mediated cleavage of G1/S specific cell cycle regulators. However, our proteomic experiments did not identify candidate substrates that function in this capacity.

We focused our efforts to understand how an otherwise apoptotic protein contributed to the G1/S phenotype. The 2D gel screen for YCA1 responsive proteins demonstrated up-regulation of the G1/S checkpoint protein RAD23. RAD23 interacts with other members of the RAD in the recognition and repair of DNA lesions. We did not observe evidence of oxidative stresses or damages that would likely contribute to a RAD23-induced nucleotide excision repair checkpoint. RAD23 also functions in proteasomal delivery of ubiquitinated substrates (Chen and Madura 2002), a function which may complement the cell stress we observed in later experiments. For example, we noted activation of stress response pathways, autophagic vacuolization and accumulated insoluble aggregate material in *Δyca1* cells.

4.1.2 YCA1 and stress response chaperones

Quantitative examination of wild-type and *Δyca1* proteomes by iTRAQ revealed the presence of stress-related pathways that may contribute to the delay in G1/S

progression. Specifically, we observed substantial up-regulation of HSP family proteins and vacuolar peptidases in *Δyca1*. Consistent with our iTRAQ results, caspase mutants accumulate autophagic bodies indicative of an autophagic process. We screened YCA1-TAP interactors during log-phase growth and observed that YCA1-TAP directly interacts with many of the same HSP family proteins and co-localizes with them *in-vivo* which together suggest a conserved cell function between YCA1 and HSP family chaperones.

The iTRAQ experiment revealed numerous *yca1* responsive protein species. Small heat shock proteins and other chaperones of the HSP70/90/104 families were significantly up-regulated in *Δyca1* when compared to wild-type. In particular, the small heatshock protein HSP12 exhibited the most variation of all proteins in the iTRAQ experiment. Expression of HSPs is not exclusive to a heat specific environment, but rather a response which facilitates protein refolding in times of stress. HSP12 is readily expressed in most stress conditions and is used in commercial and industrial processes as a general stress marker (Karreman and Lindsey 2005). In addition to expression of other HSPs, the ~3-fold induction of HSP12 during log phase growth marks the *Δyca* strain as inherently stressed, suggesting that YCA1 acts to maintain yeast fitness during log growth. We also observed substantial up-regulation of most constituent peptidases of the yeast vacuole in *Δyca1* cells. Consistent with this finding both *Δyca1* and, to a lesser extent, the C297A caspase inactivation mutant accumulated autophagic vacuoles during growth which together indicate the activation of an autophagic program. Interestingly, autophagy specifically alters the cell cycle in late G1 resulting in prolonged G1/S progression or complete G1 arrest in affected cells (Tasdemir, Maiuri et al. 2007). These data suggest that the prolonged G1/S phase observed in *Δyca1* cells results from a stress

response-mediated reduction in cell fitness (owing to excess protein accumulation) and the consequent induction of an autophagic program.

We observed that multiple HSP family chaperones were expressed in response to YCA1 ablation. YCA1-TAP interactors were substantially enriched for HSP40 and HSP70 chaperones. YCA1 co-localized *in situ* with aggregate re-modeling chaperones of the HSP40/70/104 families (Lee, Brunette and Megeney; unpublished observation), a system of chaperones that co-ordinate the dismantling and re-solublization of aggregated protein (Glover and Lindquist 1998; Rikhvanov, Romanova et al. 2007). Specifically, YCA1 robustly associated with HSP104 foci during heat stress and in stationary phase cultures marking sites of protein aggregation. This is the first observation of physical interactions between metacaspases and chaperones; however, mammalian chaperones are known to regulate and interact with mammalian initiator caspases, effector caspases and apoptotic machinery. HSP70 is capable of directly binding the pro-forms of effector caspases -3 and -7 in U-937 leukemia cells and substantially inhibits/postpones DEVDase activity in apoptotic NS0/1 cells (Komarova, Afanasyeva et al. 2004). HSP70 also inhibits mitochondrial death pathways by inhibiting the translocation of BAX, AIF and EndoG (Lanneau, de Thonel et al. 2007). Estradiol induced HSP27 in C2C12 cells binds to and inhibits maturation of caspase-3 and eventual death in response to H_2O_2 (Vasconsuelo, Milanesi et al. 2009). The HSP27-Caspase-3 interaction similarly protects monocytes by binding caspase-3 in non-apoptotic cells (Voss, Batra et al. 2007). HSP90α analogously reduce autocatalytic activation of the initiator caspase-2 (Bouchier-Hayes, Oberst et al. 2009). HSP90β inhibits formation of the apoptosome by binding APAF-1 and is itself a substrate of initiator caspase-10 during UVB mediated apoptosis (Chen,

Xia et al. 2009). In contrast, HSP60D advances *D. melanogaster* apoptosis and is required to remove the caspase inhibitor DIAP1 from drosophila caspases (Arya and Lakhotia 2008). Similarly, HSP70 promotes caspase-9 activation by co-ordinating the formation of the ring-like apoptosome structure (Kim, Jiang et al. 2008). Thus, HSP70 is capable of both inhibiting and promoting caspase dependent apoptosis, presumably through the activation of opposing molecular mechanisms. The compensatory expression of HSPs, direct YCA1-TAP interactions and the in-vivo co-localization between YCA1 and HSP-family fusions strongly suggest that caspase/HSP co-operation is not only conserved but may also regulate vital non-death functions.

4.1.3 A model for YCA1 in aggregate removal

Our data suggested that YCA1 co-operated with HSP family chaperones possibly by contributing to protein quality control. We hypothesized that YCA1 might directly participate in the removal of protein aggregates. Interestingly, this model depicts a novel role for YCA1 with implications for metacaspase and caspase-like function in aging and neurodegenerative disease models.

To address the validity of our hypothesis we quantified the detergent-insoluble aggregate fraction of wild-type and caspase mutant cells during log growth and observed a substantial increase of protein aggregates in the caspase mutants. Specifically, we examined the NP-40 insoluble protein aggregate fraction from log phase yeast by filter trap and 1D gel electrophoresis. These experiments demonstrated that the protein aggregate fraction of wild-type and *Δyca1* cells share a similar constitution; however, these aggregates accumulated to far greater extents in log-phase metacaspase deletion and inactivation mutants as determined by both assays. The HSP70 family chaperone SSA1

was up-regulated in *Δyca1* as determined by iTRAQ. SSA1 was also a predominant interactor in YCA1-TAP gels and specifically accumulated in the insoluble fraction of *Δyca1* extracts. This distribution of SSA1 suggested that the expression and aggregate targeting function of SSA1 may directly compensate for YCA1 ablation. From these and our previous data we have developed a model whereby YCA1 promotes the removal of protein aggregates by the targeted degradation or stabilization of aggregate re-modeling complexes on the aggregate itself. The deletion/inactivation of YCA1 in our model results in the accumulation of cytosolic aggregates which promotes expression of heat shock-responsive aggregate re-modeling chaperones. Furthermore, deletion and inactivation mutants continue through log-phase growth with markers of autophagy.

Previously, autophagy was thought to be a distinct form of PCD whereby a starving autophagic cell would completely degrade its own cytosolic material. However, autophagy is arguably a stress response process that occurs concurrently with death processes not to promote death, but to prolong cell viability through times of moderate stress (Thorburn 2008). Autophagy serves protective functions in the cell by removing larger aggregated material from the intracellular milieu (Eisenberg, Knauer et al. 2009; Madeo, Eisenberg et al. 2009) which has particular relevance to neurodegenerative diseases in the removal of amyloid inclusions (Rideout, Lang-Rollin et al. 2004; Iwata, Riley et al. 2005; Komatsu, Ueno et al. 2007; Hetz, Thielen et al. 2009). In our model, the induction of autophagic processes and vacuolization encourage the compensatory degradation of the accumulating aggregate material thus supporting the continued growth of metacaspase deficient mutants. We observed the formation of fluorescent foci of YCA1 and C297A fusions in aged and heat stressed cultures but we did not observe

substantial formation of the catalytic fragments in response to non-lethal heat stress. The vacuolation and aggregate retention phenotypes were both apparent in the C297A catalytic inactivation mutant (a mutant that is incapable of forming catalytic fragments); however, these phenotypes were less striking in the C297A strain when compared to the *yca1* deletion mutant. These observations suggest that both the enzymatic activity and the non-enzymatic function of YCA1 contribute to aggregate removal.

The dynamics of protein aggregate formation and dissipation have relevance to stress, disease and, in particular, the replicative/chronological aging process (Grune, Jung et al. 2004). Replicative and chronological aging of *E. coli* is typified by accumulation of aggregated proteins which reduces clonogenicity and pre-disposes aged cells to death (Maisonneuve, Ezraty et al. 2008; Maisonneuve, Fraysse et al. 2008). Similarly, oxidative damaged proteins and protein aggregates are retained by mother cells during replicative aging in yeast, contributing to the increased fitness of daughter cells and the relatively decreased fitness of aging mother cells (Aguilaniu, Gustafsson et al. 2003; Lindner, Madden et al. 2008). Accumulation of carbonylated protein aggregates by asymmetric division may hence represent a major factor contributing to the declined fitness of replicatively aging cells (Lindner, Madden et al. 2008; Maisonneuve, Fraysse et al. 2008). Increased caspase activity has been observed in chronologically aging cells and is thought to contribute to apoptotic death of cells within aging tissue (Zhang, Chong et al. 2002; Zhang, Zhang et al. 2003). Similarly, metacaspase activity increases in aged yeast cells possibly due to age specific accumulation of ROS concurrent with a loss of clonogenecity in aged *Δyca1* cultures. This observation suggests a role for YCA1 in chronological aging in log-phase and stationary-phase cultures (Herker, Jungwirth et al.

2004). Interestingly, we observed that YCA1-GFP co-localized with HSP104-RFP positive foci in three day old stationary cultures. In the context of our model this finding suggests that YCA1 may support clearance of carbonylated protein aggregates or other damaged protein inclusions during chronological aging thus promoting the fitness of aging stationary phase cultures. To a similar effect, *Δyca1* cells were demonstrated to accumulate a greater proportion of protein carbonyls in comparison to wild-type cells during mild oxidative stress (Khan, Chock et al. 2005). This was a perplexing phenotype which can also be explained by our proposed model for YCA1 function. Here, YCA1 would promote the general removal of aggregated material including aggregates of oxidative damaged proteins that accrue in response to non-lethal oxidative stress. In this regard, our model suggests that YCA1 contributes to the fitness of aging cells in log-phase and stationary-phase cultures.

4.1.4 Caspases and amyloid aggregates

Caspases are recognized as significant contributors to the pathology of mammalian neurodegenerative diseases. Caspase dependent cleavage of Tau, Huntington and APP are all thought to contribute to the formation of tightly tangled amyloid fibrils within affected cells. The order of events is controversial as it is not clear whether or not caspase cleavage of these amyloidogenic proteins occurs before or after the formation of the initial aggregates (Weidemann, Paliga et al. 1999; Soriano, Lu et al. 2001; Cotman, Poon et al. 2005; Hanger, Anderton et al. 2009).

Heterologous expression of pathological huntington fragments and mammalian α-synuclein in *S. cerevisiae* promote apoptosis-like death similar to that of mammalian neurons in the presence of toxic amyloids (Outeiro and Lindquist 2003; Sokolov,

Pozniakovsky et al. 2006; Braun, Buttner et al. 2009). Accordingly, yeast have been used to model the toxicity and death associated with amyloidogenic proteins involved with the pathogenesis of neurodegenerative diseases. There is evidence that metacaspases may process or promote the disaggregation of mammalian proteins that contribute to neurodegenerative diseases. Expression of an expanded polyglutamine (poly-Q) repeat from huntingtin protein results in the accumulation of nuclear aggregates and death with apoptotic markers (Sokolov, Pozniakovsky et al. 2006). Intriguingly, deletion of YCA1 did not greatly improve the viability of poly-Q expressing cells. Instead the polyglutamine aggregates accumulated in the cytoplasm. The solubility and proteolytic processing of the poly-Q construct were not demonstrated in this work. However, one can hypothesize in the context of our observations that the YCA1 knockout impairs the dispersion of cytoplasmic poly-Q aggregates resulting in their cytosolic accumulation. To a similar effect, in a yeast synucleinopathy study *Δyca1* cells had a greater reduction in growth and even higher retention of cytosolic aggregates in comparison to wild-type cells (Griffioen, Duhamel et al. 2006). The intention of these studies was to determine whether or not the apoptosis-like death that occurs in response to the expression of toxic amyloid was metacaspase-dependent; yet, careful examination of such data suggests YCA1 may elicit a beneficial role, through the dissipation of toxic amyloids.

There is evidence that mammalian caspases directly target and are activated at amyloid inclusions. For example, caspase-8 associated with the insoluble protein fraction in cells of Huntington's disease patients and actively co-localized with expanded poly-Q repeats in cultured neurons leading to enzymatic activation of caspase-8 (Sanchez, Xu et al. 1999). Similarly, caspase-8 activity was enhanced by expression of a poly-Q construct

in P19 cells; however this induced activity did not contribute to cell death (Kouroku, Fujita et al. 2000). Initiator caspases -8 and -10 were both directly recruited to nuclear poly-Q aggregates in human ovarian cancer cells resulting in their respective activation (U, Miyashita et al. 2001). The amyloid-targeting function is thought to promote proximity induced caspase activation and the formation of tighter fibrils leading to apoptosis. Initiator caspase-12 may be activated by an analogous recruitment strategy (Kouroku, Fujita et al. 2002). Similarly, tagged initiator caspase-2 condenses into foci during heat shock resulting in proximity induced caspase-2 activation. Formation of these foci is dependent on the expression of an aggregate-prone adaptor protein RAIDD which contains a CARD domain (Jabado, Wang et al. 2004; Bouchier-Hayes, Oberst et al. 2009). Together these findings suggest that caspases are capable of targeting amyloids of various compositions either directly or via secondary interactions with their N-terminal pro-domains. The prevailing assumption with these studies is that caspase processing of amyloidogenic proteins leads to pathological outcomes. However, our model suggests that caspase-amyloid interactions may originate from a more general aggregate-targeting function. Furthermore, it is possible that the intensity of caspase activation is proportional to aggregate concentration whereby a heavily aggregated state could promote unrestricted caspase activity and an apoptotic fate. The corollary to this supposition is that modest caspase activity is required to maintain long term cell viability.

4.2 A paradigm shift for the interpretation of caspase activity

Our data suggests a role for metacaspases in protein quality control. It is currently unknown whether or not this function is conserved in higher eukaryotes. However, these studies demonstrate that the antagonistic death and non-death functions for caspase

proteases may have originated in single-celled organisms. To this effect, enhanced caspase and metacaspase activity should not immediately imply evidence of a death-specific process. Rather, the most reasonable interpretation suggests that a continuum of caspase activity will influence multiple cell fate responses.

Our results suggest that baseline YCA1 expression and activity contributes to the fitness and adaptability of yeast. In our model, smaller scale but continual activity of the yeast metacaspase contributes to the processing of aggregated material in cooperation with heat shock chaperones. Previous findings in vertebrate and invertebrate animals have demonstrated that a controlled pulse of caspase activity is required for terminal differentiation of numerous cell lineages. Here, caspase activity remodels the cell and promotes a genomic reprogramming event to establish differentiation specific gene expression patterns (Larsen et al. 2010; in press). Clearly, caspase activity is tightly regulated to perform non-death functions, a response that is consistent with co-operative interactions with chaperones and other regulatory complexes. Caspase activity is thus not likely to contribute to molecular processes as a binary on/off regulatory switch, but acts instead as a tune-able parameter in a larger, complex signalling network (Lazebnik 2004).

4.3 Conclusions and future directions

The yeast metacaspase YCA1 has been previously characterized as an ancestral regulator of apoptosis in yeast. However, it remains unclear what selective pressures would promote the emergence and retention of a death-centric protease in a single celled eukaryote. As such, we hypothesized that the role of YCA1 was not exclusive to yeast apoptosis but also contributed to non-death functions that would encourage organism robustness and evolutionary retention. Here, we have demonstrated a number of fitness

defects associated with deletion and inactivation of YCA1, observations that have led us to suggest a novel model of metacaspase function. Our cell-cycle study has demonstrated that YCA1 encourages timely passage through the cell cycle. Furthermore, we have shown that caspase ablation and inhibition promotes an autophagic stress response simultaneous with the accumulation of protein aggregates. These stresses are capable of prolonging the cell cycle proper and are likely contributors to the observed G1/S phenotype. Our model for YCA1 in the dissipation of protein aggregates suggests that the teleology of metacaspases and the selective pressure that shaped the caspase family may have originated from a basic function independent of cell death. This model offers plausible explanations for a number of puzzling phenotypes associated with YCA1 ablation or inhibition. Furthermore, our model suggests that baseline metacaspase function protects cells against by-products of the aging process and toxic amyloids. A protective function in these processes would have particular importance in mammals should the caspase family retain a homologous function; however, characterizing the exact role of mammalian caspases in aggregate dispersion will require further directed studies.

The molecular mechanism by which YCA1 prevents the accumulation of protein aggregates has not been determined. Understanding these mechanisms at the molecular level will help to answer the question of whether or not this function is conserved across phyla. We speculate that the N-terminal pro-domain is a substantial contributor to the aggregate targeting ability of YCA1. Here, the glutamine and asparagine-rich pro-domain of YCA1 may act as an interactive surface to target aggregates. The protease activity of YCA1 or the re-folding activity of a metacaspase-chaperone complex stabilized on an

aggregate surface may act together to prevent aggregate accumulation. Further studies should be performed to examine these possibilities and elaborate on the precise mechanisms. For example, a domain based study using a series of N- or C-terminal YCA1 truncation mutants can be generated to examine the affinity of YCA1 fragments with aggregates. Here, the association of various regions of YCA1 with aggregates can be assessed during log-growth, heat stress or with pre-formed aggregates *in-vitro*. Similarly, the aggregate binding affinity of a series of chaperone-fluorescent protein fusions can be examined in either the presence or absence of YCA1 or YCA1 fragments to determine the contribution of YCA1 to chaperone-aggregate stability.

Initiator caspases -8 and -10 are capable of interacting with poly-Q amyloids which suggests that caspases may retain a general aggregate targeting function. It would be of particular interest to test mammalian initiator caspases for homologous function in yeast. Heterologous expression of mammalian caspases -8 and -10 in yeast was observed to promote apoptosis-like death (Kang, Schaber et al. 1999; Lisa-Santamaria, Neiman et al. 2009); however, expression of initiator caspases in these studies was induced over long periods of time under control of the strong Gal promoter. As such, long term expression of a protease under the Gal promoter may itself predispose these cells to an apoptotic phenotype. Mammalian initiator caspases -2, -8, -9 and -10 should be expressed in the *yca1* locus or under a titratable promoter in yeast to determine if they are capable of performing analogous function at physiologic expression levels. Heterologous expression under these conditions can be used to examine the mechanism of caspase action in yeast and to test for phenotypic complementation of the *Δyca1* strain.

To date there are no known substrates of YCA1. The only known substrate of any metacaspase is the *P. abies* tudor staphylococcal nuclease, paTSN, which is cleaved by the type-II metacaspase mcII-Pa. Intriguingly, TSN1 is a conserved substrate for the Norway spruce metacaspase as well as mammalian caspase-3 during developmental and stress-induced PCD (Sundstrom, Vaculova et al. 2009). It is particularly interesting that a PCD-specific target of a homologous substrate is conserved between caspases and metacaspases given the disparity of their respective enzymatic properties. This observation suggests that cleavage of specific substrates is dependent on substrate presentation in addition to sequence specificity. In this regard it is possible that homologous enzymes with dissimilar tetrapeptide specificities can have a conserved substrate pool by targeting different sequences within the same labile domain. Yeast does not have a characterized TSN homologue, and accordingly, there are no predicted YCA1 substrates whatsoever. Context sensitive characterization of *in-situ* substrates of YCA1 will elaborate our understanding of metacaspase function in death and protein quality control. However, it remains possible that primordial caspase enzymes such as YCA1 do not retain defined substrate specificity, rather the function of YCA1 may be to target protein aggregates independent of any defined substrate relationship. In this scenario, metacaspase and caspase substrate specificity may be a more recent adaptation.

In our model for the yeast metacaspase, YCA1 promotes cell fitness by preventing the accumulation of protein aggregates. This model suggests an alternative interpretation of metacaspase influence and activity. Herein we have only described a few possible routes of further investigation that detail and extend our model beyond yeast. Depending on the results of these experiments, subsequent studies may be directed at

mammalian pathology. It will be of particular interest to determine whether caspase/metacaspase function is a conserved component of an anti-aging and/or anti-amyloid molecular machine in vertebrate organisms.

References:

Aguilaniu, H., L. Gustafsson, et al. (2003). "Asymmetric inheritance of oxidatively damaged proteins during cytokinesis." Science **299**(5613): 1751-3.

Alam, A., L. Y. Cohen, et al. (1999). "Early activation of caspases during T lymphocyte stimulation results in selective substrate cleavage in nonapoptotic cells." J Exp Med **190**(12): 1879-90.

Alberti, S., R. Halfmann, et al. (2009). "A systematic survey identifies prions and illuminates sequence features of prionogenic proteins." Cell **137**(1): 146-58.

Allen, C., S. Buttner, et al. (2006). "Isolation of quiescent and nonquiescent cells from yeast stationary-phase cultures." J Cell Biol **174**(1): 89-100.

Ambit, A., N. Fasel, et al. (2008). "An essential role for the Leishmania major metacaspase in cell cycle progression." Cell Death Differ **15**(1): 113-22.

Arya, R. and S. C. Lakhotia (2008). "Hsp60D is essential for caspase-mediated induced apoptosis in Drosophila melanogaster." Cell Stress Chaperones **13**(4): 509-26.

Baker, S. J. and E. P. Reddy (1998). "Modulation of life and death by the TNF receptor superfamily." Oncogene **17**(25): 3261-70.

Bao, Q. and Y. Shi (2007). "Apoptosome: a platform for the activation of initiator caspases." Cell Death Differ **14**(1): 56-65.

Basu, A., V. P. Castle, et al. (2006). "Crosstalk between extrinsic and intrinsic cell death pathways in pancreatic cancer: synergistic action of estrogen metabolite and ligands of death receptor family." Cancer Res **66**(8): 4309-18.

Beckham, C., A. Hilliker, et al. (2008). "The DEAD-box RNA helicase Ded1p affects and accumulates in Saccharomyces cerevisiae P-bodies." Mol Biol Cell **19**(3): 984-93.

Bell, B. D., S. Leverrier, et al. (2008). "FADD and caspase-8 control the outcome of autophagic signaling in proliferating T cells." Proc Natl Acad Sci U S A **105**(43): 16677-82.

Boatright, K. M. and G. S. Salvesen (2003). "Caspase activation." Biochem Soc Symp(70): 233-42.

Boatright, K. M. and G. S. Salvesen (2003). "Mechanisms of caspase activation." Curr Opin Cell Biol **15**(6): 725-31.

Bossy-Wetzel, E. and D. R. Green (1999). "Caspases induce cytochrome c release from mitochondria by activating cytosolic factors." J Biol Chem **274**(25): 17484-90.

Bouchier-Hayes, L., A. Oberst, et al. (2009). "Characterization of cytoplasmic caspase-2 activation by induced proximity." Mol Cell **35**(6): 830-40.

Bozhkov, P. V., L. H. Filonova, et al. (2004). "VEIDase is a principal caspase-like activity involved in plant programmed cell death and essential for embryonic pattern formation." Cell Death Differ **11**(2): 175-82.

Bozhkov, P. V., M. F. Suarez, et al. (2005). "Cysteine protease mcII-Pa executes programmed cell death during plant embryogenesis." Proc Natl Acad Sci U S A **102**(40): 14463-8.

Brachmann, C. B., A. Davies, et al. (1998). "Designer deletion strains derived from Saccharomyces cerevisiae S288C: a useful set of strains and plasmids for PCR-mediated gene disruption and other applications." Yeast **14**(2): 115-32.

Braun, R. J., S. Buttner, et al. (2009). "Nervous yeast: modeling neurotoxic cell death." Trends Biochem Sci.

Buchan, J. R., D. Muhlrad, et al. (2008). "P bodies promote stress granule assembly in Saccharomyces cerevisiae." J Cell Biol **183**(3): 441-55.

Buttner, S., T. Eisenberg, et al. (2007). "Endonuclease G regulates budding yeast life and death." Mol Cell **25**(2): 233-46.

Buttner, S., T. Eisenberg, et al. (2006). "Why yeast cells can undergo apoptosis: death in times of peace, love, and war." J Cell Biol **175**(4): 521-5.

Canu, N., L. Dus, et al. (1998). "Tau cleavage and dephosphorylation in cerebellar granule neurons undergoing apoptosis." J Neurosci **18**(18): 7061-74.

Cashikar, A. G., M. Duennwald, et al. (2005). "A chaperone pathway in protein disaggregation. Hsp26 alters the nature of protein aggregates to facilitate reactivation by Hsp104." J Biol Chem **280**(25): 23869-75.

Causton, H. C., B. Ren, et al. (2001). "Remodeling of yeast genome expression in response to environmental changes." Mol Biol Cell **12**(2): 323-37.

Cerretti, D. P., C. J. Kozlosky, et al. (1992). "Molecular cloning of the interleukin-1 beta converting enzyme." Science **256**(5053): 97-100.

Chen, H., Y. Xia, et al. (2009). "Caspase-10-mediated heat shock protein 90 beta cleavage promotes UVB irradiation-induced cell apoptosis." Mol Cell Biol **29**(13): 3657-64.

Chen, L. and K. Madura (2002). "Rad23 promotes the targeting of proteolytic substrates to the proteasome." Mol Cell Biol **22**(13): 4902-13.

Chipuk, J. E. and D. R. Green (2005). "Do inducers of apoptosis trigger caspase-independent cell death?" Nat Rev Mol Cell Biol **6**(3): 268-75.

Coquelle, A., S. Mouhamad, et al. (2006). "Enrichment of non-synchronized cells in the G1, S and G2 phases of the cell cycle for the study of apoptosis." Biochem Pharmacol **72**(11): 1396-404.

Cotman, C. W., W. W. Poon, et al. (2005). "The role of caspase cleavage of tau in Alzheimer disease neuropathology." J Neuropathol Exp Neurol **64**(2): 104-12.

Deng, X., F. Gao, et al. (2003). "Bcl2 retards G1/S cell cycle transition by regulating intracellular ROS." Blood **102**(9): 3179-85.

Desjardins, P. and S. Ledoux (1998). "The role of apoptosis in neurodegenerative diseases." Metab Brain Dis **13**(2): 79-96.

DiPaola, R. S. (2002). "To arrest or not to G(2)-M Cell-cycle arrest : commentary re: A. K. Tyagi et al., Silibinin strongly synergizes human prostate carcinoma DU145 cells to doxorubicin-induced growth inhibition, G(2)-M arrest, and apoptosis. Clin. cancer res., 8: 3512-3519, 2002." Clin Cancer Res **8**(11): 3311-4.

Duke, R. C., R. Chervenak, et al. (1983). "Endogenous endonuclease-induced DNA fragmentation: an early event in cell-mediated cytolysis." Proc Natl Acad Sci U S A **80**(20): 6361-5.

Eisenberg, T., H. Knauer, et al. (2009). "Induction of autophagy by spermidine promotes longevity." Nat Cell Biol **11**(11): 1305-14.

Ellis, H. M. and H. R. Horvitz (1986). "Genetic control of programmed cell death in the nematode C. elegans." Cell **44**(6): 817-29.

Erjavec, N., L. Larsson, et al. (2007). "Accelerated aging and failure to segregate damaged proteins in Sir2 mutants can be suppressed by overproducing the protein aggregation-remodeling factor Hsp104p." Genes Dev **21**(19): 2410-21.
Fabrizio, P., L. Battistella, et al. (2004). "Superoxide is a mediator of an altruistic aging program in Saccharomyces cerevisiae." J Cell Biol **166**(7): 1055-67.
Fadok, V. A., D. R. Voelker, et al. (1992). "Exposure of phosphatidylserine on the surface of apoptotic lymphocytes triggers specific recognition and removal by macrophages." J Immunol **148**(7): 2207-16.
Faleiro, L. and Y. Lazebnik (2000). "Caspases disrupt the nuclear-cytoplasmic barrier." J Cell Biol **151**(5): 951-9.
Fernando, P., S. Brunette, et al. (2005). "Neural stem cell differentiation is dependent upon endogenous caspase 3 activity." Faseb J **19**(12): 1671-3.
Fernando, P., J. F. Kelly, et al. (2002). "Caspase 3 activity is required for skeletal muscle differentiation." Proc Natl Acad Sci U S A **99**(17): 11025-30.
Fernando, P. and L. A. Megeney (2007). "Is caspase-dependent apoptosis only cell differentiation taken to the extreme?" Faseb J **21**(1): 8-17.
Fisher, S. A., B. L. Langille, et al. (2000). "Apoptosis during cardiovascular development." Circ Res **87**(10): 856-64.
Foghsgaard, L., D. Wissing, et al. (2001). "Cathepsin B acts as a dominant execution protease in tumor cell apoptosis induced by tumor necrosis factor." J Cell Biol **153**(5): 999-1010.
Frohlich, K. U., H. Fussi, et al. (2007). "Yeast apoptosis-From genes to pathways." Semin Cancer Biol **17**(2): 112-21.
Frohlich, K. U. and F. Madeo (2000). "Apoptosis in yeast--a monocellular organism exhibits altruistic behaviour." FEBS Lett **473**(1): 6-9.
Fu, X., C. Ng, et al. (2003). "Cdc48p is required for the cell cycle commitment point at Start via degradation of the G1-CDK inhibitor Far1p." J Cell Biol **163**(1): 21-6.
Giannattasio, S., N. Guaragnella, et al. (2005). "Acid stress adaptation protects Saccharomyces cerevisiae from acetic acid-induced programmed cell death." Gene **354**: 93-8.
Gietz, R. D. and R. H. Schiestl (2007). "High-efficiency yeast transformation using the LiAc/SS carrier DNA/PEG method." Nat Protoc **2**(1): 31-4.
Gilot, D., A. L. Serandour, et al. (2005). "A role for caspase-8 and c-FLIPL in proliferation and cell-cycle progression of primary hepatocytes." Carcinogenesis **26**(12): 2086-94.
Glover, J. R. and S. Lindquist (1998). "Hsp104, Hsp70, and Hsp40: a novel chaperone system that rescues previously aggregated proteins." Cell **94**(1): 73-82.
Gonzalez, I. J., C. Desponds, et al. (2007). "Leishmania major metacaspase can replace yeast metacaspase in programmed cell death and has arginine-specific cysteine peptidase activity." Int J Parasitol **37**(2): 161-72.
Grably, M. R., A. Stanhill, et al. (2002). "HSF and Msn2/4p can exclusively or cooperatively activate the yeast HSP104 gene." Mol Microbiol **44**(1): 21-35.
Granot, D. and N. Dai (1997). "Sugar induced cell death in yeast is dependent on the rate of sugar phosphorylation as determined by Arabidopsis thaliana hexokinase." Cell Death Differ **4**(7): 555-9.

Granot, D., A. Levine, et al. (2003). "Sugar-induced apoptosis in yeast cells." FEMS Yeast Res **4**(1): 7-13.
Granot, D. and M. Snyder (1993). "Carbon source induces growth of stationary phase yeast cells, independent of carbon source metabolism." Yeast **9**(5): 465-79.
Greenhalf, W., C. Stephan, et al. (1996). "Role of mitochondria and C-terminal membrane anchor of Bcl-2 in Bax induced growth arrest and mortality in Saccharomyces cerevisiae." FEBS Lett **380**(1-2): 169-75.
Griffioen, G., H. Duhamel, et al. (2006). "A yeast-based model of alpha-synucleinopathy identifies compounds with therapeutic potential." Biochim Biophys Acta **1762**(3): 312-8.
Gross, A., J. Jockel, et al. (1998). "Enforced dimerization of BAX results in its translocation, mitochondrial dysfunction and apoptosis." Embo J **17**(14): 3878-85.
Grossmann, J. (2002). "Molecular mechanisms of "detachment-induced apoptosis--Anoikis"." Apoptosis **7**(3): 247-60.
Grune, T., T. Jung, et al. (2004). "Decreased proteolysis caused by protein aggregates, inclusion bodies, plaques, lipofuscin, ceroid, and 'aggresomes' during oxidative stress, aging, and disease." Int J Biochem Cell Biol **36**(12): 2519-30.
Guaragnella, N., A. Bobba, et al. (2009). "Yeast acetic acid-induced programmed cell death can occur without cytochrome c release which requires metacaspase YCA1." FEBS Lett.
Guaragnella, N., C. Pereira, et al. (2006). "YCA1 participates in the acetic acid induced yeast programmed cell death also in a manner unrelated to its caspase-like activity." FEBS Lett **580**(30): 6880-4.
Guscetti, F., N. Nath, et al. (2005). "Functional characterization of human proapoptotic molecules in yeast S. cerevisiae." FASEB J **19**(3): 464-6.
Hanada, M., C. Aime-Sempe, et al. (1995). "Structure-function analysis of Bcl-2 protein. Identification of conserved domains important for homodimerization with Bcl-2 and heterodimerization with Bax." J Biol Chem **270**(20): 11962-9.
Hanger, D. P., B. H. Anderton, et al. (2009). "Tau phosphorylation: the therapeutic challenge for neurodegenerative disease." Trends Mol Med **15**(3): 112-9.
Haslbeck, M., A. Miess, et al. (2005). "Disassembling protein aggregates in the yeast cytosol. The cooperation of Hsp26 with Ssa1 and Hsp104." J Biol Chem **280**(25): 23861-8.
He, R., G. E. Drury, et al. (2008). "Metacaspase-8 modulates programmed cell death induced by ultraviolet light and H2O2 in Arabidopsis." J Biol Chem **283**(2): 774-83.
Helfer, B., B. C. Boswell, et al. (2006). "Caspase-8 promotes cell motility and calpain activity under nonapoptotic conditions." Cancer Res **66**(8): 4273-8.
Herker, E., H. Jungwirth, et al. (2004). "Chronological aging leads to apoptosis in yeast." J Cell Biol **164**(4): 501-7.
Hetz, C., P. Thielen, et al. (2009). "XBP-1 deficiency in the nervous system protects against amyotrophic lateral sclerosis by increasing autophagy." Genes Dev **23**(19): 2294-306.
Hirsch, T., I. Marzo, et al. (1997). "Role of the mitochondrial permeability transition pore in apoptosis." Biosci Rep **17**(1): 67-76.

Hitomi, J., T. Katayama, et al. (2004). "Apoptosis induced by endoplasmic reticulum stress depends on activation of caspase-3 via caspase-12." Neurosci Lett **357**(2): 127-30.
Hsu, S. L., C. T. Yu, et al. (2006). "Caspase 3, periodically expressed and activated at G2/M transition, is required for nocodazole-induced mitotic checkpoint." Apoptosis **11**(5): 765-71.
Huh, G. H., B. Damsz, et al. (2002). "Salt causes ion disequilibrium-induced programmed cell death in yeast and plants." Plant J **29**(5): 649-59.
Ishizaki, Y., M. D. Jacobson, et al. (1998). "A role for caspases in lens fiber differentiation." J Cell Biol **140**(1): 153-8.
Itoh, N., S. Semba, et al. (2002). "Phosphorylation of Akt/PKB is required for suppression of cancer cell apoptosis and tumor progression in human colorectal carcinoma." Cancer **94**(12): 3127-34.
Iwata, A., B. E. Riley, et al. (2005). "HDAC6 and microtubules are required for autophagic degradation of aggregated huntingtin." J Biol Chem **280**(48): 40282-92.
Jabado, O., Q. Wang, et al. (2004). "RAIDD aggregation facilitates apoptotic death of PC12 cells and sympathetic neurons." Cell Death Differ **11**(6): 618-30.
Jabbour, A. M., P. K. Ho, et al. (2004). "The Caenorhabditis elegans CED-9 protein does not directly inhibit the caspase CED-3, in vitro nor in yeast." Cell Death Differ **11**(12): 1309-16.
Jacobson, M. D., M. Weil, et al. (1997). "Programmed cell death in animal development." Cell **88**(3): 347-54.
James, C., S. Gschmeissner, et al. (1997). "CED-4 induces chromatin condensation in Schizosaccharomyces pombe and is inhibited by direct physical association with CED-9." Curr Biol **7**(4): 246-52.
Journo, D., G. Winter, et al. (2008). "Monitoring autophagy in yeast using FM 4-64 fluorescence." Methods Enzymol **451**: 79-88.
Joza, N., S. A. Susin, et al. (2001). "Essential role of the mitochondrial apoptosis-inducing factor in programmed cell death." Nature **410**(6828): 549-54.
Kang, J. J., M. D. Schaber, et al. (1999). "Cascades of mammalian caspase activation in the yeast Saccharomyces cerevisiae." J Biol Chem **274**(5): 3189-98.
Karreman, R. J. and G. G. Lindsey (2005). "A rapid method to determine the stress status of Saccharomyces cerevisiae by monitoring the expression of a Hsp12:green fluorescent protein (GFP) construct under the control of the Hsp12 promoter." J Biomol Screen **10**(3): 253-9.
Kennedy, N. J., T. Kataoka, et al. (1999). "Caspase activation is required for T cell proliferation." J Exp Med **190**(12): 1891-6.
Kerr, J. F., A. H. Wyllie, et al. (1972). "Apoptosis: a basic biological phenomenon with wide-ranging implications in tissue kinetics." Br J Cancer **26**(4): 239-57.
Khan, M. A., P. B. Chock, et al. (2005). "Knockout of caspase-like gene, YCA1, abrogates apoptosis and elevates oxidized proteins in Saccharomyces cerevisiae." Proc Natl Acad Sci U S A **102**(48): 17326-31.
Kim, H. E., X. Jiang, et al. (2008). "PHAPI, CAS, and Hsp70 promote apoptosome formation by preventing Apaf-1 aggregation and enhancing nucleotide exchange on Apaf-1." Mol Cell **30**(2): 239-47.

Kim, M., K. Murphy, et al. (2005). "Caspase-mediated specific cleavage of BubR1 is a determinant of mitotic progression." Mol Cell Biol **25**(21): 9232-48.
King, D. A., D. M. Hannum, et al. (2004). "HOCl-mediated cell death and metabolic dysfunction in the yeast Saccharomyces cerevisiae." Arch Biochem Biophys **423**(1): 170-81.
Kinnally, K. W. and B. Antonsson (2007). "A tale of two mitochondrial channels, MAC and PTP, in apoptosis." Apoptosis **12**(5): 857-68.
Knorre, D. A., E. A. Smirnova, et al. (2005). "Natural conditions inducing programmed cell death in the yeast Saccharomyces cerevisiae." Biochemistry (Mosc) **70**(2): 264-6.
Komarova, E. Y., E. A. Afanasyeva, et al. (2004). "Downstream caspases are novel targets for the antiapoptotic activity of the molecular chaperone hsp70." Cell Stress Chaperones **9**(3): 265-75.
Komatsu, M., T. Ueno, et al. (2007). "Constitutive autophagy: vital role in clearance of unfavorable proteins in neurons." Cell Death Differ **14**(5): 887-94.
Koren, A. (2006). "Is Saccharomyces cerevisiae apoptotic cell death associated with gene transfer?" IUBMB Life **58**(4): 203-7.
Korsmeyer, S. J., J. R. Shutter, et al. (1993). "Bcl-2/Bax: a rheostat that regulates an anti-oxidant pathway and cell death." Semin Cancer Biol **4**(6): 327-32.
Kouroku, Y., E. Fujita, et al. (2002). "Polyglutamine aggregates stimulate ER stress signals and caspase-12 activation." Hum Mol Genet **11**(13): 1505-15.
Kouroku, Y., E. Fujita, et al. (2000). "Caspases that are activated during generation of nuclear polyglutamine aggregates are necessary for DNA fragmentation but not sufficient for cell death." J Neurosci Res **62**(4): 547-56.
Kroemer, G., W. S. El-Deiry, et al. (2005). "Classification of cell death: recommendations of the Nomenclature Committee on Cell Death." Cell Death Differ **12 Suppl 2**: 1463-7.
Kuida, K., T. F. Haydar, et al. (1998). "Reduced apoptosis and cytochrome c-mediated caspase activation in mice lacking caspase 9." Cell **94**(3): 325-37.
Lamkanfi, M., W. Declercq, et al. (2002). "Alice in caspase land. A phylogenetic analysis of caspases from worm to man." Cell Death Differ **9**(4): 358-61.
Lanneau, D., A. de Thonel, et al. (2007). "Apoptosis versus cell differentiation: role of heat shock proteins HSP90, HSP70 and HSP27." Prion **1**(1): 53-60.
Laun, P., A. Pichova, et al. (2001). "Aged mother cells of Saccharomyces cerevisiae show markers of oxidative stress and apoptosis." Mol Microbiol **39**(5): 1166-73.
Lazebnik, Y. (2004). "Can a biologist fix a radio? -- Or, what I learned while studying apoptosis, (Cancer Cell. 2002 Sep;2(3):179-82)." Biochemistry (Mosc) **69**(12): 1403-6.
Lee, N., S. Gannavaram, et al. (2007). "Characterization of metacaspases with trypsin-like activity and their putative role in programmed cell death in the protozoan parasite Leishmania." Eukaryot Cell **6**(10): 1745-57.
Lee, R. E. and L. A. Megeney (2005). "The yeast kinome displays scale free topology with functional hub clusters." BMC Bioinformatics **6**: 271.
Lee, R. E., L. G. Puente, et al. (2008). "A non-death role of the yeast metacaspase: Yca1p alters cell cycle dynamics." PLoS One **3**(8): e2956.

Leist, M. and M. Jaattela (2001). "Four deaths and a funeral: from caspases to alternative mechanisms." Nat Rev Mol Cell Biol **2**(8): 589-98.
Levine, B. and J. Yuan (2005). "Autophagy in cell death: an innocent convict?" J Clin Invest **115**(10): 2679-88.
Li, J., W. M. Brieher, et al. (2007). "Caspase-11 regulates cell migration by promoting Aip1-Cofilin-mediated actin depolymerization." Nat Cell Biol **9**(3): 276-86.
Li, L. Y., X. Luo, et al. (2001). "Endonuclease G is an apoptotic DNase when released from mitochondria." Nature **412**(6842): 95-9.
Li, P., D. Nijhawan, et al. (1997). "Cytochrome c and dATP-dependent formation of Apaf-1/caspase-9 complex initiates an apoptotic protease cascade." Cell **91**(4): 479-89.
Ligr, M., F. Madeo, et al. (1998). "Mammalian Bax triggers apoptotic changes in yeast." FEBS Lett **438**(1-2): 61-5.
Lindner, A. B., R. Madden, et al. (2008). "Asymmetric segregation of protein aggregates is associated with cellular aging and rejuvenation." Proc Natl Acad Sci U S A **105**(8): 3076-81.
Lippert, D. N., S. G. Ralph, et al. (2009). "Quantitative iTRAQ proteome and comparative transcriptome analysis of elicitor-induced Norway spruce (Picea abies) cells reveals elements of calcium signaling in the early conifer defense response." Proteomics **9**(2): 350-67.
Lisa-Santamaria, P., A. M. Neiman, et al. (2009). "Human initiator caspases trigger apoptotic and autophagic phenotypes in Saccharomyces cerevisiae." Biochim Biophys Acta **1793**(3): 561-71.
Liu, X., H. Zou, et al. (1997). "DFF, a heterodimeric protein that functions downstream of caspase-3 to trigger DNA fragmentation during apoptosis." Cell **89**(2): 175-84.
Madeo, F., T. Eisenberg, et al. (2009). "Autophagy for the avoidance of neurodegeneration." Genes Dev **23**(19): 2253-9.
Madeo, F., E. Frohlich, et al. (1999). "Oxygen stress: a regulator of apoptosis in yeast." J Cell Biol **145**(4): 757-67.
Madeo, F., E. Herker, et al. (2002). "A caspase-related protease regulates apoptosis in yeast." Mol Cell **9**(4): 911-7.
Maisonneuve, E., B. Ezraty, et al. (2008). "Protein aggregates: an aging factor involved in cell death." J Bacteriol **190**(18): 6070-5.
Maisonneuve, E., L. Fraysse, et al. (2008). "Carbonylated proteins are detectable only in a degradation-resistant aggregate state in Escherichia coli." J Bacteriol **190**(20): 6609-14.
Manon, S., B. Chaudhuri, et al. (1997). "Release of cytochrome c and decrease of cytochrome c oxidase in Bax-expressing yeast cells, and prevention of these effects by coexpression of Bcl-xL." FEBS Lett **415**(1): 29-32.
Matsuyama, S., S. L. Schendel, et al. (1998). "Cytoprotection by Bcl-2 requires the pore-forming alpha5 and alpha6 helices." J Biol Chem **273**(47): 30995-1001.
Mazzoni, C. and C. Falcone (2008). "Caspase-dependent apoptosis in yeast." Biochim Biophys Acta **1783**(7): 1320-7.
Mazzoni, C., E. Herker, et al. (2005). "Yeast caspase 1 links messenger RNA stability to apoptosis in yeast." EMBO Rep **6**(11): 1076-81.

McKinnell, I. W., J. Ishibashi, et al. (2008). "Pax7 activates myogenic genes by recruitment of a histone methyltransferase complex." Nat Cell Biol **10**(1): 77-84.
Mitchell, L., J. P. Lambert, et al. (2008). "Functional dissection of the NuA4 histone acetyltransferase reveals its role as a genetic hub and that Eaf1 is essential for complex integrity." Mol Cell Biol **28**(7): 2244-56.
Mitsui, K., D. Nakagawa, et al. (2005). "Valproic acid induces apoptosis dependent of Yca1p at concentrations that mildly affect the proliferation of yeast." FEBS Lett **579**(3): 723-7.
Miura, M., X. D. Chen, et al. (2004). "A crucial role of caspase-3 in osteogenic differentiation of bone marrow stromal stem cells." J Clin Invest **114**(12): 1704-13.
Mogi, M. and A. Togari (2003). "Activation of caspases is required for osteoblastic differentiation." J Biol Chem **278**(48): 47477-82.
Muzio, M., B. R. Stockwell, et al. (1998). "An induced proximity model for caspase-8 activation." J Biol Chem **273**(5): 2926-30.
Narasimhan, M. L., B. Damsz, et al. (2001). "A plant defense response effector induces microbial apoptosis." Mol Cell **8**(4): 921-30.
Nemecek, J., T. Nakayashiki, et al. (2009). "A prion of yeast metacaspase homolog (Mca1p) detected by a genetic screen." Proc Natl Acad Sci U S A **106**(6): 1892-6.
Nissan, T. and R. Parker (2008). "Analyzing P-bodies in Saccharomyces cerevisiae." Methods Enzymol **448**: 507-20.
Ortolan, T. G., L. Chen, et al. (2004). "Rad23 stabilizes Rad4 from degradation by the Ub/proteasome pathway." Nucleic Acids Res **32**(22): 6490-500.
Outeiro, T. F. and S. Lindquist (2003). "Yeast cells provide insight into alpha-synuclein biology and pathobiology." Science **302**(5651): 1772-5.
Parsell, D. A., A. S. Kowal, et al. (1994). "Protein disaggregation mediated by heat-shock protein Hsp104." Nature **372**(6505): 475-8.
Perera, D. and R. Freire (2005). "Human spindle checkpoint kinase Bub1 is cleaved during apoptosis." Cell Death Differ **12**(7): 827-30.
Pitti, R. M., S. A. Marsters, et al. (1996). "Induction of apoptosis by Apo-2 ligand, a new member of the tumor necrosis factor cytokine family." J Biol Chem **271**(22): 12687-90.
Puente, L. G., R. E. Lee, et al. (2009). "Reconstructing regulatory kinase pathways from phosphopeptide data: a bioinformatics approach." Methods Mol Biol **527**: 311-9, x.
Puente, L. G., S. Voisin, et al. (2006). "Reconstructing the regulatory kinase pathways of myogenesis from phosphopeptide data." Mol Cell Proteomics **5**(12): 2244-51.
Puryer, M. A. and C. J. Hawkins (2006). "Human, insect and nematode caspases kill Saccharomyces cerevisiae independently of YCA1 and Aif1p." Apoptosis **11**(4): 509-17.
Rand, J. D. and C. M. Grant (2006). "The thioredoxin system protects ribosomes against stress-induced aggregation." Mol Biol Cell **17**(1): 387-401.
Reiter, J., E. Herker, et al. (2005). "Viral killer toxins induce caspase-mediated apoptosis in yeast." J Cell Biol **168**(3): 353-8.

Richie, D. L., M. D. Miley, et al. (2007). "The Aspergillus fumigatus metacaspases CasA and CasB facilitate growth under conditions of endoplasmic reticulum stress." Mol Microbiol **63**(2): 591-604.
Rideout, H. J., I. Lang-Rollin, et al. (2004). "Involvement of macroautophagy in the dissolution of neuronal inclusions." Int J Biochem Cell Biol **36**(12): 2551-62.
Rigaut, G., A. Shevchenko, et al. (1999). "A generic protein purification method for protein complex characterization and proteome exploration." Nat Biotechnol **17**(10): 1030-2.
Rikhvanov, E. G., N. V. Romanova, et al. (2007). "Chaperone effects on prion and nonprion aggregates." Prion **1**(4): 217-22.
Robinson, M. D., J. Grigull, et al. (2002). "FunSpec: a web-based cluster interpreter for yeast." BMC Bioinformatics **3**: 35.
Sanchez, I., C. J. Xu, et al. (1999). "Caspase-8 is required for cell death induced by expanded polyglutamine repeats." Neuron **22**(3): 623-33.
Sato, T., M. Hanada, et al. (1994). "Interactions among members of the Bcl-2 protein family analyzed with a yeast two-hybrid system." Proc Natl Acad Sci U S A **91**(20): 9238-42.
Sattler, M., T. Winkler, et al. (1999). "Hematopoietic growth factors signal through the formation of reactive oxygen species." Blood **93**(9): 2928-35.
Schauber, C., L. Chen, et al. (1998). "Rad23 links DNA repair to the ubiquitin/proteasome pathway." Nature **391**(6668): 715-8.
Schmitt, M. J. and F. Breinig (2006). "Yeast viral killer toxins: lethality and self-protection." Nat Rev Microbiol **4**(3): 212-21.
Sedlak, T. W., Z. N. Oltvai, et al. (1995). "Multiple Bcl-2 family members demonstrate selective dimerizations with Bax." Proc Natl Acad Sci U S A **92**(17): 7834-8.
Severin, F. F. and A. A. Hyman (2002). "Pheromone induces programmed cell death in S. cerevisiae." Curr Biol **12**(7): R233-5.
Shevchenko, A., H. Tomas, et al. (2006). "In-gel digestion for mass spectrometric characterization of proteins and proteomes." Nat Protoc **1**(6): 2856-60.
Shevchenko, A., M. Wilm, et al. (1996). "Mass spectrometric sequencing of proteins silver-stained polyacrylamide gels." Anal Chem **68**(5): 850-8.
Shi, M., C. J. Vivian, et al. (2009). "DNA-PKcs-PIDDosome: a nuclear caspase-2-activating complex with role in G2/M checkpoint maintenance." Cell **136**(3): 508-20.
Shimizu, S., M. Narita, et al. (1999). "Bcl-2 family proteins regulate the release of apoptogenic cytochrome c by the mitochondrial channel VDAC." Nature **399**(6735): 483-7.
Silva, R. D., R. Sotoca, et al. (2005). "Hyperosmotic stress induces metacaspase- and mitochondria-dependent apoptosis in Saccharomyces cerevisiae." Mol Microbiol **58**(3): 824-34.
Sokolov, S., A. Pozniakovsky, et al. (2006). "Expression of an expanded polyglutamine domain in yeast causes death with apoptotic markers." Biochim Biophys Acta **1757**(5-6): 660-6.
Soriano, S., D. C. Lu, et al. (2001). "The amyloidogenic pathway of amyloid precursor protein (APP) is independent of its cleavage by caspases." J Biol Chem **276**(31): 29045-50.

Spellman, P. T., G. Sherlock, et al. (1998). "Comprehensive identification of cell cycle-regulated genes of the yeast Saccharomyces cerevisiae by microarray hybridization." Mol Biol Cell **9**(12): 3273-97.
Stanger, B. Z., P. Leder, et al. (1995). "RIP: a novel protein containing a death domain that interacts with Fas/APO-1 (CD95) in yeast and causes cell death." Cell **81**(4): 513-23.
Stennicke, H. R., J. M. Jurgensmeier, et al. (1998). "Pro-caspase-3 is a major physiologic target of caspase-8." J Biol Chem **273**(42): 27084-90.
Suarez, M. F., L. H. Filonova, et al. (2004). "Metacaspase-dependent programmed cell death is essential for plant embryogenesis." Curr Biol **14**(9): R339-40.
Sulston, J. E., E. Schierenberg, et al. (1983). "The embryonic cell lineage of the nematode Caenorhabditis elegans." Dev Biol **100**(1): 64-119.
Sundstrom, J. F., A. Vaculova, et al. (2009). "Tudor staphylococcal nuclease is an evolutionarily conserved component of the programmed cell death degradome." Nat Cell Biol **11**(11): 1347-54.
Susin, S. A., H. K. Lorenzo, et al. (1999). "Molecular characterization of mitochondrial apoptosis-inducing factor." Nature **397**(6718): 441-6.
Szallies, A., B. K. Kubata, et al. (2002). "A metacaspase of Trypanosoma brucei causes loss of respiration competence and clonal death in the yeast Saccharomyces cerevisiae." FEBS Lett **517**(1-3): 144-50.
Talanian, R. V., X. Yang, et al. (1997). "Granule-mediated killing: pathways for granzyme B-initiated apoptosis." J Exp Med **186**(8): 1323-31.
Tao, W., D. W. Walke, et al. (1999). "Oligomerized Ced-4 kills budding yeast through a caspase-independent mechanism." Biochem Biophys Res Commun **260**(3): 799-805.
Tasdemir, E., M. C. Maiuri, et al. (2007). "Cell cycle-dependent induction of autophagy, mitophagy and reticulophagy." Cell Cycle **6**(18): 2263-7.
Thorburn, A. (2008). "Studying autophagy's relationship to cell death." Autophagy **4**(3): 391-4.
Thornberry, N. A., H. G. Bull, et al. (1992). "A novel heterodimeric cysteine protease is required for interleukin-1 beta processing in monocytes." Nature **356**(6372): 768-74.
Timmer, J. C. and G. S. Salvesen (2007). "Caspase substrates." Cell Death Differ **14**(1): 66-72.
U, M., T. Miyashita, et al. (2001). "Extended polyglutamine selectively interacts with caspase-8 and -10 in nuclear aggregates." Cell Death Differ **8**(4): 377-86.
Uren, A. G., K. O'Rourke, et al. (2000). "Identification of paracaspases and metacaspases: two ancient families of caspase-like proteins, one of which plays a key role in MALT lymphoma." Mol Cell **6**(4): 961-7.
Vachova, L. and Z. Palkova (2005). "Physiological regulation of yeast cell death in multicellular colonies is triggered by ammonia." J Cell Biol **169**(5): 711-7.
Vachova, L. and Z. Palkova (2007). "Caspases in yeast apoptosis-like death: facts and artefacts." FEMS Yeast Res **7**(1): 12-21.
Van Noorden, C. J. (2001). "The history of Z-VAD-FMK, a tool for understanding the significance of caspase inhibition." Acta Histochem **103**(3): 241-51.

Vandenabeele, P., T. Vanden Berghe, et al. (2006). "Caspase inhibitors promote alternative cell death pathways." Sci STKE **2006**(358): pe44.
Varfolomeev, E. E., M. Schuchmann, et al. (1998). "Targeted disruption of the mouse Caspase 8 gene ablates cell death induction by the TNF receptors, Fas/Apo1, and DR3 and is lethal prenatally." Immunity **9**(2): 267-76.
Vasconsuelo, A., L. Milanesi, et al. (2009). "Participation of HSP27 in the antiapoptotic action of 17beta-estradiol in skeletal muscle cells." Cell Stress Chaperones.
Vercammen, D., W. Declercq, et al. (2007). "Are metacaspases caspases?" J Cell Biol **179**(3): 375-80.
Vercammen, D., B. van de Cotte, et al. (2004). "Type II metacaspases Atmc4 and Atmc9 of Arabidopsis thaliana cleave substrates after arginine and lysine." J Biol Chem **279**(44): 45329-36.
Verdoodt, B., I. Decordier, et al. (1999). "Induction of polyploidy and apoptosis after exposure to high concentrations of the spindle poison nocodazole." Mutagenesis **14**(5): 513-20.
Vermes, I., C. Haanen, et al. (1995). "A novel assay for apoptosis. Flow cytometric detection of phosphatidylserine expression on early apoptotic cells using fluorescein labelled Annexin V." J Immunol Methods **184**(1): 39-51.
Voss, O. H., S. Batra, et al. (2007). "Binding of caspase-3 prodomain to heat shock protein 27 regulates monocyte apoptosis by inhibiting caspase-3 proteolytic activation." J Biol Chem **282**(34): 25088-99.
Wang, Y. and D. J. Burke (1995). "Checkpoint genes required to delay cell division in response to nocodazole respond to impaired kinetochore function in the yeast Saccharomyces cerevisiae." Mol Cell Biol **15**(12): 6838-44.
Wang, Y., A. B. Meriin, et al. (2009). "Abnormal proteins can form aggresome in yeast: aggresome-targeting signals and components of the machinery." Faseb J **23**(2): 451-63.
Watanabe, N. and E. Lam (2005). "Two Arabidopsis metacaspases AtMCP1b and AtMCP2b are arginine/lysine-specific cysteine proteases and activate apoptosis-like cell death in yeast." J Biol Chem **280**(15): 14691-9.
Weidemann, A., K. Paliga, et al. (1999). "Proteolytic processing of the Alzheimer's disease amyloid precursor protein within its cytoplasmic domain by caspase-like proteases." J Biol Chem **274**(9): 5823-9.
Weil, M., M. C. Raff, et al. (1999). "Caspase activation in the terminal differentiation of human epidermal keratinocytes." Curr Biol **9**(7): 361-4.
Wellington, C. L., R. Singaraja, et al. (2000). "Inhibiting caspase cleavage of huntingtin reduces toxicity and aggregate formation in neuronal and nonneuronal cells." J Biol Chem **275**(26): 19831-8.
Wilson, M. R., T. W. Close, et al. (2000). "Cell population dynamics (apoptosis, mitosis, and cell-cell communication) during disruption of homeostasis." Exp Cell Res **254**(2): 257-68.
Wissing, S., P. Ludovico, et al. (2004). "An AIF orthologue regulates apoptosis in yeast." J Cell Biol **166**(7): 969-74.
Wright, M. E., D. K. Han, et al. (1999). "Caspase-3 inhibits growth in Saccharomyces cerevisiae without causing cell death." FEBS Lett **446**(1): 9-14.

Wysocki, R. and S. J. Kron (2004). "Yeast cell death during DNA damage arrest is independent of caspase or reactive oxygen species." J Cell Biol **166**(3): 311-6.

Xu, Q. and J. C. Reed (1998). "Bax inhibitor-1, a mammalian apoptosis suppressor identified by functional screening in yeast." Mol Cell **1**(3): 337-46.

Yuan, J., S. Shaham, et al. (1993). "The C. elegans cell death gene ced-3 encodes a protein similar to mammalian interleukin-1 beta-converting enzyme." Cell **75**(4): 641-52.

Yuan, J. Y. and H. R. Horvitz (1990). "The Caenorhabditis elegans genes ced-3 and ced-4 act cell autonomously to cause programmed cell death." Dev Biol **138**(1): 33-41.

Zermati, Y., C. Garrido, et al. (2001). "Caspase activation is required for terminal erythroid differentiation." J Exp Med **193**(2): 247-54.

Zhang, J. H., Y. Zhang, et al. (2003). "Caspases, apoptosis and aging." Ageing Res Rev **2**(4): 357-66.

Zhang, N. N., D. D. Dudgeon, et al. (2006). "Multiple signaling pathways regulate yeast cell death during the response to mating pheromones." Mol Biol Cell **17**(8): 3409-22.

Zhang, Q., H. K. Chieu, et al. (2003). "Schizosaccharomyces pombe cells deficient in triacylglycerols synthesis undergo apoptosis upon entry into the stationary phase." J Biol Chem **278**(47): 47145-55.

Zhang, Y., E. Chong, et al. (2002). "Age-associated increases in the activity of multiple caspases in Fisher 344 rat organs." Exp Gerontol **37**(6): 777-89.

Zuzarte-Luis, V. and J. M. Hurle (2005). "Programmed cell death in the embryonic vertebrate limb." Semin Cell Dev Biol **16**(2): 261-9.

Appendix 1. Extended Materials and methods

Single step TAP purifications:

To prepare beads, 2 mL of dimethylformamide (DMF) was added to 60 mg of dry M-270 epoxy Dynabeads (Invitrogen). Beads were vortexed for 2 minutes and stored indefinitely at 4°C. IgG crosslinked beads were made within 2 week of each TAP purification experiment. Briefly, 200μL of beads suspended in DMF were isolated on a Dynal MPC magnet (Invitrogen). The separated beads were washed and isolated 3 times in 1mL of sodium phosphate buffered at pH 7.4 (NaPB). The wash buffer was completely removed. The dry beads were immediately re-suspended in 230μL of NaPB. 10μL of non-specific Rabbit IgG (PP64, Chemicon) from a 10.3 mg/mL stock was added and then supplemented with 120μL of ammonium sulphate buffer (ammonium sulphate dissolved in NaPB to a final concentration of 3M). The suspension was incubated at 37°C for 16-24 hours on a nutator mixer. The beads were isolated and subjected to a series of washes/isolations with end-over-end rotation as follows: 4x1 minute in 1 mL of PBS (pH 7.4), 1x10 minutes in PBS + 1% Triton-X 100, 2x1 minute PBS, 4x10 minutes in citric acid buffer (0.1M citric acid, pH 3.1 with NaOH), 2x10 minute wash in PBS. The post washed beads were separated on the magnet and re-suspended to a final volume of 400μL in PBS.

Lysates were prepared from 200mL liquid yeast cultures by glass bead agitation in Tackett extraction buffer (20mM HEPES pH7.4, 0.1% Tween20, 2mM $MgCl_2$, 300mM NaCl with protease inhibitors) and clarified by centrifugation at 20000×g for 15 minutes. Protein concentrations were normalized and equal volumes corresponding to 17mg of protein were retained for analysis. 100μL of IgG conjugated beads were added

to the protein extract and the resulting slurry rotated at 4°C for 2-3 hours. The target bound beads were subsequently washed 5 times in 1 mL of Tackett extraction buffer. The TAP tagged target and complexed material were then eluted from the beads by heating for 10 minutes at 65°C in 40μL of sample buffer (50mM Tris pH6.8, 2%SDS, 0.1% bromophenol blue, 10% glycerol, 150mM NaCl). The beads were discarded and beta-2-mercaptoethanol was added to each sample to a final concentration of 100mM. The samples were finally boiled at 100°C and analysed by SDS-PAGE.

Genomic DNA extraction from yeast:

5mL of overnight cultures were pelleted and re-suspended in 40μL of breaking buffer (2% Triton X-100, 1% SDS, 100mM NaCl, 10mM Tris-HCl pH 8.0, 1mM EDTA) and 40μL of phenol:chloroform:isoamyl alcohol (25:24:1). A small amount of acid washed glass beads were added and the slurry was vortexed at max speed for 3 minutes. The debris was spun down and the supernatant was collected. The DNA was precipitated by addition of cold 100% ethanol. The DNA was pelleted in a centrifuge at 13000·g for 5 minutes, the pellet was dried and the purified genomic DNA was resuspended in 40μL sterile water.

General PCR program:

The following PCR reaction was used as a first pass protocol for amplification of most constructs. The reaction mixture consisted of 5μL of 5x reaction buffer, 10mM each dNTP, forward and reverse primers at 12.5pmol, 12.5-100 ng of DNA, 0.25μL (0.25 units) of Phusion DNA polymerase (NEB). The reaction mixture was topped to 25μL

with sterile water. The polymerase chain reaction occurred with the following thermal cycler settings: Step1: 98°C for 1 min

Step2: 98°C for 10 seconds

Step3: 50°C for 20 seconds

Step4: 72°C for 1 minute

Step5: Repeat steps 2-4 29 times for a final total of 30 cycles

Step6: 72°C for 10 minutes

Step7: 4° hold

As required, the 72°C polymerase elongation step was lengthened to accommodate the amplification of larger constructs. Similarly, the 50°C annealing temperature was adjusted as required for specificity. PCR products were resolved on 1% agarose gels.

Yeast transformation:

Yeast cultures were grown to an OD660 of 0.8-1.0 in 50mL of media (YPD or synthetic media as required). Yeast cells were pelleted by centrifugation at 3000·g and washed in sterile water. The washed cells were re-suspended in 1mL of 100mM LiAc, pelleted and suspended in 200μL of 100 mM LiAc. This suspension was transferred into 50μL aliquots for individual transformations. Cells were pelleted again and the supernatant was removed. 240μL of 50% Polyethylene glycol 3350 (Sigma), 36μL of 1M LiAc, 50μL denatured carrier DNA (from a stock of 2mg/mL DNA sodium salt from salmon testes) and 36μL of sterile water with plasmid or insert DNA (0.1-10μg) were added in order. The cell pellet was re-suspended and incubated at 42°C for 1 hour. The transformed yeast were then grown on selective plates.

Appendix 2. Additional Publications

2.1 Article: The Yeast Kinome Displays Scale Free Topology with Functional Hub Clusters

RECL: Designed the study, performed experiments, analyzed the data and wrote the manuscript.

LAM: Designed the study, contributed materials and wrote the manuscript.

This research was originally published in BMC Bioinformatics. Lee and Megeney. The Yeast Kinome Displays Scale Free Topology with Functional Hub Clusters. *BMC Bioinformtics*. 2005; **5**(271).

BMC Bioinformatics

BioMed Central

Research article

Open Access

The yeast kinome displays scale free topology with functional hub clusters

Robin EC Lee[1,2] and Lynn A Megeney*[1,2]

Address: [1]Ottawa Health Research Institute, Molecular Medicine Program, Ottawa, Canada and [2]University of Ottawa, Department of Cellular and Molecular Medicine, Ottawa, Canada

Email: Robin EC Lee - rolee@ohri.ca; Lynn A Megeney* - lmegeney@ohri.ca

* Corresponding author

Published: 09 November 2005

BMC Bioinformatics 2005, 6:271 doi:10.1186/1471-2105-6-271

Received: 12 May 2005

Accepted: 09 November 2005

This article is available from: http://www.biomedcentral.com/1471-2105/6/271

Abstract

Background: The availability of interaction databases provides an opportunity for researchers to utilize immense amounts of data exclusively *in silico*. Recently there has been an emphasis on studying the global properties of biological interactions using network analysis. While this type of analysis offers a wide variety of global insights it has surprisingly not been used to examine more localized interactions based on mechanism. In as such we have particular interest in the role of key topological components in signal transduction cascades as they are vital regulators of healthy and diseased cell states.

Results: We have used publicly available databases and a novel software tool termed Hubview to model the interactions of a subset of the yeast interactome, specifically protein kinases and their interaction partners. Analysis of the connectivity distribution has inferred a fat-tailed degree distribution with parameters consistent with those found in other biological networks. In addition, Hubview identified a functional clustering of a large group of kinases, distributed between three separate groupings. The complexity and average degree for each of these clusters is indicative of a specialized function (cell cycle propagation, DNA repair and pheromone response) and relative age for each cluster.

Conclusion: Using connectivity analysis on a functional subset of proteins we have evidence that reinforces the scale free topology as a model for protein network evolution. We have identified the hub components of the kinase network and observed a tendency for these kinases to cluster together on a functional basis. As such, these results suggest an inherent trend to preserve scale free characteristics at a domain based modular level within large evolvable networks.

Background

The Barabási and Albert scale free network model is a mathematical precept that describes the innate connectivity and distribution within complex networks. These scale free networks defy the traditional random graph model of Erdös and Renyi and display a connectivity distribution where the occurrence of highly interacting components of the network, defined as nodes decay as a power law, $P(k) \sim k^{\gamma}$ [1-3]. In turn, growth of a scale free network is characterized by a preferential attachment scheme in which new nodes attach to older more connected nodes with a higher probability [2,4,5]. This model facilitates a rich-get-richer schema and allows for the existence of a very important class of highly connected hubs [1,6]. These

hubs are largely responsible for the non-Gaussian connectivity distribution of scale free networks and are commonly orders of magnitude more connected than the average node. The existence of the hubs also provide a robust environment that is tolerant of random attack and failure but is very sensitive to hub perturbation [3,7-10].

This scale free topology has been demonstrated in a variety of man-made networks such as the World Wide Web and the actor collaboration network [1,2]. Scale free principles have also been noted in biologic systems such as the yeast protein-protein interaction dataset and the metabolic protein network [3,6]. Nevertheless, the suitability of the static scale free construct across diverse biologic systems has been challenged as a universal principle. For example, the yeast protein interaction network has been described as a date and party hub scale free network, in which these hubs are defined by variable or consistent interactions, respectively [10]. More critically, mathematical models of network growth have shown that preferential attachment may follow a random geometric topology rather than a scale free distribution [11]. Another study uses a learning algorithm to infer duplication-mutation-complementation as the central topology mechanism in the Drosophila melanogaster protein interaction network [12]. Indeed, it has been reported that the essential proteins within the larger yeast protein interaction network form an exponential connectivity distribution rather than a scale free distribution [13]. These observations raise intriguing possibilities, one of which suggests that broader scale free systems may evolve from a compilation of sub networks of different topology. Alternatively, this non-scale free structure may be an anomaly that originates from examining essential hubs versus non-essential hubs in the framework of an already established network.

Within this context, phosphorylation dependent signal transduction pathways provide an interesting venue to examine network behavior. In eukaryotic organisms, kinase directed phosphorylation is one of the most common forms of post-translational modification and as such this protein class is noted as a vital regulator of cellular function [14-16]. In addition, kinase families are well conserved across diverse phyla, suggesting that network organization may be similarly conserved. However, phosphorylation pathways are commonly studied as linear events connecting stimulus to response through a simple ladder of molecular interactions, a concept that is based largely on experimental perturbation and observation of directly connected proteins.

As such, identification of the select kinase hubs and interaction profiling should offer an insight into the functional complexities of cellular signaling in yeast and higher eukaryotes. Here, we examined the subset of the *S. cerevisiae* interaction data, which include protein kinases and their direct protein interactions. In all cases, analysis was performed on filtered datasets available in public databases to identify likely hub kinases and their interactivity. We confirmed scale free behaviour of this dataset using connectivity analysis and observed parameters as applied to a novel computer program/visualization tool we termed Hubview [17]. Interactions between the 19 most connected kinases, which we identified as super-hubs,

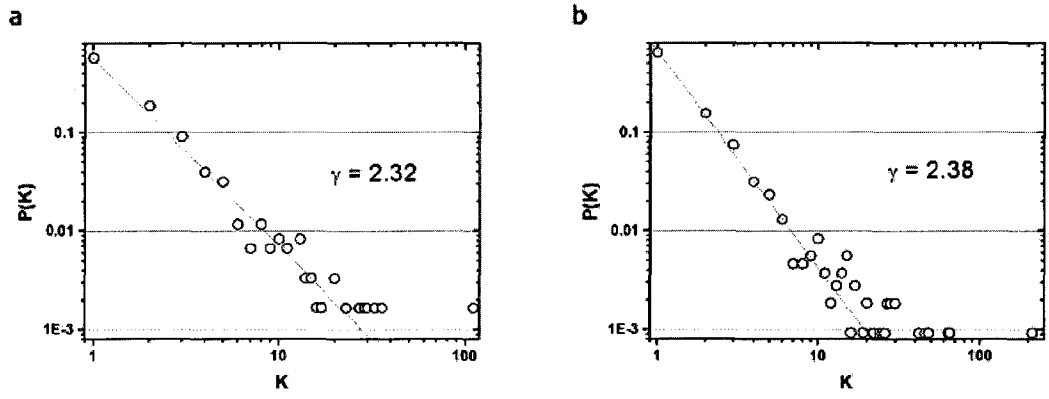

Figure 1
Degree distributions giving the probability that a given protein will interact with exactly k other proteins for: a. the core KPI with γ_{core} = 2.32 b. the complete KPI with $\gamma_{complete}$ = 2.38. In both cases γ determined by maximum likeliness estimation (MLE) and goodness of fit determined by Kolomogorov-Smirnov (KS) test. The self organization of scale free topology is normally associated with much larger datasets yet we still find the scale free characteristics.

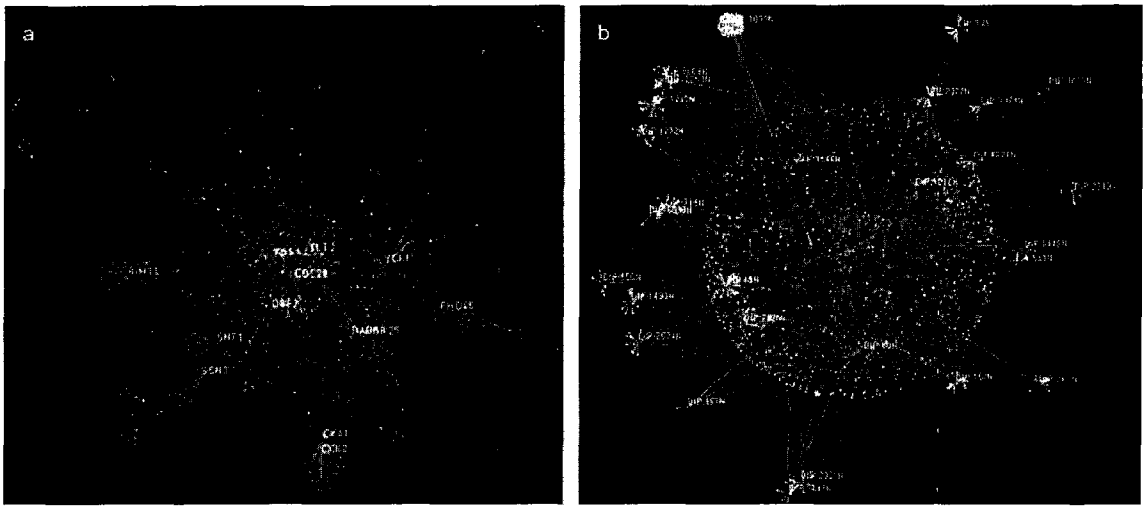

Figure 2
a. Hubview Fruchterman-Rheingold visualization of Core KPI (607 nodes, 834 interactions) b. Hub-Star-Satellite output of Hubview of complete KPI (1085 nodes with 1481 interactions) with hub degree cut-off of 15 yields 28 hubs.

were mapped along with less connected hub kinases. From this map we were able to discern three distinct clusters of kinase proteins, with each cluster retaining a common biologic function, i.e. cell cycle control, DNA repair/recombination and the pheromone/mating response. Together these observations suggest that scale free topology of the yeast kinome co-evolved with the emergence of distinct biologic domains.

Results and discussion

To study the topological properties of kinase mediated phosphorylation it was necessary to isolate the signaling component of the S. Cerevisiae proteome which we refer to as the *Kinase-Partner Interaction* set (KPI). The KPI node set was assembled from the concatenation of kinases from the database of interacting proteins (DIP) kinase search, the yeast kinases identified by Hunter and Plowman [18] and their non-kinase interaction partners. The interactions of the KPI nodes were considered bidirectional, as no directionality can be consistently inferred in most experimental conditions, and consisted of kinase-kinase and kinase-non-kinase interactions only (i.e. any potential interactions between non-kinases have been filtered). The core and complete KPI consisted of 607 nodes with 834 interactions and 1085 nodes and 1481 interactions respectively. Analysis using maximum likelihood estimation (MLE) of the degree distributions (Figure 1) resulted in derived γ values of $\gamma = 2.32$ in the core KPI and $\gamma = 2.38$ in the complete KPI which is in the biologically robust range of $2 < \gamma < 3$ [19]. The Kolmogorov-Smirnov test for Power Law Distribution [20] of both MLEs (Core: N = 500, K = 0.021; Complete: N = 1000, K = 0.015) support the hypothesis that the KPI networks are indeed both power-law distributions and hence scale free in topology. The γ-values found for the KPIs are very consistent with reports from complete protein interaction data analysis and the deterministic scale free model [21,22] which confirms that the selection criteria for the KPI is not biased to any connectivity class. A study of metabolic networks has shown that the largest most connected part of a network (in the case of metabolic networks the largest component is less than 33% the size of the full network) tends to dominate the parameters found through topological analysis [23]. Here the degree distribution is challenged as a global property and treated as a local property of the network. It is worth noting that while the KPI does contain a limited number of segregated modules, the size of the largest component accounts for roughly 95% of the network and the degree distribution does represent a global property of the network.

The KPI interaction data was analyzed by our visualization tool, Hubview. The hub-star-satellite view separates nodes with degrees higher than a user defined cut-off and their substrates of unary degree, groups the rest of the nodes within a sphere, and places the hub-stars around the sphere as satellites. The core and complete KPI were viewed with a cut-off of 10 and 15 respectively (Figure 2) and in both cases resulted in 28 satellites responsible for about 69% and 71% of the interactions respectively. The average node degree for both the core and complete KPI was found to be $\langle k \rangle \cong 1.3$.

Table 1: Summary of hub kinases as identified by Hubview: Weighted mean calculated by giving double weight to degrees listed in the *core KPI dataset. Hubs with knockout lethal phenotype listed as identified by Giaver et al [35].*

Name	DIP Node Number	Knockout Lethal	Weighted Degree	Confidence as a super-hub
CDC28	DIP:1039N	yes	150 ± 40	High
CKA1	DIP:48N	no	50 ± 10	High
HRR25	DIP:157N	yes	40 ± 10	High
SLT2	DIP:1448N	no	37 ± 5	High
YCK1	DIP:719N	no	34 ± 7	High
KSS1	DIP:60N	no	33 ± 5	High
SNF1	DIP:18N	no	24 ± 1	High
PHO85	DIP:1493N	no	22 ± 2	High
RAD53	DIP:2322N	yes	22 ± 2	High
CKB2	DIP:262N	no	19 ± 5	High
CDC7	DIP:1235N	yes	19 ± 6	High
RIM11	DIP:1566N	no	19 ± 3	High
SSN3	DIP:2574N	no	17	High
DBF2	DIP:2319N	no	17 ± 2	High
DUN1	DIP:1772N	no	16 ± 6	Uncertain
MKK2	DIP:1447N	no	16 ± 2	High
CDC5	DIP:2321N	yes	14 ± 1	High
STE11	DIP:861N	no	14 ± 1	High
PKC1	DIP:1516N	yes	14 ± 1	High
TPK3	DIP:550N	no	14 ± 1	High
CKA2	DIP:1038N	no	13 ± 5	Uncertain
SPS1	DIP:6598N	no	13 ± 2	Uncertain
CLA4	DIP:2276N	no	13	Uncertain
YAK1	DIP:1374N	no	12 ± 4	Uncertain
STE20	DIP:712N	no	12 ± 1	Uncertain
FUS3	DIP:714N	no	12 ± 1	Uncertain
CHK1	DIP:1253N	no	12 ± 2	Uncertain
KIN2	DIP:6276N	no	12 ± 2	Uncertain
BUD32	DIP:5008N	no	11 ± 9	Uncertain
SWE1	DIP:2410N	no	11	Low
CKB1	DIP:282N	no	11 ± 7	Uncertain
GIN4	DIP:2260N	no	11 ± 1	Low
BCY1	DIP:551N	no	10 ± 3	Low

The putative hubs identified by Hubview were compiled into a list of 33 distinct nodes and ranked by average degree where the degree found in the core KPI was given twice the weight (Table 1). Defining the actual cut-off degree for a hub is a subjective task, here we defined 13 (10*<k>) as the cut-off for high confidence in super-hub status. This cut-off retains 19 proteins as high confidence hubs that still maintain ~64% of KPI interactions which suggests that less understood signaling systems in higher eukaryotes may be studied with higher efficiency by identifying likely hub kinases (using expression and activity profiling) and mapping the complete set of their immediate interaction partners.

The 124 members of the protein kinase superfamily list [18] were cross referenced with the list of essential yeast proteins [24] to identify the yeast kinases with known knockout lethal phenotypes. Of the 124 kinases only 16 were deemed to be lethal deleterious mutants yielding a 13% chance of lethality in an instance of random single kinase deletion. In contrast, 6 of the 19 hubs named as *high confidence* in table 1 are listed as essential resulting in a 32% chance of lethality attributed to random deletion of one of the 19 high confidence hubs. This marked increase in lethality associated with directed hub attack is consistent with existing studies of scale free networks [3] and indicates a likely tendency for hub kinases to be preserved in an evolutionary perspective.

24 of the 33 hubs listed in table 1 were found to interact with one another. The interplay between these 24 connected hubs forms a kinase signaling backbone (figure 3a) through which 3 distinct groups of interacting hubs (forthwith these interacting hubs are referred to as hub clusters) can be identified. Presumably, the hub clusters would provide vital functions as whole as in most cases

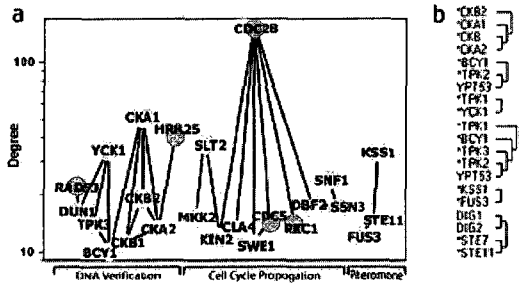

Figure 3

a. Interplay between 24 of the hubs identified by HubView constituting the signaling backbone. Red hubs are deemed as lethal knockout phenotypes as described in the systematic deletion project [35]. The nodes are separated by degree along the ordinate to illustrate a possible relationship between the degree of a hub and its phylogenetic age while the arrangement along the abscissa is purely aesthetic. The proposed function of the 3 clusters from left to right are: DNA damage/repair, cell cycle propagation and pheromone response. b. The dendrogram to the right confirms functional interactions for a number of the backbone hubs using redundancy clustering of the entire KPI as described by Samanta & Liang [28]. Only clusters containing a hub kinase are depicted in the dendrogram.

the constituent hubs are not directly essential themselves. The structure of this backbone may offer some insight in identifying synthetic lethality strategies, i.e. CKA1 and CKA2 knockouts are both viable but double deletion mutant has a lethal phenotype [25]. Backbone hubs have been ordered by degree to illustrate a possible correlation between degree and phylogenetic age where, by direct consequence of the growth and preferential attachment conditions in scale free systems, more connected hubs are likely to be older than less connected hubs [26]. A cross genome study of four organisms from different regions of the phylogenetic tree has been used to identify connectivity and emergence time of yeast proteins [5]. The results of this study support the preferential attachment and growth criteria as outlined by the scale free theory. Older proteins appear to be more connected than younger proteins. Another explanation of the degree arrangement is that the average size or degree of a cluster is associated with the evolutionary age of the clusters functional class [27]. This perspective is based on a similar study using a more rigorous phylogenetic profiling technique. The results suggest a modified form of scale free preferential attachment whereby proteins bind preferentially within their own functional class and not globally or promiscuously. By this model a younger protein may be more connected than an older one simply because it is part of an older and more connected functional grouping which emerged during an earlier phylogenetic period. Here the average connectivity of the functional group is proportional to the age of that group i.e. older eukaryotic proteins are shown to be more connected than yeast specific proteins. This perspective is very plausible as it suggests that proteins of similar function will interact within the same pool.

In response to the latter interpretation we examined the basic purpose of the individual hubs and observed a common functional theme concomitant with each cluster. The largest cluster, containing cdc28, is functionally associated with cell cycle propagation through the various phases. The second cluster, with CKA1 as a peak, is generally associated with kinase proteins that manipulate response to DNA damage and the final KSS/MAPK cluster is involved with the regulation of the pheromone response. These results seem to offer a reasonable order to the emergence of specialized functions central to all eukaryotes i.e., the cell division cycle predates the DNA verification mechanisms, which in turn predates the youngest reproductive module, the mating response.

The entire core and complete kinomes were clustered using the probabilistic method described by Samanta and Liang [28]. This method identifies functional relationships between proteins through redundancy of interaction partners. A number of the associations in the backbone clusters were confirmed using this algorithm (figure 3b). Interestingly the proteins in the cell cycle propagation cluster did not appear as functionally redundant in the clustering. Presumably the three clusters converge downstream to some extent but at the hub level this indicates that these components offer highly specialized non redundant services to the cell cycle cluster likely due to the ancient nature of their function. This method can also be used to identify likely synthetic lethality as many viable knockouts are rescued through redundant interactions. The full results of the clustering is available as supporting information (see additional file 1) or can be generated using Hubview.

In addition to the scale free topology, modeling of the yeast kinome using the Hubview cascade crawler function revealed other notable characteristics. Specifically, individual clusters containing hub kinases also include kinases that interact both inside and outside the scope of the immediate functional cluster. This characteristic was generally not observed with non-hub clusters. For example, the cluster of kinases involved in the MAPK cascade (a functional cluster with hub kinases) retain interactions with a number of non-MAPK kinases i.e. single points that interact both within and outside of the MAPK class. This is a feature we refer to as an open loop signal (Figure 4). Identifying open points within a cluster provides the user with probable targets for regulation of that functional

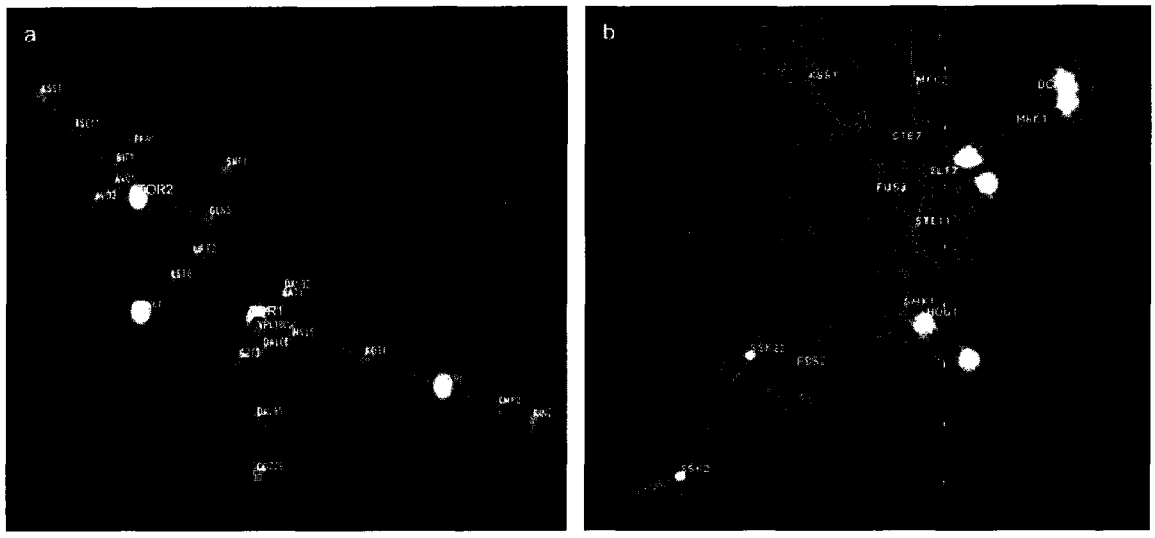

Figure 4
Cascade crawler output of Hubview. Gray spheres represent non-kinases while all other colored spheres represent kinases of varying degree. a) Depiction of closed loop TOR signaling: neither TOR protein is directly connected to another kinase indicating highly specified reaction. b) Depiction of open loop MAPK signaling: white spheres denote non-MAPK kinases that interact within and outside of the MAPK clusters representing possible regulatory and cross-talk channels associated with more complicated cellular behaviour.

cluster or even likely paths for signaling crosstalk. Open loop kinase cascades appear to reflect robust cellular responses that require multiple alterations and as such would require direct communication and signal propagation between numerous key regulatory factors/kinases themselves. However, non hub kinase clusters such as the TOR kinase cascade do not retain direct interactions between unclustered kinases and as such conform to a closed loop structure (Figure 4). Closed loop structures are likely to be kinase directed cascades that perform a very discrete cellular function in response to a limited or very specific initiating event.

The network of essential yeast proteins has been compiled and identified as an exponential distribution [13]. This distribution is normally associated with more stochastic evolutionary mechanisms. It has been argued that this network may represent an ancestral core about which the rest of the yeast interactome has formed [13]. The existence of an exponential core does not directly contradict the scale free topology observed in the protein interaction network but may simply exist as a scaffold for scale free mechanisms to adhere to. This possibility is interesting as it may also suggest that different parts of the interactome may have evolved by different evolutionary pressures causing unequal distribution of topological properties within the same interactome.

A recent investigation concerning the effects of sampling on topology adds a small shard of doubt to studies of protein network topology. In this study the effects of various large scale experiments were simulated by first generating different networks of known topology and then sampling interactions in a scale mimicking yeast two hybrid and co-affinity purification [29]. They found that under some conditions that non-scale free topologies (i.e. Erdös and Renyi network with <K> = 10), when sampled, can generate sub-networks with scale free properties. Here the kinome benefits from the fact that it is a widely studied mechanistic class and many of the interactions, especially in the core kinome, have been identified in smaller scale experiments and not exclusively large scale experiments. This suggests that the much smaller kinome network may not suffer as much as networks derived solely from large scale experiments. The results of this study certainly insist on the caveat that the results of our KPI network cannot be extrapolated to the complete yeast protein interaction network with any amount of confidence.

Conclusion

Our analysis suggests that the yeast kinome is an evolved scale free system. Moreover, these observations suggest the intriguing possibility that the scale free topology of the global protein-protein interaction network or any larger biologic network may be the composite of smaller evolving topologies (such as the kinome), all of which are subject to their own selective pressures.

Methods

Interaction database

Both the core and complete yeast interaction data of the manually curated DIP [30] were used as interaction data sets. The complete dataset consists largely of high throughput interaction data [19,31-33]. The core DIP dataset consists of interactions found in small scale experiments, two or more independent larger scale experiments and, when paralogous interaction data exist, the Paralogous Verification Method PVM [31,32]. The core dataset is believed to correctly identify the core of interacting proteins in yeast and provides a minimal interaction view of the yeast interactome. For our purposes the complete yeast interaction set is viewed as a hypothetical maximal interaction set. The many false positives, negatives and unlikely biologic interactions [19] available in the complete dataset are still valuable as they may be representative of interactions in a diseased state based on possible spatial and temporal protein delocalization. The DIP is available online at http://dip.doe-mbi.ucla.edu.

Interaction filter

Both datasets were filtered to include only kinases and direct interaction partners with kinases as found in the DIP node search in conjunction with kinases listed in the protein kinase superfamily found by Hunter and Plowman [18]. The resulting Kinase-Partner Interaction dataset (KPI) consisted of 607 nodes with 834 interactions in the case of the core dataset and 1085 nodes with 1481 interactions in the case of the complete dataset.

Hubview description

We developed a program called Hubview to help us analyze the KPI network and visualize the hubs and hub interactions found in the datasets. The degree distribution of the loaded network can be obtained by pressing the probability distribution button. The main program and OpenGL network interface utilize an undirected binary adjacency matrix which is then interpreted in real-time 3D. Yeast specific information such as the naming convention (DIP number, ORF and common name) and protein type (kinase or non-kinase) is hard coded into Hubview minimizing the amount of data required to generate an interaction network. The 3D representation is geared towards identifying nodes with degrees higher than a user-defined cut-off and displaying them in either a hub-star-satellite view whereby hub degree and inter-hub interactions are plainly visible or a Fruchterman-Rheingold (FR) force-directed placement arrangement [34] which offers a less tangled, more visually appealing interpretation.

Briefly, the FR algorithm causes the system to untangle itself through iterative simulation of mechanical and electrostatic forces. A connection between a pair of nodes is treated as though a spring were connecting those nodes creating attractive forces between all connected pairs. Repulsive electrostatic forces are also generated by considering each node as a negative point charge. The nodes in the analogous system move in 3 dimensional space according to the attractive and repulsive forces. The final arrangement is displayed once the system has evolved through a set number of iterations resulting in an intelligible and appealing graph.

The hub-star-satellite view is generated by placing all nodes randomly within a sphere of radius r_i. All nodes with connectivity higher than the user defined cutoff are identified as hubs and projected outside of the sphere to a radial position, r_f, outside the confines of the initial sphere ($r_f > r_i$). Any substrates of the new hub with unary degree are also moved to positions spherically centered near the newly placed hub generating a hub-star-satellite. The algorithm ends once all hubs are processed similarly. The advantage of this view type is that it allows interactions between hubs to be quickly and easily identified as all visually interfering substrates remain pooled within the initial sphere.

Another useful visualization method included in Hubview is the cascade crawler function. This view type is geared towards depiction of smaller cascades (the immediate and remote neighbors of a chosen protein) within the complete network. The cascade crawler function is controlled by a point and click interface whereby the user can define a specific protein(s) as a starting point and display all of its substrates by clicking on it. Clicking subsequent nodes will display their interaction partners in turn. Using this function along with the FR algorithm one can develop appealing visual interpretations of specific cascades and interactions (figure 4).

Hubview also utilizes the clustering method proposed by Samanta & Liang [28]. The main suggestion of this algorithm is that if two proteins in a network share a significantly larger number of common interaction partners than what is expected from a similar random network then the pair of proteins likely share a close functional relationship. This process assigns a P value between every pair of proteins in the network representing the probability that an association between proteins is random i.e. a

higher P score means that the pair is not functionally associated. The algorithm then merges the pair sharing the lowest P value into a cluster and recalculates P values for all possible pairs again treating the newly formed cluster as though it were a single protein. This process repeats until all P values are higher than a user defined cutoff. Once a network is loaded one can access this method by clicking the cluster button. Here a cutoff value can be defined which represents the probability that a particular association is random and a dendrogram is produced (which can be saved as a .BMP file), Samanta & Liang reported successful clustering of a large portion of the yeast interactome (N = 4692) using a cutoff value of up to 2×10^{-4} [28] indicating that this cutoff can be considered sharp and biologically relevant in our much smaller KPI networks (N_{core} = 607 and $N_{complete}$ = 1085).

Topology analysis

To counter the distortion associated with log-log data transformation the γ-value associated with the degree distribution of the KPI was analyzed using maximum likelihood estimation of the zeta function (MLE) and goodness of fit confirmed by the Kolmogorov-Smirnov test for power law distributions [20]. Briefly, the γ parameter associated with the pure power law,

$$P(k) = \frac{k^{-\gamma}}{\zeta(\gamma)} \qquad [1]$$

is best approximated by the solution of:

$$\frac{\partial\zeta(\gamma)/\partial\gamma}{\zeta(\gamma)} = -\frac{\sum_{i=1}^{N} Log(k_i)}{N} \qquad [2]$$

Where:

- $\zeta(\gamma)$ is the Riemann Zeta function

$$\sum_{k=1}^{\infty} k^{(-\gamma)} \qquad [3]$$

- k_i is the i^{th} non-zero observed degree of the P(k) vs. k distribution.

- γ is the power law exponent [20]

Protein essentiality

Phenotypic profiles of gene-deletion mutants (nearly 96% of known ORFs) have been systematically constructed and analyzed by a PCR-based gene deletion strategy [35]. A list of essential ORFs has been generated [24] and can be used to predict a lethal protein knockout or disruption phenotype.

Authors' contributions

RECL participated in the projects design and coordination, carried out programming, informatics, and drafted the manuscript. LAM conceived the study, participated in its design and coordination and drafted the manuscript.

Additional material

Additional File 1

The software Hubview has been successfully tested and used on a number of recent generation PCs with the Windows XP operating system. Suggested systems should have more than 256 Megs of ram and an OpenGL compliant video card with onboard ram. The software requires the windows operating system. Installation: Simply unzip all files into the same folder. Supplementary Material.doc: Microsoft Word Document, Complete results of redundancy clustering. Hubview.zip: Winzip archive, Reviewer copy of Hubview program used to develop data for this manuscript.

Click here for file

[http://www.biomedcentral.com/content/supplementary/1471-2105-6-271-S1.doc]

Acknowledgements

The authors would like to thank Drs. Pasan Fernando, Lawrence Puente and Lukasz Salwinski for helpful discussions. This work was supported by grants to L.A.M. from the Canadian Institutes of Health Research (CIHR) and the Heart and Stroke Foundation of Canada. L.A.M. is the Mach-Gaennelsen chair in cardiac research at the Ottawa Health Research Institute.

References

1. Albert R, Jeong H, Barabási AL: Internet: Diameter of the World-Wide Web. *Nature* 1999, **401(6749):**130-131.
2. Barabasi AL, Albert R: **Emergence of scaling in random networks.** *Science* 1999, **286(5439):**509-512.
3. Jeong H, Mason SP, Barabasi AL, Oltvai ZN: **Lethality and centrality in protein networks.** *Nature* 2001, **411(6833):**41-42.
4. Barabasi AL, Albert R, Jeong H: **Mean-Field theory for scale-free random networks.** *Physica A* 1999, **272:**173-187.
5. Eisenberg E, Levanon EY: **Preferential attachment in the protein network evolution.** *Phys Rev Lett* 2003, **91(13):**138701.
6. Jeong H, Tombor B, Albert R, Oltvai ZN, Barabasi AL: **The large-scale organization of metabolic networks.** *Nature* 2000, **407(6804):**651-654.
7. Callaway DS, Newman ME, Strogatz SH, Watts DJ: **Network robustness and fragility: percolation on random graphs.** *Phys Rev Lett* 2000, **85(25):**5468-5471.
8. Sole RV, Montoya JM: **Complexity and fragility in ecological networks.** *Proc R Soc Lond B Biol Sci* 2001, **268(1480):**2039-2045.
9. Shargel B, Sayama H, Epstein IR, Bar-Yam Y: **Optimization of robustness and connectivity in complex networks.** *Phys Rev Lett* 2003, **90(6):**68701.
10. Han JD, Bertin N, Hao T, Goldberg DS, Berriz GF, Zhang LV, Dupuy D, Walhout AJ, Cusick ME, Roth FP, Vidal M: **Evidence for dynamically organized modularity in the yeast protein-protein interaction network.** *Nature* 2004, **430(6995):**88-93.
11. Przulj N, Corneil DG, Jurisica I: **Modeling interactome: scale-free or geometric?** *Bioinformatics* 2004, **20(18):**3508-3515.

12. Middendorf M, Ziv E, Wiggins CH: **Inferring network mechanisms: The Drosophila melanogaster protein interaction network.** *Proc Natl Acad Sci U S A* 2005.
13. Pereira-Leal JB, Audit B, Peregrin-Alvarez JM, Ouzounis CA: **An Exponential Core in the Heart of the Yeast Protein Interaction Network.** *Mol Biol Evol* 2004.
14. Manning G, Whyte DB, Martinez R, Hunter T, Sudarsanam S: **The protein kinase complement of the human genome.** *Science* 2002, **298(5600)**:1912-1934.
15. Hunter T: **Signaling--2000 and beyond.** *Cell* 2000, **100(1)**:113-127.
16. Holmberg CI, Tran SE, Eriksson JE, Sistonen L: **Multisite phosphorylation provides sophisticated regulation of transcription factors.** *Trends Biochem Sci* 2002, **27(12)**:619-627.
17. **Hubview** [http://www.ogic.ca/projects/hubview/hubview.html]
18. Hunter T, Plowman GD: **The protein kinases of budding yeast: six score and more.** *Trends Biochem Sci* 1997, **22(1)**:18-22.
19. von Mering C, Krause R, Snel B, Cornell M, Oliver SG, Fields S, Bork P: **Comparative assessment of large-scale data sets of protein-protein interactions.** *Nature* 2002, **417(6887)**:399-403.
20. Goldstein ML, Morris SA, G.G. Y: **Problems with fitting to the power-law distribution.** *Eur Phys J B* 2004, **41**:255-258.
21. Farkas I, Derenyi I, Jeong H, Neda Z, Oltvai ZN, Ravasz E, Schubert A, Barabasi AL, Vicsek T: **Networks in life: Scaling properties and eigenvalue spectra.** *Physica A* 2002, **314**:25-34.
22. Yook SH, Oltvai ZN, Barabasi AL: **Functional and topological characterization of protein interaction networks.** *Proteomics* 2004, **4(4)**:928-942.
23. Ma HW, Zeng AP: **The connectivity structure, giant strong component and centrality of metabolic networks.** *Bioinformatics* 2003, **19(11)**:1423-1430.
24. **Yeast Deletion Project** [http://www-sequence.stanford.edu/group/yeast_deletion_project/Essential_ORFs.txt]
25. Barz T, Ackermann K, Pyerin W: **Perturbation of protein kinase CK2 uncouples executive part of phosphate maintenance pathway from cyclin-CDK control.** *FEBS Lett* 2003, **537(1-3)**:210-214.
26. Wuchty S: **Evolution and topology in the yeast protein interaction network.** *Genome Res* 2004, **14(7)**:1310-1314.
27. Kunin V, Pereira-Leal JB, Ouzounis CA: **Functional evolution of the yeast protein interaction network.** *Mol Biol Evol* 2004, **21(7)**:1171-1176.
28. Samanta MP, Liang S: **Predicting protein functions from redundancies in large-scale protein interaction networks.** *Proc Natl Acad Sci U S A* 2003, **100(22)**:12579-12583.
29. Han JD, Dupuy D, Bertin N, Cusick ME, Vidal M: **Effect of sampling on topology predictions of protein-protein interaction networks.** *Nat Biotechnol* 2005, **23(7)**:839-844.
30. **Database of Interacting Proteins** [http://dip.doe-mbi.ucla.edu/]
31. Deane CM, Salwinski L, Xenarios I, Eisenberg D: **Protein interactions: two methods for assessment of the reliability of high throughput observations.** *Mol Cell Proteomics* 2002, **1(5)**:349-356.
32. Salwinski L, Miller CS, Smith AJ, Pettit FK, Bowie JU, Eisenberg D: **The Database of Interacting Proteins: 2004 update.** *Nucleic Acids Res* 2004, **32 Database issue**:D449-51.
33. Xenarios I, Rice DW, Salwinski L, Baron MK, Marcotte EM, Eisenberg D: **DIP: the database of interacting proteins.** *Nucleic Acids Res* 2000, **28(1)**:289-291.
34. Fruchterman TMJ, Reingold EM: **Graph Drawing by Force-directed Placement.** *Softw Exp Pract* 1991, **21(11)**:1129-1164.
35. Giaever G, Chu AM, Ni L, Connelly C, Riles L, Veronneau S, Dow S, Lucau-Danila A, Anderson K, Andre B, Arkin AP, Astromoff A, El-Bakkoury M, Bangham R, Benito R, Brachat S, Campanaro S, Curtiss M, Davis K, Deutschbauer A, Entian KD, Flaherty P, Foury F, Garfinkel DJ, Gerstein M, Gotte D, Guldener U, Hegemann JH, Hempel S, Herman Z, Jaramillo DF, Kelly DE, Kelly SL, Kotter P, LaBonte D, Lamb DC, Lan N, Liang H, Liao H, Liu L, Luo C, Lussier M, Mao R, Menard P, Ooi SL, Revuelta JL, Roberts CJ, Rose M, Ross-Macdonald P, Scherens B, Schimmack G, Shafer B, Shoemaker DD, Sookhai-Mahadeo S, Storms RK, Strathern JN, Valle G, Voet M, Volckaert G, Wang CY, Ward TR, Wilhelmy J, Winzeler EA, Yang Y, Yen G, Youngman E, Yu K, Bussey H, Boeke JD, Snyder M, Philippsen P, Davis RW, Johnston M: **Functional profiling of the Saccharomyces cerevisiae genome.** *Nature* 2002, **418(6896)**:387-391.

2.2 Article: Reconstructing the regulatory kinase pathways of myogenesis from phosphopeptide data

Author contributions:

LGP: Designed the study, performed experiments, analyzed the data and wrote the manuscript.

SV: Designed the study and performed experiments.

RECL: Analyzed the data and wrote the manuscript.

LAM: Designed the study, contributed materials and wrote the manuscript.

This research was originally published in Molecular & Cellular Proteomics. Puente, Voisin, Lee and Megeney. Reconstructing the Regulatory Kinase Pathways of Myogenesis from Phosphopeptide Data. *Mol Cell Proteomics*. 2006; **5**(12):2244-51.

Reconstructing the Regulatory Kinase Pathways of Myogenesis from Phosphopeptide Data*[S]

Lawrence G. Puente‡‖, Sébastien Voisin§¶, Robin E. C. Lee‡‖, and Lynn A. Megeney‡‖**

Multiple kinase activities are required for skeletal muscle differentiation. However, the mechanisms by which these kinase pathways converge to coordinate the myogenic process are unknown. Using multiple phosphoprotein and phosphopeptide enrichment techniques we obtained phosphopeptides from growing and differentiating C2C12 muscle cells and determined specific peptide sequences using LC-MS/MS. To place these phosphopeptides into a rational context, a bioinformatics approach was used. Phosphorylation sites were matched to known site-specific and to site non-specific kinase-substrate interactions, and then other substrates and upstream regulators of the implicated kinases were incorporated into a model network of protein-protein interactions. The model network implicated several kinases of known relevance to myogenesis including AKT, GSK3, CDK5, p38, DYRK, and MAPKAPK2 kinases. This combination of proteomics and bioinformatics technologies should offer great utility as the volume of protein-protein and kinase-substrate information continues to increase. ***Molecular & Cellular Proteomics 5:2244–2251, 2006.***

The process of skeletal muscle formation, or myogenesis, has been intensely studied because of the medical significance of muscle self-repair and as a model for cellular differentiation in general. During embryonic development, secreted factors including Shh and Wnts drive the commitment and formation of myogenic progenitor cells (1). Myoblasts, proliferating myogenic progenitors that express MyoD and Myf5, differentiate into non-proliferating myocytes that express myogenin and MRF4 (2). Subsequently these myocytes fuse into multinucleated syncytia that mature into contractile myofibers. This process of myoblast proliferation, cell cycle arrest, and myocyte fusion is recapitulated in injury repair and in cell culture models of myoblast differentiation such as the murine C2C12 muscle cell line. Transcriptional control of myogenesis has been extensively studied, firmly establishing the essential role of the myogenic regulatory factors (MRFs)[1] Myf5, MyoD, myogenin, and MRF4. Accordingly recent interest has focused on defining the kinase signal transduction mechanisms that also modulate this process.

The best characterized kinase signaling factors in myogenesis are the p38 mitogen-activated protein kinases. Inhibitors of p38 signaling block muscle-specific gene expression and myotube formation (3, 4). There is evidence that p38 acts through multiple mechanisms including phosphorylation of the MRF cofactor myocyte enhancer factor 2 (4–6), phosphorylation of the MyoD cofactor E47, and enhanced recruitment of the SWI/SNF chromatin-remodeling complex to MRF-targeted promoters (7). Another key signaling kinase in muscle is AKT1. Stimulation of AKT1 by IGF-1 or insulin induces muscle hypertrophy, whereas inhibition of AKT1 by glucocorticoids promotes muscle atrophy. Hypertrophy is associated with AKT-mediated mTOR (mammalian target of rapamycin) activation and GSK3B repression (8). Conversely AKT1 inhibition leads to dephosphorylation and activation of FOXO transcription factors resulting in atrophy (9). Although some kinase activities are required for normal muscle development, others must be suppressed. JNK1 is normally inactive during myogenesis, and its activation leads to muscle pathology (10). In addition to these kinases numerous other kinase proteins have been implicated as regulators of the differentiation process. For example CDK5 expression and activity increases during early myogenesis, and expression of dominant-negative forms of CDK5 inhibits muscle formation (11, 12). However, an important unresolved question is how these different

From the ‡Ottawa Health Research Institute, Molecular Medicine Program, Ottawa Hospital, Ottawa, Ontario K1H 8L6, Canada, §Institute for Biological Sciences, National Research Council, Ottawa, Ontario K1A 0R6, Canada, and ‖Department of Cellular and Molecular Medicine and Centre for Neuromuscular Disease, Faculty of Medicine, University of Ottawa, Ottawa, Ontario K1H 8M5, Canada

Received, April 12, 2006, and in revised form, August 3, 2006
Published, MCP Papers in Press, September 13, 2006, DOI 10.1074/mcp.M600134-MCP200

[1] The abbreviations used are: MRF, myogenic regulatory factor; 2D-GE, two-dimensional gel electrophoresis; CDK, cyclin-dependent kinase; CRHSP, calcium-regulated heat stable protein; CRMP, collapsin response mediator protein; dH_2O, deionized water; DYRK, dual specificity tyrosine (Y) phosphorylation-regulated kinase; ERK, extracellular signal-regulated kinase; FOXO, forkhead box (transcription factor); GSK, glycogen synthase kinase; IGF, insulin-like growth factor; JNK, c-Jun NH_2-terminal kinase; MAPKAPK, mitogen-activated protein kinase-activated protein kinase; PEA, phosphoprotein enriched in astrocytes; PKC, protein kinase C; STAT, signal transducer and activator of transcription; HNRNPK, heterogeneous nuclear ribonucleoprotein K; CK, casein kinase.

pathways are integrated into an overall network of kinase-substrate interactions to control myogenic differentiation.

Previously we profiled changes to protein phosphorylation during myogenesis on a proteome-wide scale by using phosphoprotein enrichment and comparative two-dimensional gel electrophoresis (13). Here we extend those findings by mapping sequence-specific sites of protein phosphorylation in growing and differentiating C2C12 cells. To place these results in a systems context, we took advantage of recent advances in the availability of protein-protein interaction databases. Databases of protein-protein interactions have been constructed from yeast, fruit fly, worm, and human cells using yeast two-hybrid, tag/pulldown, and literature search approaches (14). Subsets of the total protein-protein interaction set such as kinase-substrate interaction maps have also been constructed (15). To date, however, relatively few studies have leveraged this type of information to assist in the interpretation of results. Here we used kinase-substrate interaction databases to bioinformatically reconstruct a kinase signaling network based upon our experimentally identified phosphorylation events. This approach yielded a model kinase-substrate network that predicted several known features of myogenic signaling and revealed the potential relevance of newly identified phosphorylation events in relation to known muscle-related biochemical pathways.

EXPERIMENTAL PROCEDURES

Cells and Sample Preparation—C2C12 myoblasts were cultured in growth medium (10% fetal bovine serum, Dulbecco's modified Eagle's medium), and whole cell lysates were collected either 0 or 24 h after a change to differentiation medium (2% horse serum, Dulbecco's modified Eagle's medium) as described previously (13).

Phosphoprotein Enrichment—Phosphoprotein enrichment was performed by affinity column purification of total myoblast proteins using PhosphoProtein Purification kits (Qiagen) as described previously (13).

Analysis of Putative Phosphoproteins by One-dimensional Gel Electrophoresis—Phosphoprotein-enriched samples (typically 100–150 μg) were washed in water and concentrated using Amicon 10,000 molecular weight cutoff ultrafiltration columns (Millipore). Aliquots of retentate were separated by SDS-PAGE (12.5% acrylamide "mini" format). Gels were stained with Bio-Safe colloidal G-250 Coomassie Blue (Bio-Rad). 23 1-mm gel sections were excised from each lane, and in-gel digest and extraction of proteins was performed.

In-gel Digest—Gel pieces cut into 1-mm cubes were destained in 100 mM ammonium bicarbonate (NH_4HCO_3) in 30% ACN. Destained gel pieces were washed in dH_2O and shrunk in ACN. Gel pieces were incubated for 1 h at 56 °C in 10 mM DTT, 50 mM NH_4HCO_3; washed in 50 mM NH_4HCO_3; and incubated for 1 h at room temperature in 55 mM iodoacetamide, 50 mM NH_4HCO_3. Gel pieces were shrunk with ACN and reswollen in 50 mM NH_4HCO_3 with Promega modified trypsin (10 ng/μl). Sufficient 50 mM NH_4HCO_3 was added to cover the gel pieces, and sealed tubes were incubated overnight at 37 °C.

Preparation of Samples for IMAC—Approximately 15 μg of phosphoprotein-enriched protein extract was suspended in 50 mM NH_4HCO_3 containing Promega modified trypsin (10 ng/μl). After overnight incubation at 37 °C digest solutions were concentrated to ~40 μl and desalted through 20-μl GELoader tips (Eppendorf) packed with 20 μl of OligoR3 resin (Applied Biosystems) as described previously (16). Peptides were washed once by 20 μl of 1% acetic acid and eluted by 20 μl of 50% ACN, 1% acetic acid. Elution solvent was removed by SpeedVac and replaced by 40 μl of the appropriate IMAC binding buffer (see below).

Preparation of Metal-chelating Resin for IMAC—A 50% slurry of POROS 20MC resin (Applied Biosystems) or Propac-IMAC resin (Dionex) was prepared in dH_2O. Resin was washed twice in water, stripped by 50 mM EDTA, washed in dH_2O, and then washed in 1% acetic acid. Resin was incubated in 100 mM iron chloride, 1% acetic acid for 15 min with agitation. Activated resin was rinsed in 30% ACN, 1% acetic acid and then in 1% acetic acid.

IMAC Enrichment Using GELoader Tips—30 μl of prepared IMAC resin was added to the peptide sample in binding buffer (100 mM NaCl in 1% acetic acid) and agitated for 15 min before loading into a GELoader tip. Resin was rinsed once by 20 μl of a solution of 100 mM NaCl in 30% acetonitrile and 1% acetic acid and eluted in two steps by 250 mM ammonium phosphate, pH 9. In the first step, 5 μl was pushed into the resin and left for 5 min to neutralize the remaining acetic acid. In the second step, 15 μl of the elution buffer was pushed through the resin. The 20 μl of phosphopeptide-carrying eluate was evaporated by SpeedVac, and the phosphopeptides were suspended in 20 μl of 5% acetonitrile in 0.1% acetic acid.

IMAC Enrichment Using Pierce Phosphopeptide Isolation Kit—Gallium-chelated columns were used according to the manufacturer's recommendation with the following modifications. Using 40 μl of a solution of 5% acetic acid as binding buffer, the tryptic peptides were transferred to a Pierce column, left for 15 min at room temperature, and then centrifuged for 1 min at 3000 × g. The Gallium-chelated disc was rinsed twice with 50 μl of 100 mM NaCl in 1% acetic acid, twice with 30% acetonitrile in 1% acetic acid, and once with dH_2O and then eluted by three additions of 20 μl of 250 mM ammonium phosphate, pH 9. Eluates were pooled and evaporated by SpeedVac, and phosphopeptides were suspended in 20 μl of 5% ACN, 0.1% acetic acid before MS analysis.

Q-TOF Analyses—A fraction of each tryptic digest (typically 5–10 μl) was analyzed by nano-LC-MS/MS using a Q-TOF Ultima hybrid quadrupole time-of-flight mass spectrometer coupled to a CapLC capillary HPLC system (Waters, Milford, MA). Digests were separated on a 75-μm-inner diameter × 150-mm Inertsil ODS 3, 5-μm nano-HPLC column (Dionex/LC Packings, Sunnyvale, CA) using the following gradient conditions: 5–60% ACN, 0.2% formic acid in 30 min, and 60–90% ACN in 5 min. The mass spectrometer was set to automatically acquire MS/MS spectra on doubly, triply, and quadruply charged ions. The MS survey scan range was 400–1600 *m/z*; the MS/MS range was 50–2000. After the first LC-MS/MS run, an exclusion file was created listing all previously analyzed ions that appeared to represent non-phosphorylated peptides, and a second fraction of each tryptic digest was injected with the mass spectrometer set to ignore the ions selected during the first run.

Data Processing—Database searching was carried out using Mascot Daemon™ (Matrix Science) against the National Center for Biotechnology Information (NCBI) genome sequence database. In addition to carbamidomethylcysteines and oxidized methionine, Mascot was asked to search for the potential presence of phosphate groups on serine, threonine, or tyrosine residues by looking in the MS/MS fragmentation spectra for the mass of a HPO_3 group on these residues or for ions resulting from a neutral loss of HPO_3 or H_3PO_4 (79.9663 and 97.9769 Da, respectively). All putative phosphopeptide MS/MS spectra identified by Mascot were manually verified for both the presence of a phosphate group and the peptide sequence. In many cases, the MS/MS spectrum allowed precise identification of the modified residue.

Identification of Phosphopeptides in Existing LC-MS/MS Data—Previously phosphoprotein-enriched samples were separated by 2D-

TABLE I
Peptides sequenced by MS/MS

Gene symbol indicates the protein identity that best matches the indicated peptide. Mod. indicates the identity and sequence position of the modified residue(s) in the context of the matching protein. In the deduced peptide sequences the sites of phosphorylation are indicated with the letter "p," and missed trypsin cleavage sites are indicated with a hyphen. ND, not determined; CAMK, calcium/calmodulin-dependent protein kinase.

Gene symbol	Mod.	Peptide	Rpts[a]	Notes[b]	Potential kinases[c]
1200015F23Rik	Thr-117	TLDSP**p**THLR	1	c, f	
Acsl3 (Facl3)	Tyr-591	LQAGE**p**YVSLGK	1	b, f	
Btf3	Ser-105	QLTEMLP**p**SILNQLGADSLTSLR	1	b, d	
Btf3	Thr-100	QL**p**TEMLPSILNQLGADSLTSLR	1	b, d	
Calr	Tyr-150	VHVIFN**p**YK	1	c, d	
Canx	Ser-582	AEEDEILNR-**p**SPR	2	a, b, e, f	
Carhsp1	Ser-2	**p**SSEPPPPPLQPPTHQTSVGLLDTPR	1	b, d	
Carhsp1	Ser-31 + Ser-33	DR**p**SP**p**SPLR	1	c, f	DYRK2
Carhsp1	Ser-42	GNVVP**p**SPLPTR	7 (4)	a, b, c, d, e, f	DYRK2
Carhsp1	Ser-53	TF**p**SATVR	1	a, c, f	AKT1, AKT3
Cfl1	Ser-3	A**p**SGVAVSDGVIK + acetyl	3	a, b, c, d	LIMK1
Crmp4	Ser-522	G**p**SPTRPNPPVR	1	c, e	DYRK2
Csda	ND	SRPLNAVSQDGK	1	b, f	
D111	Ser-942	**p**SLVK-GMITAPK	1	b, f	PKC-δ*
Dap1	Ser-51	DK-DDQEWEST**p**SPPKPTVFISGVIAR	1 (2)	b, e	
Ddx21	Ser-99	EIITEEP**p**SEEEADMPKPK	1	b, e	
G3bp	Ser-231	ST**p**SPAPADVAPAQEDLR	3 (2)	a, b, c, d, e	
gi|63578930	Thr-110	VLDFEHFLPML**Q**p**T**VAK	1	c, d	
Hdgf	Ser-165	AGDVLED**p**SPK	3	a, b, c, d, f	
Hnrpk	Ser-284	DYDDM**p**SPR	1	c, f	ERK1/ERK2
Hspb1	Ser-15	SP**p**SWEPFR	1 (2)	a, b, e	MAPKAPK2
Hspb1	Ser-86	QL**p**SSGVSEIR	4 (4)	a, b, c, d, e, f	MAPKAPK2
Hspca	Ser-262	ESDDKPEIEDVG**p**SDEEEEEK-K	2	a, b, c, f	CK2
Hspcb	Ser-225	EKE**p**SDDEAEEEKGEK	1	a, c, d	CK2
Hspcb	Ser-254	IEDVG**p**SDEEDDSGK	3	a, b, c, d, f	CK2*
Lmna/c	Ser-22	SGAQASSTPL**p**SPTR	1	a, b, f	
Lmna/c	Ser-390	LR-L**p**SPSPTSQR	1	a, b, e	
Lmna/c	Ser-390 + Ser-392	LR-L**p**SP**p**SPTSQR	1	a, b, e	
Marcks	Ser-163	LSGF**p**SFK-K	1 (3)	a, b, e	PRK1, PKC
Mlp	Ser-103	LSGL**p**SFK-R	1 (2)	b, e	
Naca	Ser-132	IEDL**p**SQQAQLAAAEK	1	b, d	
Nedd5	Ser-218	IYHLPDAE**p**SDEDEDFKEQTR	1	c, f	CK2*
Npm1	Ser-82	M**p**SVQPTVSLGGFEITPPVVLR	1	b, d	
Pea15[d]	Ser-116	QP**p**SEEEIIK	3	a, b, d	CAMK2
Pea15	Thr-6	AEYG**p**TLLQDLTNNITLEDLEQLK	2	b, d	
Psma6	Ser-63	LLD**p**SSTVTHLFK	3	b, c, d	
Psma6	Ser-64	LLDS**p**STVTHLFK	1	c, d	
Psmb3	Ser-181	DAV**p**SGMGVIVHVIEK	1	b, d	
Rplp2	Ser-102 + Ser-105	K-EE**p**SEE**p**SDDDMGFGLFD	1	a, b, e	BARK1/GRK2
Rplp2	Ser-6	YVA**p**SYLLAALGGNSSPSAK	3	b, c, d	
Rplp2	Ser-6 + Tyr-7	YVA**p**S**p**YLLAALGGNSSPSAK	2	b, c, d	
Rplp2	Ser-64	LA**p**SVPAGGAVAVSAAPGSAAPAAGSAPAAAEEK	3	b, c, d	
Rplp2	Tyr-3	**p**YVASYLLAALGGNSSPSAK	2	b, c, d	
Rps3	Thr-221	DEILPT**p**TPISEQK	2	a, b, c, f	

GE, and 190 proteins were identified by LC-MS/MS (13). Many of these proteins showed evidence of differential phosphorylation between the undifferentiated and differentiating states (13). These data was extensively reanalyzed against the latest available NCBInr (nonredundant) database using Mascot server software version 2.0.04 (Matrix Science) allowing up to two missed cleavages and the variable modifications protein N-terminal acetylation, carbamidomethylation, deamidation (NQ), oxidation (Met), pyro-Glu (N-terminal Gln), and phosphorylation (YST). All putative phosphopeptide MS/MS spectra were manually reviewed.

Reconstructing a Pathway Map from Phosphopeptides—For each experimentally determined phosphorylation site, any kinase(s) known to phosphorylate the site *in vivo* or *in vitro* was identified using the bioinformatics tools KinaSource (A. Knebel, Dundee, Scotland, UK) and PhosphoSite (Cell Signaling Technology, Danvers, MA). In a small number of cases where indicated, the relevant kinase was predicted using ScanSite (17). Then KinaSource was queried for other known substrates of each kinase. The process of mapping substrates to kinases was then repeated for all proteins in the model, including the kinases themselves. Database-derived results were verified and ex-

TABLE I—*continued*

Gene symbol	Mod.	Peptide	Rpts[a]	Notes[b]	Potential kinases[c]
Stmn1	Ser-24	ASGQAFELILpSPR	2 (3)	a, b, c, d, e	GSK3, CAMK, CDC2
Stmn1	Ser-37	ESVPDFPLpSPPK	2 (3)	a, b, c, d, e	GSK3, CAMK, CDC2
Tebp	Ser-113	DWEDDpSDEDMSNFDR	3 (2)	a, b, c, d, e	CK2*
Tpm1	Ser-174	KLVIIEpSDLER	1	c, d	
Tpm1	Ser-45	QLEDELVpSLQK	1	c, d	
Tuba2	Ser-275	AVCMLpSNTTAIAEAWAR	1	c, d	
Tubb5	Thr-108	MAVpTFIGNSTAIQELFK	2	c, d	
Unnamed	ND	pSGIVVK-DVSIK	1	b, e	
XP_489094	Ser-27 + Thr-30	pSEEpTVELR	1	b, f	

[a] Rpts indicates the number of independently prepared phosphoprotein-enriched samples that produced spectra matching this phosphopeptide sequence. Numbers in parentheses represent the number of repeated observations of the peptide in independent IMAC experiments done on the same protein sample.

[b] Notes: a, phosphorylation of this site has previously been reported; b, this phosphopeptide was detected in undifferentiated C2C12 cell samples; c, this phosphopeptide was detected in differentiating C2C12 cell samples; d, this phosphopeptide was detected after phosphoprotein enrichment and two-dimensional gel electrophoresis; e, this phosphopeptide was detected after phosphoprotein enrichment and IMAC; f, this phosphopeptide was detected after phosphoprotein enrichment and one-dimensional SDS-PAGE.

[c] Potential kinases are those that have been shown to phosphorylate the specific site in other studies or that are predicted to phosphorylate the target site; predicted interactions are annotated with an asterisk (*).

[d] This phosphopeptide was reported previously by us elsewhere (13) but is included here for completeness.

tended by examination of the primary research literature. The identified substrate-kinase interactions were then diagrammed using the bioinformatics tool HubView (18).

RESULTS AND DISCUSSION

53 phosphopeptides were identified from C2C12 cell cultures undergoing growth or differentiation (Table I; see Supplements 1 and 2 for additional details). 17 phosphopeptides were identified after IMAC, 17 after one-dimensional gel electrophoresis (Fig. 1), and 30 after 2D-GE and LC-MS/MS. Only nine phosphopeptides were detected by multiple methods suggesting that each method introduces a bias into the selection of peptides. The apparently greater success of the 2D-GE method may indicate a benefit from greater sample fractionation or may simply reflect the larger number of such experiments performed. All phosphopeptides listed in Table I were matched to known or predicted proteins, and in 43 cases additional non-phosphorylated peptides were identified that supported the identification. Some phosphorylations were detected only in either growing or differentiating cells (Table II). Of the 55 identified phosphopeptides, at least 21 contained phosphorylation sites that have been reported previously.

A major challenge in systems biology is to transform large datasets into biologically relevant interpretations. To address this problem, we chose to use a novel bioinformatics approach. We reasoned that because phosphopeptides are the product of protein kinase activity we could construct a proposed kinase-substrate interaction network based upon our data. To perform this task, 19 experimentally detected phosphorylations for which the responsible kinase was known or strongly predicted were used as the "bootstrap" to create an initial network of kinase-substrate interactions (Fig. 2*A*; see also Supplement 3). Then other known substrates of those kinases, as well as interactions upstream of each kinase, were determined and incorporated into the model (Fig. 2*B*). For clarity, the abundant and promiscuous kinases PKC and CK2 were excluded from the model, although PKC was included in cases where phosphorylation was attributed to a specific PKC isoform.

The generally accepted view of myogenic signaling is that AKT, p38, MAPKAPK2, and CDK5 activity promote cell cycle exit and myotube formation, whereas ERK1/2 and GSK3 activity are associated with cell cycling and maintenance of the undifferentiated state. Of 114 kinases listed in KinaSource, only 21 appeared in our extrapolated network, and satisfyingly, this group prominently featured AKT, CDK5, GSK3, and MAPKAPK2 kinases (Fig. 2*C*). Furthermore some kinase-substrate interactions known to be relevant in myogenic signaling such as CDK5-myocyte enhancer factor 2 and AKT-FOXO1A were inferred by the model. Whereas the list of phosphopeptides alone provided little biological context, the extrapolated kinase-substrate network suggested a number of features of interest, such as the implication of DYRK kinases as promyogenic factors.

DYRK—DYRK interactions were prominent in the model network. Induction of DYRK family kinases is required for muscle differentiation (19) at least in part via DYRK-mediated phosphorylation and regulation of histone deacetylases (20). Here we found that the putative DYRK substrates CRHSP24 and CRMP4 are also phosphorylated in C2C12 (Table I and Fig. 3). Bioinformatics modeling revealed five more DYRK-substrate interactions (p27kip, p21waf, FOXO1A, glycogen

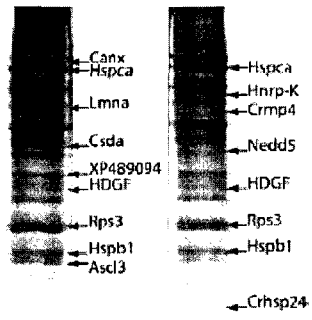

FIG. 1. **After phosphoprotein enrichment and one-dimensional SDS-PAGE, proteins were detected by G-250 Coomassie Blue stain.** *Labeled arrows* indicate identified proteins from which phosphopeptide MS/MS spectra were obtained.

TABLE II
Undifferentiated versus differentiating cells

Phosphopeptides that were detected in samples from only either undifferentiated or differentiated C2C12 but not under both conditions are listed separately. In some cases different phosphopeptides from the same protein were detected depending on the cell differentiation state, and the specific site of phosphorylation is given in these instances. Kinases proposed to be responsible for each phosphorylation are given in parentheses, MARCKS, myristoylated alanine rich protein kinase C substrate; MLP, MARCKS-like protein; NACA, nascent polypeptide-associated complex; CANX, calnexin; CALR, calreticulin; HSPCB, heat shock protein class b; CSDA, cold shock domain protein A.

Undifferentiated	Differentiating
ACSL3	CALR
BTF3	CRHSP24 Ser-31 (DYRK2)
CANX	CRHSP24 Ser-33 (DYRK2)
CRHSP24 Ser-2	CRHSP24 Ser-53 (AKT)
CSDA	CRMP4 (DYRK2)
D111 (PKC-δ)	HNRNPK (ERK1/ERK2)
DAP1	HSPCB Ser-225 (CK2)
DDX21	NEDD5 (CK2)
HSPB1 Ser-15 (MAPKAPK2)	Tropomyosin
Lamin	Tubulin
MARCKS (PKC, PRK1)	
MLP (PKC)	
NACA	
NPM1	
PEA-15 (CAMK2)	
PSMB3	
RPLP2 (GRK2)	
XP_489094	

synthase, and STAT3), suggesting additional mechanisms by which DYRK may contribute to myogenesis. Two of the phosphorylation sites ascribed to DYRK2 activity are thought to be priming sites for GSK3. In CRMP4 (Dpysl3, Drp3) Ser-522 appears to represent the priming site for a series of GSK3-mediated phosphorylations at serines 518, 514, and 509 (21). In C2C12 cells both site-specific (Table I) and general phosphorylation (13) of CRMP4 was detected only in differentiating cells, whereas Ser-522 is constitutively phosphorylated in brain. Although CRMP4 has been studied almost exclusively in the context of neurons, these data and the observation that the CRMP4 promoter contains a MyoD/myogenin binding site (22) indicate that CRMP proteins likely play an important role in muscle differentiation. eIF2B (eukaryotic translation initiation factor 2B) is also a substrate of both DYRK and GSK3. DYRK-mediated phosphorylation at Ser-539 is thought to permit subsequent phosphorylation of Ser-535 by GSK3 leading to repression of translation (23). Because muscle hypertrophy is associated with GSK3 inhibition and eIF2 derepression, this suggests that promyogenic functions of DYRK could be blocked by GSK3 activity. These observations are consistent with the model that DYRK activity is increased and GSK3 is repressed during myogenesis. In agreement with this principle, several putative GSK3 substrate proteins that were not DYRK substrates, pyruvate dehydrogenase and CRMP2, showed evidence of phosphorylation only in non-differentiated myoblasts, although specific phosphorylation sites were not determined (13).

CRHSP24—CaRHSP24/CRHSP24 is phosphoprotein of unknown function. DYRK2 can phosphorylate CRHSP24 at serines 31 and 33 *in vitro*, and Ser-43 (equivalent to Ser-42 in mouse) is phosphorylated in human embryonic kidney 293 cells (24). We detected phosphorylation at serines 31, 33, and 53 in differentiating C2C12 and constitutive phosphorylation at Ser-42 (Table I). Phosphorylation of CRHSP24 at Ser-53, ascribed to AKT activity, was also detected. CRHSP24 may play an important role in myogenesis. IGF-1 treatment, which stimulates muscle hypertrophy, stimulates phosphorylation of the Ser-53 site in human embryonic kidney 293 cells. CRHSP24 is a calcineurin substrate (25). Calcineurin activity is important in normal muscle development, and augmented calcineurin activation has been shown to limit the pathogenesis of muscular dystrophies (26).

PEA-15—Our previous observation of PEA-15 phosphorylation in C2C12 (13) was confirmed and extended with evidence of a second phosphorylation site (Table I). Ser-116 phosphorylated PEA-15 was repeatedly observed in growing cells but never in differentiating cells. This observation is consistent with the recent report that the Ser-104/Ser-116 dephosphorylated form of PEA-15 promotes cell cycle arrest via sequestration of ERK (27), and indeed, reduced ERK activity is a prerequisite for myoblast differentiation (28).

PKC-δ—A potential role for PKC-δ was inferred in the model (Fig. 2C), and the potential PKC-δ substrates 14-3-3, HMGA1 (high mobility group AT-hook 1), and HNRNPK were detected in phosphoprotein enrichment experiments (13). Although site-specific evidence of PKC-δ-mediated phosphorylation is lacking, these observations are interesting in light of a recent report that constitutively active PKC-δ promotes whereas kinase-inactive PKC-δ inhibits IGF-1-mediated pro-

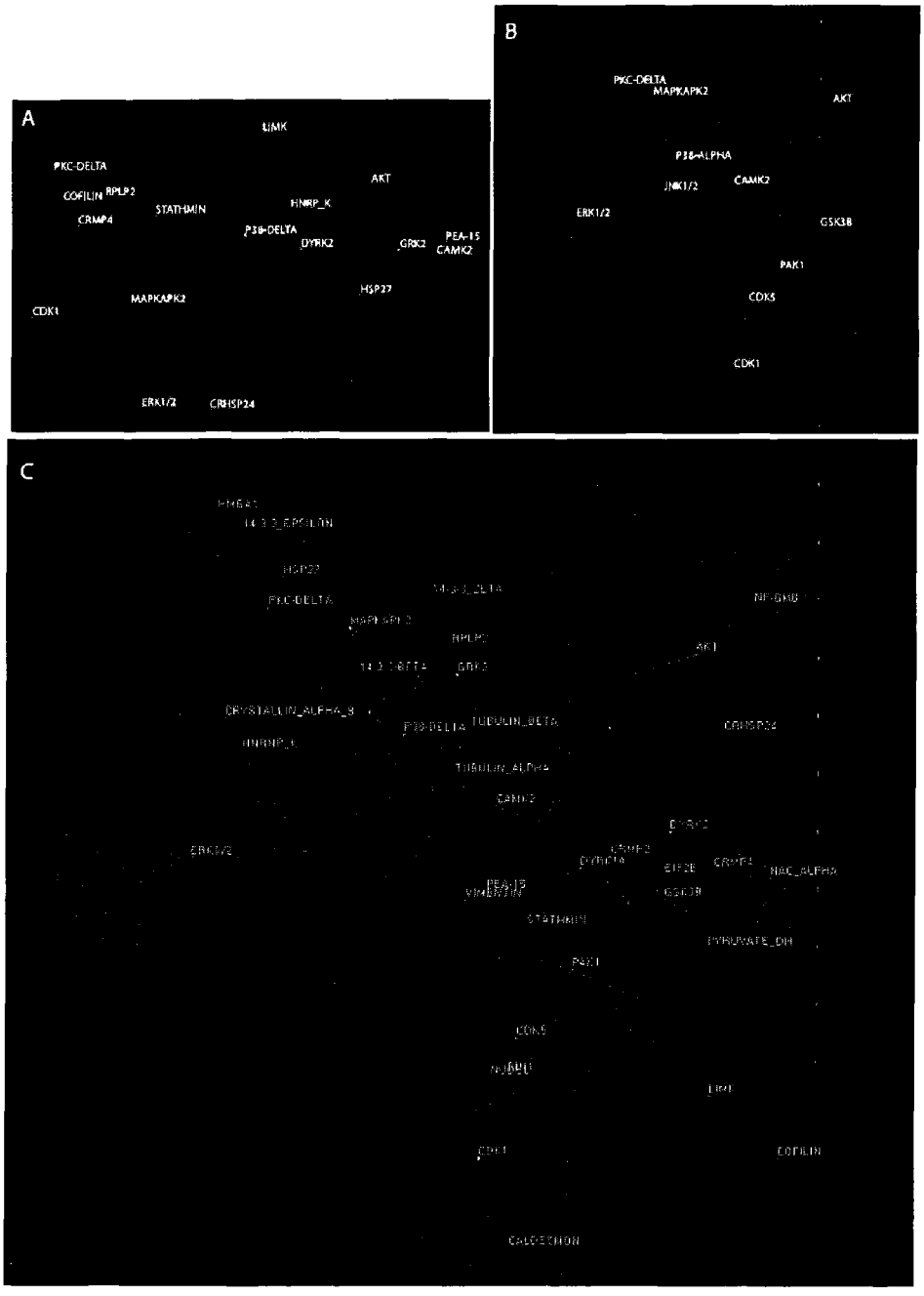

FIG. 2. **Graphical representations of kinase-substrate interaction pathways made using the bioinformatics visualization tool HubView (18).** *A*, experimentally detected phosphopeptides were matched to the corresponding kinases based on database and literature searches. Kinases are shown in *blue* (<15 substrates) or *orange* (>15 substrates), and non-kinase proteins are colored *gray*. *B*, the model network extended to include all substrates and upstream regulators of each implicated kinase. Major hub kinases are labeled. *C*, the model network with experimentally detected phosphoproteins from Table I and previous work (13) and their upstream kinases labeled. Additional visualizations can be found in Supplement 3. LIMK, LIM domain containing, protein kinase; NACA, nascent polypeptide-associated complex α; DH dehydrogenase.

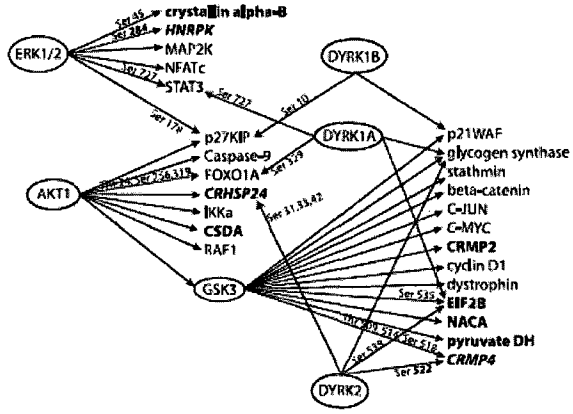

FIG. 3. **Detailed view of DYRK interactions.** Specific sites of phosphorylation are indicated where known. Proteins experimentally determined to be phosphorylated (13) are given in *bold type*, and proteins experimentally determined to be phosphorylated at specific sites (Table I) are given in *italic type*. The current model for kinase signaling in early myogenesis is that AKT is activated, GSK3 is consequently repressed, ERK activity is low, and DYRK expression and activity is increased. IKKa, inhibitor of κB kinase α; NFATc, nuclear factor of activated T cells; CSDA, cold shock domain protein A.

liferation of myoblasts (29). PKC-δ, as well as DYRK1a and ERK1/ERK2, can also phosphorylate STAT3, which is reported to promote myoblast proliferation and inhibit MyoD function and muscle differentiation (30–32). Because the aforementioned substrates contain multiple phosphorylation sites, additional studies will be required to determine the precise role of PKC.

Limitations to Application and Interpretation—Because the experimental data cover only a very small proportion of the phosphoproteome, it is important to consider the validity of extrapolating a model kinase network under these circumstances. The strategy used relies on three assumptions: that substrates have a limited number of kinases, that kinases have a large number of substrates, and that the overall topology of the kinase-substrate network is scale-free. First, if a substrate has many potential kinases then inference of specific kinase activities is not possible. Second, if a kinase has few substrates then the odds that one of those substrates will be found experimentally is extremely low. The last assumption determines whether the model is likely to encompass major features of the true *in vivo* network or if it reveals only local details. In a non-scale-free network a small data sample will show only local features, much as mapping a few roads in a city would reveal nothing about the overall layout of the traffic flow. However in a scale-free network, any two points on the network are connected by a very small number of interactions, and the overall picture emerges quickly, just as a sampling of commercial airline flights would quickly reveal the existence of traffic hubs at the major airports. Work on kinase-substrate interactions in yeast supports these three assumptions. An exhaustive evaluation of 1325 phosphoproteins and 87 kinases by Ptacek *et al.* (15) found that 73% of substrates were associated with only one or two kinases but that most kinases had multiple substrates. Analysis of the kinase-substrate subset of the extensive protein-protein interaction data available for yeast confirmed that this network is scale-free (18).

Another consideration was protein abundance. If myogenesis resulted in altered protein phosphorylation in only a subset of very low abundance proteins against a large backdrop of abundant invariant phosphoproteins then no relevant results would have been obtained. However, we found previously that the subset of the phosphoproteome that is sufficiently abundant for silver stain detection on gels does in fact undergo extensive alteration during early myogenesis (13). The use of data obtained from two-dimensional gels was especially valuable in retaining a biologically relevant focus. Comparative analysis of gels prepared from growing *versus* differentiating myocytes allowed us to focus the MS analysis on proteins that exhibited evidence of altered post-translational modification during myogenesis. All of these factors contributed to the ability to produce a model network that exhibited relevant features of interest. However, a number of caveats remain. First, because proteome coverage is incomplete, lack of detection of phosphorylation cannot be taken as strong evidence of dephosphorylation. Second, the results are biased toward the detection of relatively abundant peptides. Third, kinase-substrate databases are far from complete, although the amount of protein-protein interaction data available is increasing rapidly. We anticipate that increased coverage should not invalidate or contradict the results presented here. Because kinase networks appear to be scale-free (18), increased data coverage would likely increase the number of substrates more rapidly than the number of kinases, limiting any changes in the overall topology of the network. However, this remains to be experimentally demonstrated. Another challenge remaining to be addressed is the role of regulated phosphatases in the network. At this time inclusion of a comprehensive phosphatase dataset is not possible given the limited experimental observations in the literature combined with the absence of robust screening tools for phosphatase activity or dephosphorylation events.

Conclusion—Experimental phosphopeptide data and bioinformatics databases of kinase-substrate interactions were used to produce a model signaling network for C2C12 myogenesis. From a relatively small number of phosphopeptides, a complex network was readily constructed that inferred the existence of several known features of myogenic signaling. In addition, places for newly described phosphorylations in signaling cascades were predicted. New protein-protein interaction datasets including kinase-substrate datasets are being produced at an increasing rate, and the utility of this approach is certain to increase as more data become available.

Acknowledgments—We thank John F. Kelly for invaluable advice and discussions and Douglas J. Borris, Wen Ding, and Luc Tessier for expert technical assistance.

* This work was supported in part by grants from the Heart and Stroke Foundation of Canada and the Muscular Dystrophy Association (United States) (to L. A. M.). The costs of publication of this article were defrayed in part by the payment of page charges. This article must therefore be hereby marked "*advertisement*" in accordance with 18 U.S.C. Section 1734 solely to indicate this fact.

[S] The on-line version of this article (available at http://www.mcponline.org) contains supplemental material.

¶ Supported by funding from the Genomic and Health Initiative.

** Holds the Mach-Gaennelsen Chair in Cardiac Research. To whom correspondence should be addressed: Ontario Genomics Innovation Centre, Ottawa Health Research Institute, 501 Smyth Rd., Ottawa, Ontario K1H 8L6, Canada. Tel.: 613-737-8899 (ext. 78618); Fax: 613-737-8803; E-mail: lmegeney@ohri.ca.

REFERENCES

1. Huh, M. S., Smid, J. K., and Rudnicki, M. A. (2005) Muscle function and dysfunction in health and disease. *Birth Defects Res.* **75,** 180–192
2. Chargé, S. B., and Rudnicki, M. A. (2004) Cellular and molecular regulation of muscle regeneration. *Physiol. Rev.* **84,** 209–238
3. Cuenda, A., and Cohen, P. (1999) Stress-activated protein kinase-2/p38 and a rapamycin-sensitive pathway are required for C2C12 myogenesis. *J. Biol. Chem.* **274,** 4341–4346
4. Zetser, A., Gredinger, E., and Bengal, E. (1999) p38 mitogen-activated protein kinase pathway promotes skeletal muscle differentiation. Participation of the Mef2c transcription factor. *J. Biol. Chem.* **274,** 5193–5200
5. de Angelis, L., Zhao, J., Andreucci, J. J., Olson, E. N., Cossu, G., and McDermott, J. C. (2005) Regulation of vertebrate myotome development by the p38 MAP kinase-MEF2 signaling pathway. *Dev. Biol.* **283,** 171–179
6. Han, J., Jiang, Y., Li, Z., Kravchenko, V. V., and Ulevitch, R. J. (1997) Activation of the transcription factor MEF2C by the MAP kinase p38 in inflammation. *Nature* **386,** 296–299
7. Lluis, F., Perdiguero, E., Nebreda, A. R., and Munoz-Canoves, P. (2006) Regulation of skeletal muscle gene expression by p38 MAP kinases. *Trends Cell Biol.* **16,** 36–44
8. Rommel, C., Bodine, S. C., Clarke, B. A., Rossman, R., Nunez, L., Stitt, T. N., Yancopoulos, G. D., and Glass, D. J. (2001) Mediation of IGF-1-induced skeletal myotube hypertrophy by PI(3)K/Akt/mTOR and PI(3)K/Akt/GSK3 pathways. *Nat. Cell Biol.* **3,** 1009–1013
9. Hoffman, E. P., and Nader, G. A. (2004) Balancing muscle hypertrophy and atrophy. *Nat. Med.* **10,** 584–585
10. Kolodziejczyk, S. M., Walsh, G. S., Balazsi, K., Seale, P., Sandoz, J., Hierlihy, A. M., Rudnicki, M. A., Chamberlain, J. S., Miller, F. D., and Megeney, L. A. (2001) Activation of JNK1 contributes to dystrophic muscle pathogenesis. *Curr. Biol.* **11,** 1278–1282
11. Lazaro, J. B., Kitzmann, M., Poul, M. A., Vandromme, M., Lamb, N. J., and Fernandez, A. (1997) Cyclin dependent kinase 5, cdk5, is a positive regulator of myogenesis in mouse C2 cells. *J. Cell Sci.* **110,** 1251–1260
12. Philpott, A., Porro, E. B., Kirschner, M. W., and Tsai, L. H. (1997) The role of cyclin-dependent kinase 5 and a novel regulatory subunit in regulating muscle differentiation and patterning. *Genes Dev.* **11,** 1409–1421
13. Puente, L. G., Carriere, J. F., Kelly, J. F., and Megeney, L. A. (2004) Comparative analysis of phosphoprotein-enriched myocyte proteomes reveals widespread alterations during differentiation. *FEBS Lett.* **574,** 138–144
14. Bork, P., Jensen, L. J., von Mering, C., Ramani, A. K., Lee, I., and Marcotte, E. M. (2004) Protein interaction networks from yeast to human. *Curr. Opin. Struct. Biol.* **14,** 292–299
15. Ptacek, J., Devgan, G., Michaud, G., Zhu, H., Zhu, X., Fasolo, J., Guo, H., Jona, G., Breitkreutz, A., Sopko, R., McCartney, R. R., Schmidt, M. C., Rachidi, N., Lee, S. J., Mah, A. S., Meng, L., Stark, M. J., Stern, D. F., De Virgilio, C., Tyers, M., Andrews, B., Gerstein, M., Schweitzer, B., Predki, P. F., and Snyder, M. (2005) Global analysis of protein phosphorylation in yeast. *Nature* **438,** 679–684
16. Stensballe, A., Andersen, S., and Jensen, O. N. (2001) Characterization of phosphoproteins from electrophoretic gels by nanoscale Fe(III) affinity chromatography with off-line mass spectrometry analysis. *Proteomics* **1,** 207–222
17. Obenauer, J. C., Cantley, L. C., and Yaffe, M. B. (2003) Scansite 2.0: Proteome-wide prediction of cell signaling interactions using short sequence motifs. *Nucleic Acids Res.* **31,** 3635–3641
18. Lee, R. E., and Megeney, L. A. (2005) The yeast kinome displays scale free topology with functional hub clusters. *BMC Bioinformatics* **6,** 271
19. Deng, X., Ewton, D. Z., Pawlikowski, B., Maimone, M., and Friedman, E. (2003) Mirk/dyrk1B is a Rho-induced kinase active in skeletal muscle differentiation. *J. Biol. Chem.* **278,** 41347–41354
20. Deng, X., Ewton, D. Z., Mercer, S. E., and Friedman, E. (2005) Mirk/dyrk1B decreases the nuclear accumulation of class II histone deacetylases during skeletal muscle differentiation. *J. Biol. Chem.* **280,** 4894–4905
21. Cole, A. R., Knebel, A., Morrice, N. A., Robertson, L. A., Irving, A. J., Connolly, C. N., and Sutherland, C. (2004) GSK-3 phosphorylation of the Alzheimer epitope within collapsin response mediator proteins regulates axon elongation in primary neurons. *J. Biol. Chem.* **279,** 50176–50180
22. Matsuo, T., Stauffer, J. K., Walker, R. L., Meltzer, P., and Thiele, C. J. (2000) Structure and promoter analysis of the human unc-33-like phosphoprotein gene. E-box required for maximal expression in neuroblastoma and myoblasts. *J. Biol. Chem.* **275,** 16560–16568
23. Woods, Y. L., Cohen, P., Becker, W., Jakes, R., Goedert, M., Wang, X., and Proud, C. G. (2001) The kinase DYRK phosphorylates protein-synthesis initiation factor eIF2B[epsilon] at Ser539 and the microtubule-associated protein tau at Thr212: potential role for DYRK as a glycogen synthase kinase 3-priming kinase. *Biochem. J.* **355,** 609–615
24. Auld, G. C., Campbell, D. G., Morrice, N., and Cohen, P. (2005) Identification of calcium-regulated heat-stable protein of 24 kDa (CRHSP24) as a physiological substrate for PKB and RSK using KESTREL. *Biochem. J.* **389,** 775–783
25. Groblewski, G. E., Yoshida, M., Bragado, M. J., Ernst, S. A., Leykam, J., and Williams, J. A. (1998) Purification and characterization of a novel physiological substrate for calcineurin in mammalian cells. *J. Biol. Chem.* **273,** 22738–22744
26. St-Pierre, S. J., Chakkalakal, J. V., Kolodziejczyk, S. M., Knudson, J. C., Jasmin, B. J., and Megeney, L. A. (2004) Glucocorticoid treatment alleviates dystrophic myofiber pathology by activation of the calcineurin/NF-AT pathway. *FASEB J.* **18,** 1937–1939
27. Krueger, J., Chou, F. L., Glading, A., Schaefer, E., and Ginsberg, M. H. (2005) Phosphorylation of phosphoprotein enriched in astrocytes (PEA-15) regulates extracellular signal-regulated kinase-dependent transcription and cell proliferation. *Mol. Biol. Cell* **16,** 3552–3561
28. Dorman, C. M., and Johnson, S. E. (1999) Activated Raf inhibits avian myogenesis through a MAPK-dependent mechanism. *Oncogene* **18,** 5167–5176
29. Czifra, G., Toth, I. B., Marincsak, R., Juhasz, I., Kovacs, I., Acs, P., Kovacs, L., Blumberg, P. M., and Biro, T. (2006) Insulin-like growth factor-I-coupled mitogenic signaling in primary cultured human skeletal muscle cells and in C2C12 myoblasts. A central role of protein kinase Cδ. *Cell. Signal.* **18,** 1461–1472
30. Jo, C., Kim, H., Jo, I., Choi, I., Jung, S. C., Kim, J., Kim, S. S., and Jo, S. A. (2005) Leukemia inhibitory factor blocks early differentiation of skeletal muscle cells by activating ERK. *Biochim. Biophys. Acta* **1743,** 187–197
31. Kami, K., and Senba, E. (2002) In vivo activation of STAT3 signaling in satellite cells and myofibers in regenerating rat skeletal muscles. *J. Histochem. Cytochem.* **50,** 1579–1589
32. Kataoka, Y., Matsumura, I., Ezoe, S., Nakata, S., Takigawa, E., Sato, Y., Kawasaki, A., Yokota, T., Nakajima, K., Felsani, A., and Kanakura, Y. (2003) Reciprocal inhibition between MyoD and STAT3 in the regulation of growth and differentiation of myoblasts. *J. Biol. Chem.* **278,** 44178–44187

2.3 Book Chapter: Reconstructing regulatory kinase pathways from phosphopeptide data: a bioinformatics approach

LGP: Wrote the manuscript.

RECL: Wrote the manuscript.

LAM: Wrote the manuscript.

Chapter 23

Reconstructing Regulatory Kinase Pathways from Phosphopeptide Data: A Bioinformatics Approach

Lawrence G. Puente, Robin E.C. Lee, and Lynn A. Megeney

Summary

Protein phosphorylation is a widespread cellular process, and simplistic linear pathway models of kinase signaling likely under-represent the complexity of *in vivo* pathways. The recent massive increase in information available through protein interaction databases now allows construction of *in silico* models of protein networks that are underpinned by evidence from real biological systems. By combining protein phosphorylation data with current databases of protein–protein and kinase–substrate interactions, sophisticated models of intracellular protein phosphorylation signaling can be constructed for a system of interest. The kinase interaction network can be visualized, analyzed by graph theory, and investigated for hypotheses that are not otherwise obvious.

Key words: Bioinformatics, Scale-free networks, Kinase signaling.

1. Introduction

Reversible protein phosphorylation is one of the most common means of regulating cellular processes. Genomic studies have identified 518 kinases in humans *(1)* and 540 in mouse *(2)*, and it is estimated that up to 30% of the proteome may be subject to phosphorylation *(3)*. These numbers have led to an appreciation that systems biology and bioinformatics approaches are required in order to fully understand the role of protein phosphorylation in cellular biology. Large-scale protein–protein interaction studies have clearly demonstrated that protein–protein interactions form complex networks. The subset of protein–protein interactions composed of kinases and their substrates can also be considered as a network *(4, 5)*. Such network models can aid in gaining a

Marjo de Graauw (ed.), *Phospho-Proteomics, Methods and Protocols, vol. 527*

Book DOI: 10.1007/978-1-60327-834-8_23

thorough mechanistic understanding of the pathways, reveal unanticipated molecular interactions, and lead to novel hypotheses.

The most common network visualization technique is the connected ball and stick graph (Fig. 1), where a ball or *node* represents an individual protein and an interaction between a pair of proteins is depicted by a line or *edge* connecting the pair. In the context of kinases, the presence of a directed edge can implicitly define the kinase–substrate relationship, where the origin of the edge is the kinase and the arrow tip identifies the substrate; this is in contrast with an undirected edge, which can represent a physical/coactivation or undefined interaction.

To represent a network computationally, the interacting nodes can be recorded as pairs of node identification numbers (*see* **Table 1** for an example). For kinase networks, the identification numbers would correspond to specific proteins. Several standardized protein identification number systems exist, such as SwissProt (http://www.expasy.org). The specific system employed is not important as long as the numbers are uniquely associated with a specific protein.

Once a network has been assembled, graph theory can be used to analyze its structure. Highly connected nodes or *hubs* are one point of interest, and may represent indispensable components of the signaling network. Experimental observations of protein phosphorylation can be mapped onto a network model of the system of interest to infer which kinase pathways are most

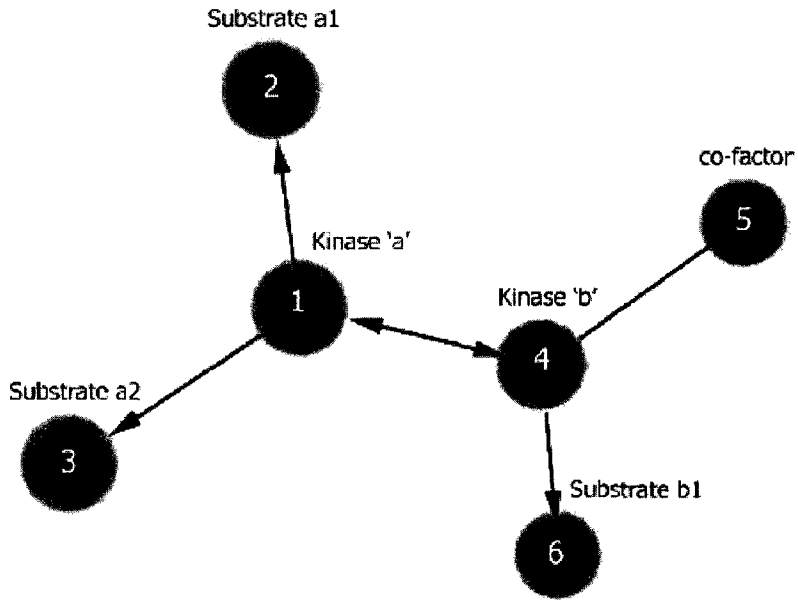

Fig. 1. A sample network. Kinase a phosphorylates substrates a1 and a2 and also phosphorylates kinase b. Kinase b phosphorylates kinase a and substrate b1 and has a nonsubstrate interaction with protein 5.

Table 1
Description of the network shown in Fig. 1

Kinase	Substrate
1	4
1	2
1	3
4	1
4	6

The table represents a directed network in which the *left side* indicates kinases and the *right side* indicates substrates. The data indicates that protein 1 phosphorylates proteins 2, 3, and 4 while protein 4 phosphorylates proteins 1 and 6. The order of the pairs implicitly indicates which proteins are kinases and which are substrates. An undirected network could contain additional pairs such as (4, 5) that do not have a kinase–substrate relationship. In an undirected network the order of the pairs does not matter so the interaction (4, 1) would automatically imply the interaction (1, 4)

likely to be active. The network will predict specific biochemical interactions that can be experimentally tested.

We previously demonstrated a general strategy for inferring networks of kinase–substrate relationships from phosphopeptide data *(5)*. This bioinformatics approach involves compiling phosphorylation site data, inferring potential kinase activities, predicting additional substrates, and visualizing and analyzing the network.

2. Materials

2.1. Bioinformatics Workstation

A basic bioinformatics workstation can be implemented on any modern personal computer system. Some specific requirements are as follows:

1. Current web browser with JavaScript support.
2. Java support. The Java runtime environment (JRE) is pre-installed on most personal computer systems and can be downloaded at no cost from http://www.java.com/en/download/manual.jsp.
3. A spreadsheet application such as Microsoft Excel (http://office.microsoft.com) or OpenOffice (http://www.openoffice.org) for basic data management.
4. High-speed Internet access.

3. Methods

By leveraging the information in bioinformatic databases of kinase–substrate interactions, protein phosphorylation data can be used to reconstruct a model network of kinase-mediated signaling in the system of interest. The approach involves several steps:

1. Acquire phosphopeptide data.
2. Identify known kinase(s) for each phosphorylated site.
3. Predict additional substrates for each kinase.
4. Extend the network model by identifying potential kinases for each known or predicted substrate.
5. Visualize the network.
6. Analyze the network and utilize the model to make testable hypotheses.

Each step is described in more detail in the following sections.

3.1. Acquire Phosphopeptide Data

Generally, proteins are purified from the system of interest, either with or without a phosphoprotein enrichment procedure. The recovered proteins are usually separated or fractionated using gel electrophoresis or liquid chromatography methods and each gel band or chromatograph fraction is proteolytically digested by trypsin. The resultant peptides may be further enriched for phosphopeptides using the methods described elsewhere in this volume. These peptides are then characterized using mass spectrometry and sites of phosphorylation are identified. Detailed methods for the acquisition of phosphopeptide data are beyond the scope of this chapter.

3.2. Map Kinase–Substrate Relationships

Several tools are available for mapping substrate-to-kinase relationships, some of which are described here.

KinaSource (http://www.kinasource.co.uk): The KinaSource web site includes a manually curated database (http://www.kinasource.co.uk/Database/welcomePage.php) of kinase–substrate pairs, emphasizing mouse and human proteins. The database can be searched by kinase or substrate. The resulting records show Swiss-Prot accession numbers, site(s) of phosphorylation where known, and corresponding literature references. Over 1,000 kinase–substrate pairs are described.

PhosphoSite (http://www.phosphosite.org): PhosphoSite is a large database of known phosphorylation sites on rodent and human proteins, maintained by the Cell Signaling Technology Corporation. The database can be searched by protein name or accession number and also by amino acid sequence, domain name, or contributing author. The resulting protein information

pages include basic information on the protein and a list of the amino acid sequences known to be phosphorylated. Individual sites of phosphorylation are linked to detailed subpages that list the methods by which the phosphorylation was characterized, literature references, and in some cases extensive information on known upstream kinases and phosphatases as well as pharmacological or biochemical treatments known to modulate the phosphorylation. Phosphosite contains a great deal of additional information such as protein name synonyms, kinase family classifications, biological function annotations, and an isoelectric point calculator for phosphorylated proteins.

ScanSite (http://scansite.mit.edu): ScanSite *(6)* is a tool for predicting sites of protein interaction based upon the presence of amino acid sequence motifs. Many kinases phosphorylate specific target motifs, and ScanSite can search protein sequences for the presence of these motifs. ScanSite also finds motifs for other protein–protein interactions, such as potential SH3 binding sites. By default, ScanSite searches for a spectrum of common motifs, including many kinase–substrate motifs. User-defined sequence patterns or scoring matrices can also be employed. Batches of accession numbers or sequences may also be submitted for analysis (http://stjuderesearch.org/scansite/).

Phospho.ELM (http://phospho.elm.eu.org/): Phospho.ELM *(7)* is a database of several thousand phosphorylation sites from multiple species. It can be searched by kinase or substrate, and can also be searched for phosphorylation sites that modulate specific protein–protein interactions (e.g., SH2 domain binding sites). Academic users may request a copy of the Phospho.ELM database for their own research (http://phospho.elm.eu.org/dataset.html), or can write programs that interface with Phospho.ELM via Web Services (a WSDL file is available at http://phospho.elm.eu.org/webservice/phosphoELMdb.wsdl).

3.3. Predict Additional Substrates

To extend the network and generate hypotheses, add other known substrates for each kinase in the model. Based on the assumption that each of the identified kinases is potentially active, additional known substrates of each kinase can be predicted to be phosphorylated and this can be tested experimentally. Tools such as KinaSource and Phospho.ELM can be used to produce lists of known substrates for a given kinase. For human cells, it is estimated that there are an average of 20 substrates per kinase *(3)*, although certain kinases have hundreds of known substrates. For the purposes of hypothesis generation, it is sometimes helpful to ignore the promiscuous kinases in favor of analyzing more specific interactions.

3.4. Extend the Network

The model network at this stage includes observed substrates, predicted kinases, and predicted substrates. Treating *all* proteins

in the model network as potential substrates, repeat the earlier process of mapping substrates to kinases. Many kinases are themselves substrates of other kinases and such kinase cascades are frequently of interest.

3.5. Network Visualization

Several tools are available for visualizing networks.

Cytoscape (http://www.cytoscape.org/): Cytoscape *(8)* is an open-source software platform specifically designed for visualizing molecular interaction networks. Cytoscape is the product of a public–private research partnership and is released under the LGPL (Lesser General Public License). Cytoscape is a Java application and can be used on any Windows, Macintosh or Linux system that supports Java.

LaNet-vi (http://xavier.informatics.indiana.edu/lanet-vi/): The LArge NETwork VIsualization tool is an online tool that constructs undirected network diagrams. To use LaNet-vi, prepare a text file representing the network as a simple list of number pairs representing nodes that interact with each other. Each pair of numbers should be separated by a space or tab, one pair per line. The input file is submitted through a web page form and the resulting network diagram is returned by e-mail. A Creative Commons license applies to the images.

Graphviz (http://www.graphviz.org/): Graphviz is an open-source graph visualization software package. It is a general-purpose package that can be customized through programming.

HubView (http://www.ogic.ca/projects/hubview/hubview.html): HubView *(4)* is a standalone Windows application specialized to the study of *Saccharomyces cerevisiae* kinase–substrate interaction networks. The application permits network visualization, clustering analysis, and the generation of user defined subnetworks. A Creative Commons license applies to use of the software.

3.6. Analysis of the Network

Once a network is assembled, graph theory can be used to analyze its structure. Topological features of the graph are studied by statistical analysis of the number of unique edges directed towards and away from each individual node. Highly connected nodes or "hub proteins" are commonly observed in eukaryotic protein interaction networks. The exact role of a hub protein can be ambiguous in the context of a network, and is best studied on a case-by-case basis but the hub-ness of a protein may offer general insight into its regulation or function. For example a hub-like kinase may provide a noise threshold by phosphorylating a large number of substrates in a promiscuous manner or the kinase itself may be temporally/spatially regulated causing a dramatic shift in substrate interactions. A hub-like substrate might act as a phospho-sink to stop a signal from being inappropriately propagated at sub-threshold levels or perhaps the substrate

requires phosphorylation at multiple unique sites in order for its function to be fully regulated.

The presence of hubs is a characteristic of scale-free networks. Scale-free networks are a specific class of networks defined by topological parameters, which have been commonly identified in natural, synthetic, and biological systems. Mathematical modeling of evolutionary conditions that favor the formation of scale-free networks has supported the proposal of a growth and preferential attachment schema *(9)*. During the growth of the network in this environment, an already well-connected node has a greater likelihood of acquiring a new interaction partners than a less-connected node. It is through this growth process over an evolutionary time scale that hubs are thought to emerge. The kinase–substrate interaction network in yeast exhibits scale-free topology *(4)*, suggesting that mammalian kinase–substrate networks are also scale free.

Complex networks can be simplified by reducing them to a set of smaller subnetworks (subgraphs), using a process called clustering. Clustering is frequently employed in functional genomics to associate nodes into a subgraph based on a common property. The actual property (parameter) used to generate a cluster depends on the object of the study. In the case of protein interaction networks, parameters include (but are not limited to) presence in the same gene ontology annotation, similar patterns of interaction partners, or involvement in the same signaling pathways. Within the individual clusters local information is more apparent and hypotheses can be made about the contacts within the cluster or about the interactions that connect different clusters. For example, consider a cluster consisting of six proteins involved in the same signaling pathway that are known to be simultaneously activated. If four of the six proteins are observed to be active in a screen, then it is reasonable to hypothesize that the remaining two may also be activated and that the pathway itself has been stimulated. Through the process of clustering information about the network under study can be used to infer information about the individual nodes. For example, it has been observed that clustering based on interaction architecture strongly correlates with clustering based on functional category *(10)*.

4. Example

In a study of mouse myoblast differentiation *(5)*, 53 protein phosphorylation events were identified, and a sample of these are listed in **Fig. 2** (left column). Using the methods described in **Subheading 3**, each of these proteins was identified as being a substrate of one or more of the kinases listed in the center column

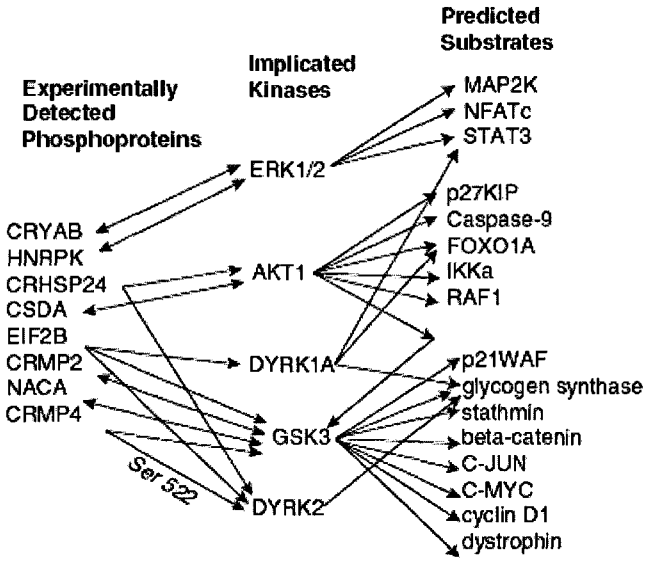

Fig. 2. Extrapolation of a network from phosphopeptide data. The proteins listed in the *left column* were experimentally determined to be phosphorylated. Using bioinformatic techniques, the kinases listed in the *center column* were proposed to be active and responsible for the observed phosphorylations. The proteins listed in the *right column* are additional predicted substrates of those kinases.

of Fig. 2. By repeated database searching, additional substrates were predicted, as shown on the right side of Fig. 2. To take a specific example, CRMP4 was found experimentally to be phosphorylated on serine 522 in differentiating myoblasts. Phosphorylation of this site has previously been ascribed to DYRK2 activity. Experimental observation of CRMP2 phosphorylation in undifferentiated cells implicated GSK3 activity. Bioinformatic searches and network modeling revealed that GSK3 can also phosphorylate CRMP4, on sites 509, 514, and 518. Interestingly, these GSK3-mediated phosphorylations are known to be dependent on phosphorylation at serine 522. Therefore, a very specific signaling module can be predicted. CRMP4 can have three phosphorylation states: unphosphorylated, completely phosphorylated on four sites, and singly phosphorylated on serine 522. The actual phosphoform present in the cell will depend on the relative activities of DYRK2 and GSK3 (the fully phosphorylated species will only be observed if GSK3 activity occurs after or simultaneously with DYRK2 activity and the singly phosphorylated species can only form if GSK3 is inactive, as occurs during differentiation). Overall, the model predicts that GSK3 and AKT activity should have a significant impact on myoblast differentiation due to their high degree of connectivity within the network (i.e., hubs). This prediction is in agreement with the known biochemistry of myoblasts, and a role in myoblast biology has already been found for many of the predicted substrates shown.

References

1. Manning, G., Whyte, D. B., Martinez, R., Hunter, T., and Sudarsanam, S. (2002) The protein kinase complement of the human genome. *Science* 298, 1912–34.
2. Caenepeel, S., Charydczak, G., Sudarsanam, S., Hunter, T., and Manning, G. (2004) The mouse kinome: discovery and comparative genomics of all mouse protein kinases. *Proc Natl Acad Sci U S A* 101, 11707–12.
3. Cohen, P. (2002) The origins of protein phosphorylation. *Nat Cell Biol* 4, E127–30.
4. Lee, R. E., and Megeney, L. A. (2005) The yeast kinome displays scale free topology with functional hub clusters. *BMC Bioinformatics* 6, 271.
5. Puente, L. G., Voisin, S., Lee, R. E., and Megeney, L. A. (2006) Reconstructing the regulatory kinase pathways of myogenesis from phosphopeptide data. *Mol Cell Proteomics* 5, 2244–51.
6. Obenauer, J. C., Cantley, L. C., and Yaffe, M. B. (2003) Scansite 2.0: proteome-wide prediction of cell signaling interactions using short sequence motifs. *Nucleic Acids Res* 31, 3635–41.
7. Diella, F., Cameron, S., Gemund, C., Linding, R., Via, A., Kuster, B., Sicheritz-Ponten, T., Blom, N., and Gibson, T. J. (2004) Phospho. ELM: a database of experimentally verified phosphorylation sites in eukaryotic proteins. *BMC Bioinformatics* 5, 79.
8. Shannon, P., Markiel, A., Ozier, O., Baliga, N. S., Wang, J. T., Ramage, D., Amin, N., Schwikowski, B., and Ideker, T. (2003) Cytoscape: a software environment for integrated models of biomolecular interaction networks. *Genome Res* 13, 2498–504.
9. Barabasi, A. L., and Albert, R. (1999) Emergence of scaling in random networks. *Science* 286, 509–12.
10. Samanta, M. P., and Liang, S. (2003) Predicting protein functions from redundancies in large-scale protein interaction networks. *Proc Natl Acad Sci U S A* 100, 12579–83.